PRODUCTION AND PURIFICATION OF CANNABIDIOL GLYCOSIDES

LE THI THUY TRINH

A Thesis Submitted in Partial Fulfillment of the Requirements for the

Degree of Doctor of Philosophy in Biotechnology

Suranaree University of Technology

Academic Year 2023

การผลิตและการทำบริสุทธิ์แคนาบิไดออลไกลโคไซด์

นางสาวลี ที ทุย ทริน

วิทยานิพนธ์นี้เป็นส่วนหนึ่งของการศึกษาตามหลักสูตรปริญญาวิทยาศาสตรดุษฎีบัณฑิต
สาขาวิชาเทคโนโลยีชีวภาพ
มหาวิทยาลัยเทคโนโลยีสุรนารี
ปีการศึกษา 2566

PRODUCTION AND PURIFICATION OF CANNABIDIOL GLYCOSIDES

Suranaree University of Technology has approved this thesis submitted in partial fulfillment of the requirements for the Degree of Doctor of Philosophy.

Thesis Examining Committee

(Assoc. Prof. Dr. Theppanya Charoenrat)
Chairperson

(Assoc. Prof. Dr. Apichat Boontawan)
Member (Thesis Advisor)

(Assoc. Prof. Dr. Mariena Ketudat-Cairns)
Member (Thesis Co-advisor)

(Prof. Dr. James Ketudat-Cairns)
Member

(Assoc. Prof. Dr. Panlada Tittabutr)
Member

(Dr. Yothin Teethaisong)
Member

(Assoc. Prof. Dr. Yupaporn Ruksakulpiwat)
Vice Rector for Academic Affairs
and Quality Assurance

(Prof. Dr. Neung Teaumroong)
Dean of Institute of Agricultural
Technology

ลี ที ทุย ทริน : การผลิตและการทำบริสุทธิ์แคนาบิไดออลไกลโคไซด์ (PRODUCTION AND PURIFICATION OF CANNABIDIOL GLYCOSIDES) อาจารย์ที่ปรึกษา :
รองศาสตราจารย์ ดร. อภิชาติ บุญทาวัน, 121 หน้า.

คำสำคัญ : แคนนาบิไดออลไกลโคไซด์/ซูโครสซินเทส/SrUGT76G1/การแสดงออกของเอนไซม์/สภาวะการเกิดไกลโคซิเลชันของ CBD

แคนนาบิไดออลไกลโคไซด์ (cannabidiol glycosides) เป็นยากลุ่มประเภทโพรดรัก (prodrug) ที่มีข้อดีหลายประการรวมถึงความสามารถในการละลายสูง ความคงสภาพ การดูดซึมทางชีวภาพ และคุณลักษณะทางเภสัชจลนศาสตร์ ปฏิกิริยาเรียงซ้อน (cascade reaction) ของเอนไซม์กลูโคซิลทรานสเฟอเรส SrUGT76G1 และซูโครสซินเทส SuSy ได้รับการพัฒนาเพื่อสังเคราะห์สารประกอบไกลโคไซด์โดยใช้ซูโครส (น้ำตาลทราย) ราคาถูกเป็นตัวให้กลูโคซิลอย่างง่าย ดังนั้นวัตถุประสงค์แรกของการศึกษานี้คือการหาอาหารเลี้ยงเชื้อที่ดีและสภาวะการแสดงออกที่เหมาะสมสำหรับการผลิต SuSy และ SrUGT76G1 ในฟลาสก์เขย่า ถังหมักขนาด 5 ลิตร และถังหมักขนาด 50 ลิตร หลังจากได้อาหารเลี้ยงเชื้อที่ดีแล้ว การออกแบบการทดลองโดยโมเดลของ Box-Benhken ได้ถูกนำมาใช้เพื่อหาสภาวะที่เหมาะสมต่อการแสดงออกของเอนไซม์ SuSy และ SrUGT76G1 โดยปรับปัจจัยสามอย่างให้เหมาะสมได้แก่ อุณหภูมิ ตัวเหนี่ยวนำแลคโตส และเวลา พบว่า การแสดงออกที่เหมาะสมถูกนำมาใช้ในฟลาสก์เขย่า ถังหมักขนาด 5 ลิตร และถังหมักขนาด 50 ลิตรได้สำเร็จ โดยผลผลิตของเอนไซม์เพิ่มขึ้นจากขวดทดลองไปจนถึงถังหมัก ความสามารถในการทำงานของเอนไซม์จำเพาะก็ไม่แตกต่างกันอย่างมีนัยสำคัญสำหรับเอนไซม์ที่ถูกทำให้บริสุทธิ์หลังการเพาะเลี้ยงจากทั้งสามระบบ

วัตถุประสงค์ที่สองคือเพื่อลดต้นทุนในการสกัดเอนไซม์ โดยใช้วิธีสกัดเอนไซม์แบบไมโครฟลูอิดิกแทนวิธีการสกัดด้วยไลโซไซม์ ผลการวิจัยพบว่าไม่มีความแตกต่างกันอย่างมีนัยสำคัญในด้านผลผลิตของเอนไซม์และความสามารถในการทำงานของเอนไซม์ระหว่างทั้งสองเทคนิค ทำให้สามารถลดต้นทุนในการผลิตเอนไซม์สำหรับการสังเคราะห์ CBD glycosides

วัตถุประสงค์ที่สามคือการหาสภาวะที่เหมาะสมสำหรับการผลิตแคนนาบิไดออลไกลโคไซด์ ในขณะเดียวกันก็ลดต้นทุนของตัวให้น้ำตาลโดยใช้ซูโครสซินเทส SuSy เพื่อสร้าง UDP-Glc ใหม่ ผลลัพธ์ได้มาจากเงื่อนไขสองประการในการสร้างผลิตภัณฑ์ที่มีขั้วน้อยหรือมากกว่านั้น โดยมีการใช้ LC/MS/MS เพื่อยืนยันมวลของผลิตภัณฑ์ CBD glycosides จากนั้นจึงตรวจสอบโครงสร้างของ CBD glycosides ที่ได้

วัตถุประสงค์สุดท้ายคือการขจัดสิ่งเจือปนส่วนใหญ่ออกจาก CBD glycosides หลังเกิดปฏิกิริยา จากซิลิกาเจลโครมาโทกราฟี พบว่าสิ่งเจือปนส่วนใหญ่จะถูกกำจัดออกโดยเฉพาะ

สารประกอบที่ชอบน้ำ ผลิตภัณฑ์ CBD-G1 ถูกแยกออกด้วยเมทานอล 5% ในสารละลายเอทิลอะซิเตตของซิลิกาเจลโครมาโตกราฟี และทำให้บริสุทธิ์มากขึ้นด้วยโครมาโทกราฟีเรซินชนิด C18 บรรจุในคอลัมน์ขนาดเล็ก สำหรับ HPLC แบบแฟลช/preparative นั้น สารผสม CBD glycosides พบอยู่ในส่วนแยกลำดับที่ 23 และ 24 ที่มีตัวทำละลายประมาณ 28% อะซีโตไนไตรล์ในน้ำ และ CBD-G2 ถูกชะล้างในส่วนแยกลำดับที่ 31 และ 32 ด้วยตัวทำละลายประมาณ 40% อะซีโตไนไตรล์ในน้ำ

สภาวะการแสดงออกของการผลิตเอนไซม์ทั้งสอง เอนไซม์สกัดแบบไมโครฟลูอิดิก ปฏิกิริยาการสังเคราะห์ CBD glycosides โดย SrUGT76G1 และเอนไซม์ SuSy เพื่อให้ได้ผลิตภัณฑ์ไกลโคไซด์ที่เป็นโพลาร์มากขึ้น และการทำให้ CBD glycosides บริสุทธิ์บางส่วน ได้ทำให้เกิดความชัดเจนจากผลการทดลองนี้ การศึกษาในอนาคตควรจะตรวจสอบการเชื่อมต่อ (Fusion) เพื่อปรับปรุงความสามารถในการละลายน้ำของเอนไซม์ที่เกี่ยวกับการผลิต CBD glycosides รวมถึงวิธีการอื่นในการทำให้บริสุทธิ์

สาขาวิชาเทคโนโลยีชีวภาพ
ปีการศึกษา 2566

ลายมือชื่อนักศึกษา _____
ลายมือชื่ออาจารย์ที่ปรึกษา _____
ลายมือชื่ออาจารย์ที่ปรึกษาร่วม _____

LE THI THUY TRINH : PRODUCTION AND PURIFICATION OF CANNABIDIOL GLYCOSIDES. THESIS ADVISOR : APICHAT BOONTAWAN, Ph.D., 121 PP.

Keyword: CANNABIDIOL GLYCOSIDES/SUCROSE SYNTHASE/SrUGT76G1/ENZYME EXPRESSION/ CBD GLYCOSYLATION CONDITIONS

Cannabidiol glycosides are prodrugs with many advantages, including high solubility, stability, bioavailability, and pharmacokinetic characteristics. The coupled SrUGT76G1 glucosyltransferase and sucrose synthase (SuSy) enzymes cascade reaction was developed to synthesize glycoside compounds using cheap sucrose as the expedient glucosyl donor. Thus, the first objective of this study was to screen for optimal medium and suitable expression conditions for SuSy and SrUGT76G1 production in shake flask, 5 L fermenter, and 50 L fermenter cultures. After the best medium was identified, Box-Benhken design was used to determine the suitable expression conditions for SrUGT76G1 and SuSy enzymes, optimizing three factors including temperature, lactose inducer, and time. For this, the suitable expression conditions were successfully applied in the shake flask, 5 L fermenter, and 50 L fermenter cultures. The yields of enzyme production were successfully increased from shake flask to fermenter. The specific activities of the enzymes were not significantly different for purified enzyme from each systems.

The second objective was to reduce cost and materials for the enzymatic extraction for which microfluidic method was used to substitute the used of lysozyme and DNase method. The results showed that there were no significant differences in the enzymes production yield and the enzyme activities between the two extraction techniques. The low-cost manufacture of enzyme materials for the synthesis of CBD glycoside was thereby facilitated.

The third objective was to obtain optimal conditions for the production of cannabidiol glycosides while reducing the cost of sugar donors by the use of sucrose synthase to regenerate UDP-Glc. Two conditions for generating either less or more polar products were drawn from the results. LC/MS/MS was used to confirm the mass of the CBD glycosides and then determine their structure.

The last objective was to partially remove most impurities from CBD glycosides after the reaction. From silica gel chromatography, most impurities especially hydrophilic compounds were removed. The CBD-G1 product was isolated by 5% methanol in ethyl acetate fractions of silica gel chromatography and purified more by mini C18-resin column chromatography. For flash/preparative HPLC, the mixed CBD glycoside formulations were found in fractions 23 and 24 at a solvent composition of around 28% acetonitrile in water, and the CBD-G2 eluted at fraction 31, 32, around 40% acetonitrile in water.

The expression conditions for both enzyme productions, the microfluidic extraction enzyme, the CBD glycoside synthesis reaction by SrUGT76G1 and SuSy enzyme for obtaining more polar glycoside products, and the partial purification of CBD glycosides were illuminated by these results. Future studies to examine the fusion for improving the enzyme-soluble forms of CBD glycosides as well as alternative methods for purification should be performed.

School of Biotechnology
Academic Year 2023

Student's Signature _____
Advisor's Signature _____
Co-advisor's Signature _____

ACKNOWLEDGEMENT

First and foremost, I would like to thank my advisor, Assoc. Prof. Dr. Apichat Boontawan, and my co-advisors, Prof. Dr. James R. Ketudat Cairns and Assoc. Prof. Dr. Mariena Ketudat-Cairns, for providing me the opportunity to study towards my Ph.D. degree and for their helpful guidance, unconditional support, and encouragement. I am most grateful for their thorough grounding in the principles of the research methodologies and also many other methodologies in life.

Besides that, I would like to thank all JKC lab members, especially Dr. Salila Pengthaisong, Ms. Chamaipon Beagbandee, and Dr. Sunaree Choknud, for their help in the preparation of my research, discussion, and suggestions on everything. I also extend my deepest appreciation to AB Lab members, especially manager Chakapong Wongsalee, Dr. Cheeranan Sriphuttha, and Mr. Phummarin Phoopong, for their help in the preparation of fermentation, microfluidization, and purification in my research.

I would also like to express my deepest gratitude to Dr. Rayudika Aprilia Patindra Purba for providing me the chance to learn Experimental design, valuable writing skills, and his advice, support, and encouragement.

I would like to thank all my friends in the School of Biotechnology at Suranaree University of Technology for their constant support and help throughout the project and in making this journey of mine relatively easy.

I wish to express my special thanks to all my Vietnamese friends at Suranaree University of Technology and close friends who are staying in Vietnam for their unconditional love, support, and encouragement.

Finally, I would like to express my appreciation to my family, my boyfriend for their unconditional love, care, support, and encouragement throughout my life.

This Ph.D. dissertation was supported by Suranaree University of Technology (SUT) and the Office of the Higher Education Commission under an OROG scholarship.

LE THI THUY TRINH

CONTENTS

Page

CONTENTS (Continued)

Page

CONTENTS (Continued)

Page

CONTENTS (Continued)

Page

CONTENTS (Continued)

Page

LIST OF TABLES

Table Page

LIST OF FIGURES

Figure Page

LIST OF FIGURES (Continued)

Figure Page

LIST OF FIGURES (Continued)

Figure Page

LIST OF FIGURES (Continued)

Figure Page

LIST OF FIGURES (Continued)

Figure Page

LIST OF ABBREVIATIONS

OD_{600}	=	Optical density measured at 600 nm
OD_{750}	=	Optical density measured at 750nm
DI	=	Deionized water
µl	=	Microliters
µg	=	Microgram
L	=	Litter
pH	=	Potential of hydrogen
TB	=	Terrific Broth (TB) medium
LB	=	Lysogeny broth
SOB	=	Super optimal broth
M9 modified	=	M9 minimal medium modified
FM	=	For medium auto-induced
h	=	hour(s)
°C	=	Degree(s) Celsius
w/w	=	Weight per weight
v/v	=	Volume per volume
g/L	=	Gram(s) per Liter
g	=	gram
Mpa	=	Megapascal
vvm	=	Volume per volume per liter of air
C2GnT-L	=	2 beta 1,6-N-acetylglucosaminyltransferase
CBD	=	Cannabidiol
DMSO	=	Dimethyl sulfoxide
DNA	=	Deoxyribonucleic acid
DNS	=	3, 5 Dinitrosalicylic acid
glc-1-P	=	Glucose 1-phosphate
GlcNAc-1-P	=	Amino sugar N-acetylglucosamine 1-phosphate
		glucuronosyltransferase

LIST OF ABBREVIATIONS (Continued)

GT42	=	Glycosyltransferase famlily 42
HPLC	=	High Performance Liquid Chromatography
IPTG	=	Isopropyl β – D -1-thiogalactopyranoside
LC/MS/MS	=	Liquid chromatography – mass spectrometry
ml	=	Milliliter(s)
mm	=	Millimeter(s)
mM	=	Millimolar
rpm	=	Rotations per minute
RSM	=	Response surface methodology
SrUGT76G1	=	*Stevia rebaudiana* Uridine 5'-diphospho-
TLC	=	Thin layer chromatography
UDP	=	Uridine diphosphate sodium salt
UDP-Glc	=	Uridine diphosphate glucose
UDP-GlcNAc	=	Uridine – diphosphate – N- acetylglucosamine
UMP	=	Uridine monophosphate
UTP	=	Uridine – 5' – triphosphate
UV	=	Ultraviolet
β-1,6-GlcNAc	=	Beta – 1,6 – N-acetylglucosamine

CHAPTER I

INTRODUCTION

1.1 Significance of the background

Cannabis is a kind of plant and a psychoactive drug used primarily for medical, food and dietary supplement. The herb cannabis contains 400 cannabinoid compounds and 60 derivative cannabinoids, including cannabidiol (CBD) and tetrahydrocannabinol (THC) (Ashton, 2001). However, THC is the main psychoactive constituent of cannabis. In contrast, CBD has been developed as an influential drug in modern medicine for treating various disorders, including schizophrenia, post-traumatic stress disorder, anxiety, graft-versus-host disease, addiction, cancer, and inflammatory bowel disease, etc. (Millar et al., 2020). In addition, CBD was also warranted by the US FDA (Food and Drug Administration) for addition to food, beverages, and dietary supplements (Corroon et al., 2020). There are many advantages of CBD; nevertheless, it has poor intrinsic features, such as low solubility in water, low bioavailability, and changeable pharmacokinetic profiles (Millar et al., 2020). The solubility of CBD in water is quite low, which reduces its bioavailability and limits transmission to target cells where it has poor membrane permeability. Several methods improve the hydrophobic property, including inclusion in liposomes, and nanoparticles, drug glycosylation, etc. However, a traditional nano-drug carrier, such as liposomes, presents a few disadvantages: poor stability, poor reproducibility, and low drug encapsulation efficiency (Idrees et al., 2020).

Glycosylation with sugar moieties, such as glucose, mannose, and galactose, can help in drug delivery systems, and it has a lot of advantages, including good biocompatibility, no notable toxicity, no immunogenicity, and biodegradability (Chen et al., 2020). Based on glycosylation, the sugar can be attached to a molecule to make it more polar by enzymes, via the hydroxyl group of the sugar. In addition,

depending on the sugar moieties, a concentration of drugs in target organs passes to the gastrointestinal tract or blood circulation (Chen and Huang, 2019). Therefore, the application of glycosylation in targeting drugs has become promising for treatment, diagnostics through carbohydrate, and receptor acceptance, with applications in brain targeting, lung targeting, and tumor cell targeting. Increasing the solubility of CBD will also improve its use in food, beverages, and dietary supplements.

In the production of glycosides, the sugar and acceptor are reacted with an acid or base catalyst, which is chemical glycosylation. It can produce a lot of waste and is not safe for the environment. Kim et al. (2021) used 80% ethanol to glycosylate MAPPD (N-Acetyl-p-phenylenediamine) to make Glc-DAPPD (glucose N,N'-diacetyl-p-phenylenediamine), which is an anti-neuroinflammatory designed for treatment of Alzheimer's disease. The yield of glycosylation was 48% (Kim et al., 2021). In comparison, glycosylation using enzymes as catalysts gives a high yield with a little waste, which is safe for the environment. Dewitte et. al. (2016) reported that the *Stevia rebaudiana* UDP-glycosyltransferase 76G1 (UGT-76G1Sr) enzyme converted curcumin to curcumin β-glycosides with 90% yield within 24 hours. Useful glycosyltransferase enzymes have been found in some sources, including *Stevia rebaudiana* which is the sweetest plant that belongs to the *Asteraceae* family. The *S. rebaudiana* SrUGT76G1 enzyme has been used for the glycosylation of cannabinoids (Hardman et al., 2017). However, the UDP-Glc was used as a sugar donor, which results in high-cost production. One way to reduce the costs for expensive nucleotide sugar is to use sucrose synthase(SuSy), which catalyzes release of fructose from sucrose and attachment of glucose to urindine diphosphate to create uridine diphosphate glucose (UDP-Glc) (Stein and Granot, 2019, Chen et al., 2020). Based on this characteristic of SuSy, coupled enzymes reactions including srUTG76G1 and SuSy can be applied to decrease the cost of producing CBD glycosides.

In this study, screening media for production of SrUGT76G1 and SuSy enzymes in *E. coli* BL21(DE3) was done. And then, the suitable expression condition was investigated by the Box-Behnken design with three factors, including lactose concentration (0 g/L to 20 g/L), temperature (20°C to 37°C), and time for expression (4 h to 24 h). These conditions for both enzymes were successfully applied in shake

flask, 5 L fermenter, and 50 L fermenter production. These enzymes were used for producing CBD glycosides. The optimization of the CBD glycosylation reaction was investigated, including concentrations of enzymes, substrates (UDP, sucrose), co-solvents (methanol, acetone) for dissolving CBD, and $MgCl_2$, along with time for reaction. Potassium phosphate buffer, pH 7.2, was applied based on a previous paper (Hardman et al., 2017). The reaction was incubated at 30°C, which was close to the temperature of 28°C in Harman et al.'s work. Thin layer chromatography (TLC) was used to detect CBD glycosides. After that, the CBD glycoside products were purified by a silica gel chromatography and flash/preparative HPLC. In the future, CBD glycosides can be a glycoside prodrug, which is promising to be applied in medicine, food, dietary supplements, and beverages for human health.

1.2 Research objectives

To produce and purify CBD glycosides by glycosylation with SrUGT76G1 and SuSy enzymes, the following objectives were targeted:

1. To obtain SrUGT76G1 enzyme from recombinant *E. coli* BL21(DE3) by cloning, expression, purification, and up-scale expression in a 50 L fermenter and investigating methods for enzyme extraction.

2. To obtain SuSy enzyme from recombinant *E. coli* BL21(DE3) by expression, purification and up-scale expression in 50 L fermenter and investigation method for enzyme extraction.

3. To find a good medium in screen media and suitable expression condition for high production of soluble enzymes.

4. To optimize the CBD glycoside reaction using SrUGT76G1 and SuSy enzymes as catalysts.

5. To partially purify the CBD glycosides products.

CHAPTER II

LITERATURE REVIEW

2.1 *Cannabis sativa L.*

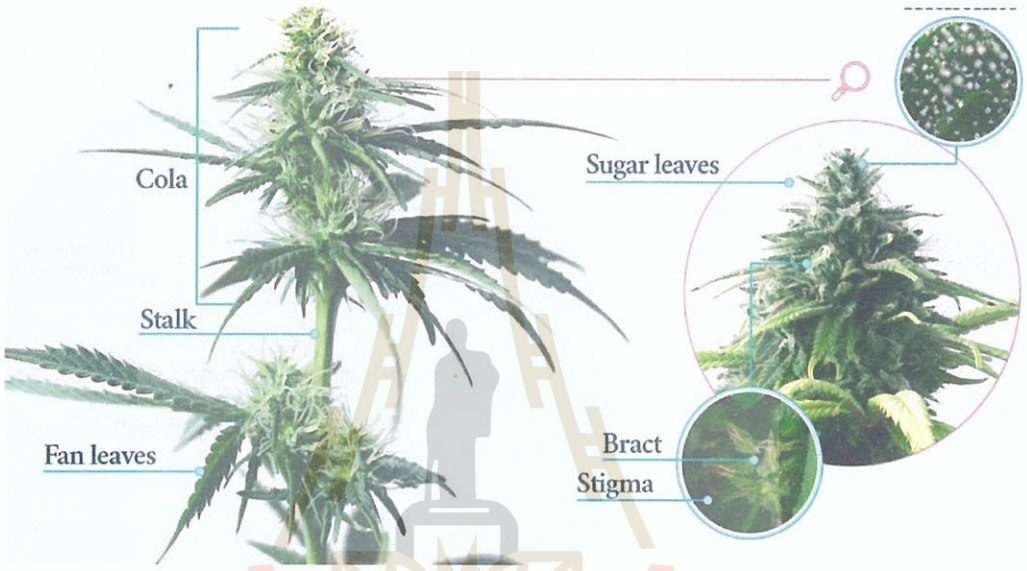

Figure 2.1 Morphology of *Cannabis sativa L.* (Geogre Mouratidis, 2020).

Cannabis sativa L. (Figure 2.1) is a kind of plant with different names like cannabis, hemp, and marijuana. It is thought to have originated from central Asia (Voeks, 2014), but now it has widespread cultivation by cosmopolitan distribution. The composition of *C. sativa* has been found to include several bioactive cannabinoid molecules with the main components that are indicated in Figure 2.2. However, delta-9-tetrahydrocannabinol (THC) and cannabidiol (CBD) have been focused on in pharmacy to treat some diseases like cancer and Autism Spectrum Disorder, and for inclusion in dietary supplements, food, and beverages. THC is a psychoactive compound, while CBD is non-psychoactive, and a correct ratio between these molecules is needed for high effectiveness for treatment (Table 2.1).

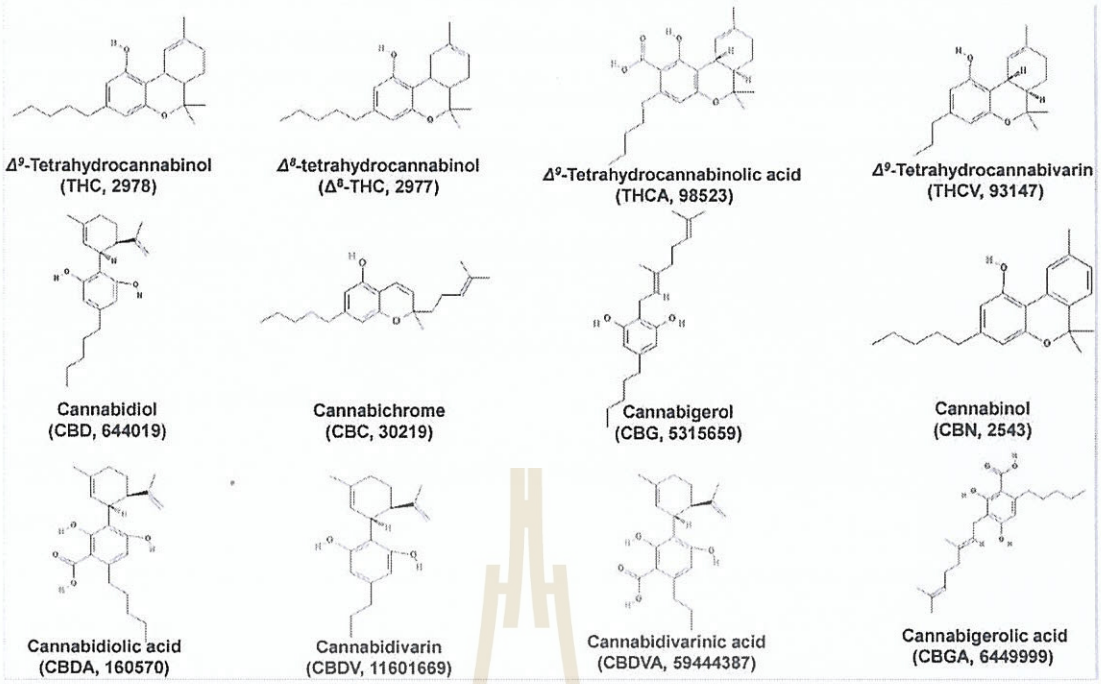

Figure 2.2 The main components of *Cannabis sativa L.* extract (Aliferis and Bernard-Perron, 2020).

Supporting medical purposes, *C. sativa* is growing in Suranaree University of Technology. Cannabis can be harvested and purified to collect THC and CBD for some applications. The advantage of CBD and THC are shown in Tables 2.1 and 2.2. However, CBD and THC are not very soluble in water. The glycosylation can be applied to change to derivatives that are highly soluble in water. Scientists have tried to look for enzymes that can help in glycosylation. In *S. rebaudiana*, 44 uridine diphosphate glucose glucosyltransferase (UGTs) enzymes have been found for glycosylation with glucose (Zhang et al., 2020). The details of *S. rebaudiana* are described in the next section.

Table 2.1 Medical characteristics of cannabis.

Medicine	Medical characteristics	References
CBD: THC Ratio (20:1)	Pediatric epilepsy treated 74 patients were 2016 (age range 1-18 years)	(Tzadok et al., 2016)
CBD:THC (20:1) twice a day	Autism Spectrum Disorder and epilepsy	(Ponton et al., 2020)
CBD (combining 5 ug/ml CBD and 4 gray of radiation)	Cancer treatment (in vitro)	(Yasmin-Karim et al., 2018)
CBD: THC Ratio (1:1)	Attention-deficit hyperactivity disorder (ADHD)	(Black et al., 2019)

Table 2.2 Cannabis in cosmetic, dietary supplement, food and beverages.

APPLICATION	REFERENCES
- Coca-Cola are planning to supplement some of their products with CBD; cosmetic industry used hempseed oil as a sun cream due to UV absorption and high vitamin E content; hemp oil was used as cooking oil like olive oil, which has established benefits for cardiovascular health; dietary supplement	(Cerino et al., 2021)
- Dietary supplement	(Corroon et al., 2020)
- Cannabidiol coffee	(Monshouwer et al., 2011) (Wouters et al., 2012)
- Acne treatment	(Spleman et al., 2018)

2.2 Characterization of cannabinoids (THC and CBD)

The aim of cannabinoids characterization is to provide pharmacokinetic information on cannabinoids when fed in oral administration. It has four parts absorption, distribution, metabolism, and excretion.

2.2.1 Absorption

In oral administration, absorption of cannabinoids involves transport across membranes of the epithelial cells in the gastrointestinal tract. The first organ

is the stomach, which has a relatively large epithelial surface, but its thick mucous layer and short transit time limit cannabinoid absorption. The cannabinoids are sent to the small intestine, where cannabinoids can absorb into the small intestine epithelium as shown in Figure 2.3. The absorption of exogenous molecules in the small intestine occurs by transcellular transport, active transport, facilitated diffusion, receptor-mediated endocytosis, paracellular transport and pinocytosis (Boyle, 2005). However, the cannabinoids are nonpolar and can diffuse directly across the membrane, followed by transcellular transport into the bloodstream (Wakshlag et al., 2020).

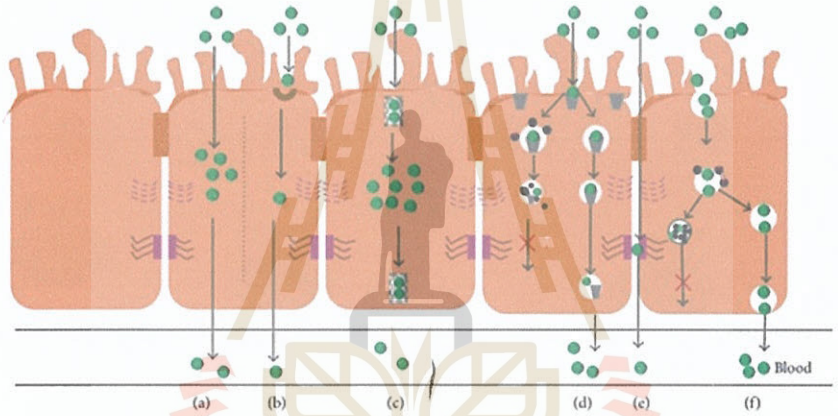

Figure 2.3 The absorption of molecules in the small intestine. (a) Transcellular transport; (b) active transport; (c) facilitated diffusion; (d) receptor-mediated endocytosis; (e) paracellular transport; (f) pinocytosis (Xu et al., 2013).

2.2.2 Distribution

After cannabinoids absorb into the bloodstream, the cannabinoids are distributed to everywhere in our body. Based on the property of cannabinoids, they can interact with blood proteins like plasma albumin to move in the circulatory systems. In an effective amount, cannabinoids will target organs to work in the human endocannabinoid system. In the previous study, 97% of the cannabinoid bound to the plasma protein and was distributed to the circulatory system (Millar et al., 2018). Depending on the specific molecule, cannabinoids can be strongly bound or weakly bound. When bound with albumin, another cannabinoid can bind to

albumin and free THC or CBD. THC is highly lipophilic and can diffuse across membranes based on concentration gradients when unbound. Cannabinoid transporters pump THC back into the plasma, limiting access to the blood-brain barrier. In our body, the system barrier has an assignment to protect some organs like the blood-brain barrier, blood - testicular barrier and blood – placental barrier (Figure 2.4).

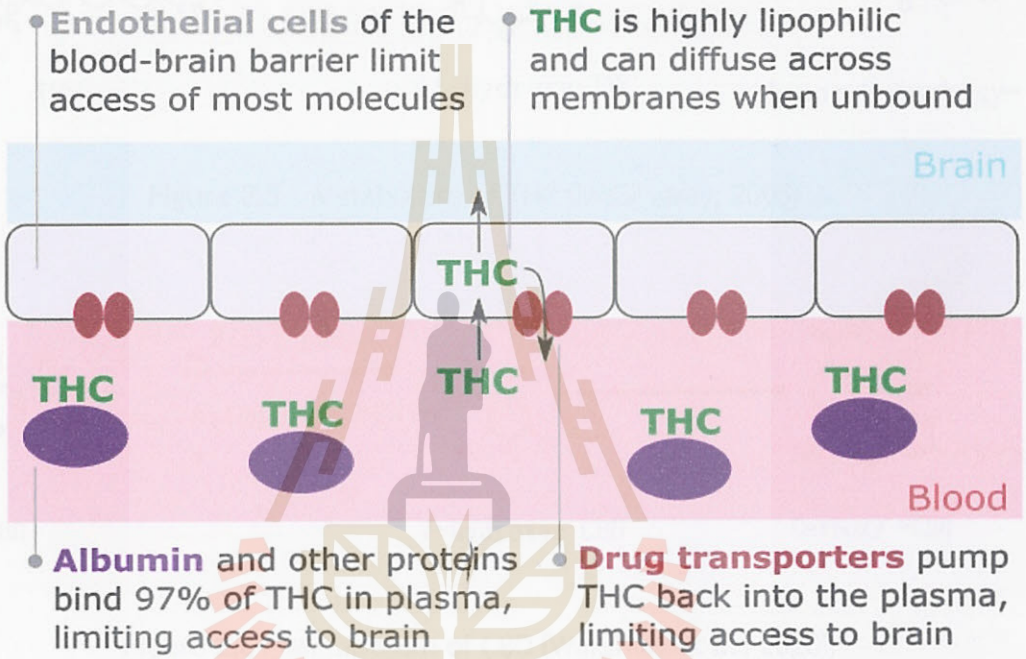

Figure 2.4 Distribution of THC in the bloodstream (Trad-Paulo Gómzer, 2017).

2.2.3 Metabolism

Metabolism of cannabinoids includes several chemical reactions that change the structure of cannabinoids to another molecule, which can be activated or inactivated the cannabinoids and can target them for excretion. Cannabinoids are carried in the blood directly to the liver, where they will be metabolized in some manner. This is called the first-pass metabolism, referring to the first pass of cannabinoids through the liver and this will typically greatly reduce the bioavailability of cannabinoids. In certain cases, metabolism in the liver actually activates cannabinoids, but this is less common, and the first pass effect can inactivate over

90% of orally administered cannabinoids before they are able to reach the general circulation. This must be taken into account when determining the appropriate dosage.

In this case, cannabinoids will react with cytochrome P450 in the liver and change to another molecule, as summarized in Figures 2.5 and 2.6.

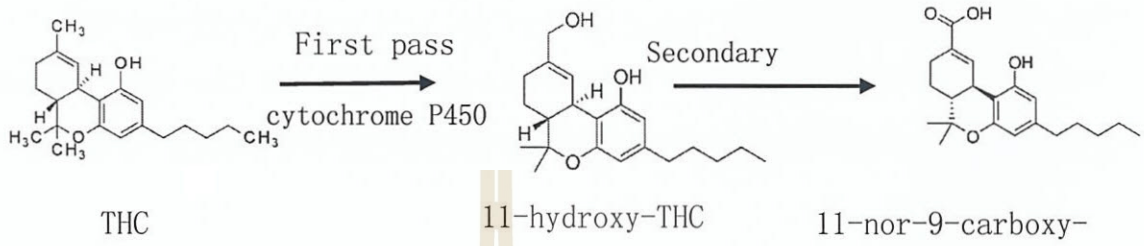

Figure 2.5 Metabolism of THC (McGilveray, 2005).

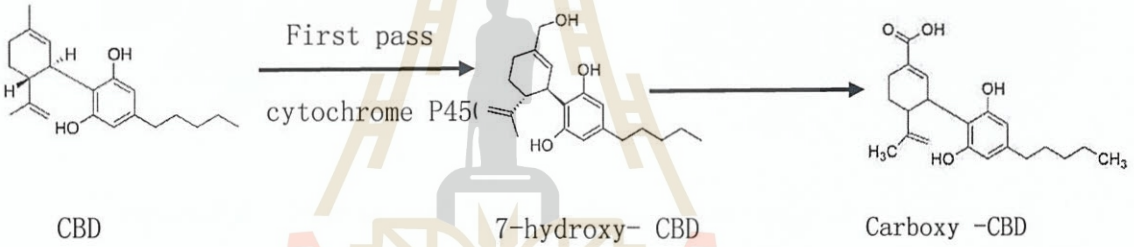

Figure 2.6 Metabolism of CBD (Wakshlag et al., 2020).

2.2.4 Excretion

Finally, cannabinoids will exit the body by urination, defecation, exhalation and sweating, which depends on the administration of cannabinoids. Normally with oral administration, the kidneys are heavily involved in this process, as they must remove poisonous substances from the bloodstream (Rimmington, 2020).

2.3 Endocannabinoid system

The endocannabinoid system is a biological system of endocannabinoids, it includes the receptors CB1 and CB2, which are G protein-coupled receptors, endocannabinoids (2-arachidonoyl-glycerol (2-AG), anandamide (AEA), the enzymes for synthesis of endocannabinoids (diacylglycerol lipase (DAGL), N-acylphosphatidyl-

ethanolamine phospholipase D (NAPE-PLD)), degradation (fatty acid amide hydrolase (FAAH) and monoacylglycerol lipase (MGL) (Kienzl et al., 2020 and Cristino et al., 2020). The endocannabinoid system is a prevalent neuromodulatory system that has significant roles in central nervous system development, synaptic plasticity, immune cells, and the response to endogenous and environmental insults (Lu and MacKie, 2016)

Phytocannabinoids are the naturally occurring cannabinoids found in the cannabis plant such as tetrahydrocannabinol (THC) and cannabidiol (CBD). They also can activate the receptors CB1 and CB2, and have similar effects to endocannabinoids.

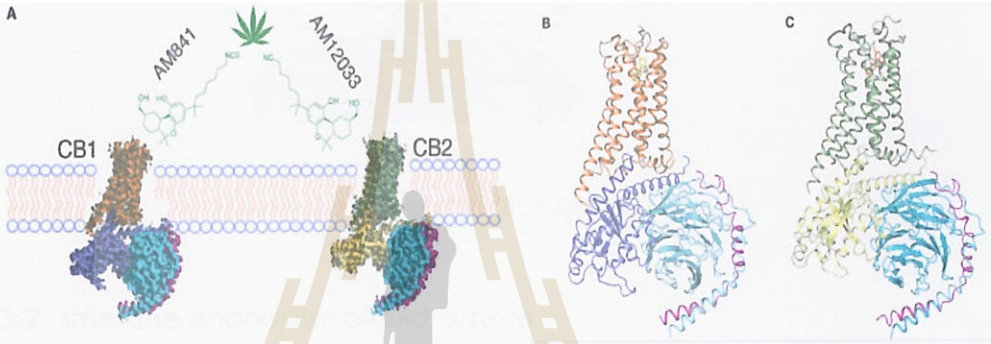

Figure 2.7 Structures of CB1 and CB2 receptors (Hua et al., 2020).

2.3.1 Central nervous system

In response to increased intracellular Ca^{2+} concentration, both endocannabinoids are produced on demand. AEA is synthesized from N-acyl-phosphatidylethanolamine (NAPE) by NAPE-specific phospholipase D (NAPE-PLD) and 2-AG is produced from diacylglycerol (DAG) by DAG lipase (Zou and Kumar, 2018). After synthesis, endocannabinoids are released into the intracellular space. Because endocannabinoids are uncharged hydrophobic molecules, they cross directly through the membrane based on concentration gradients (Boyle, 2005). Endocannabinoids will bind to the receptor CB1, and it will activate the transient receptor potential cation channel subfamily V member 1 to inhibit L-type Ca^{2+} channels. Activated CB1 will then inhibit neurotransmitter release through the suppression of calcium influx. The functions of the endocannabinoids in the central nervous system include memory, motor coordination, pain perception, feeding, appetite, and coping with stress, and it is related to the defects schizophrenia and epilepsy (Fride, 2005). The CB2 receptor has

been identified at lower levels in the brain (Zou and Kumar, 2018). Intracellular CB2 inhibits neuronal firing in medical prefrontal cortical pyramidal neurons by activating Ca^{+2}-activated chloride channels, indicating that it is involved in the regulation of neuronal activity (Zou and Kumar, 2018).

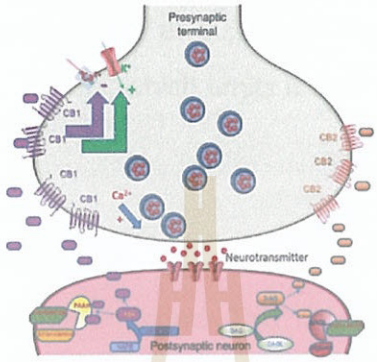

Figure 2.8 Endocannabinoid system.

2.3.2 Immune endocannabinoid system

Immune cells have many types such as CD^{8+} T cells, CD^{4+} T cells, B lymphocytes, NK cells, neutrophils, eosinophils, mast cells, monocytes, tumor-associated macrophages, dendritic cells and myeloid-derived suppressor cells as is shown in Figure 2.9 (Kienzl et al., 2020). With different effects on immune cells, the immune-endocannabinoid system contributes to the balance between neuroinflammation and neurodegeneration in the human body (Tanasescu and Constantinescu, 2010).

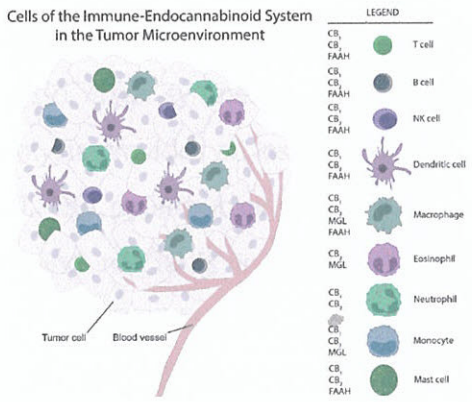

Figure 2.9 The immune endocannabinoid system (Kienzl et al., 2020).

Moreover, due to the barrier complexity of some parts of the human body, conventional drugs cannot easily be distributed and absorbed into targeted tissues. In the instance of the blood-brain barrier, the combination of cannabidiol (CBD) and tetrahydrocannabinol (THC) was used as a medicine for brain treatment, such as autism spectrum disorder, and epilepsy (Ponton et al., 2020), and attention-deficit hyperactivity disorder (Black et al., 2019). However, the drug transporter can pump THC back into the plasma, which limits it to the brain (Calapai et al., 2020).

2.4 Glycosides

In chemistry, a glycoside is a molecule in which a sugar is bound to another functional group via a glycosidic bond. This linkage is broken by acid or enzyme hydrolysis and both glycone and aglycone parts are separated. The glycone part is water-soluble but insoluble in organic solvents, whereas aglycone part may have opposing properties. They are formed by the biochemical glycosylation reaction which makes water-insoluble compounds more polar and the water-soluble. In the glycosides, the classification of glycosides can be based on linkage, based on nature of glycone, based on nature of aglycone and based on therapeutic activity (Mistry, 2021). For examples based on linkage, glycosides are separated into C-glycosides, O-glycosides (Figure 2.10), S-glycosides, and N-glycosides.

The catalyst for glycoside formation is acid, base, or enzyme, which have been shown as examples in Table 2.4. However, enzymatic synthesis has proven itself to be a promising alternative to the laborious chemical synthesis of glycosides by avoiding the necessity of numerous protecting group strategies needed in chemical synthesis because the reactions often lacking regio- and stereoselectivity (Hayes et al., 2017, Mestrom et al., 2019). The synthesis for the glycoside prodrugs of daunorubicin with chemical catalysts provides an instance of the laborious procedure required (De Graaf et al., 2003). The daunorubicin prodrug was synthesized in four reactions with many catalysts and reactants including (i) Ag_2O-CH_3CN; (ii) $NaBH_4$, $CHCl_3$-iPrOH; (iii) DSC-Et_3N, CH_3CN; (iv) DMF-Et_3N; and (v) MeOH-MeONa (Ghosh et al., 2000). In another example of use of chemical catalysts, the synthesis of glycosyloxymethyl prodrugs had two steps with many chemical catalysts that were described in Elferink et al., 2022.

Based on natural glycosylation, the synthesis of glycosides is easily accomplished by glycosyltransferases and transglycosidases. With curcumin glycosides, a glucosyltransferase from *Phytolacca americana* and a cyclodextrin glucanotransferase (a transglycosidase) from *Bacillus macerans* were used to synthesize curcumin D-glucoside and curcumin oligosaccharides, respectively (Wang, 2009). Natural glycoside production is most extensively done in plants in which glycosylation is catalyzed by uridine diphosphate (UDP) glycosyltransferases (UGTs), primarily from family 1 of glycosyltransferases (Wang, 2009). These plant UGTs catalyze glycosyl transfer via a direct displacement S_N2-like mechanism, similar to other inverting glycosyltransferases (GTs) (Wang, 2009). Scientists have found a large number of UGT enzymes that have evolved for the glycosylation of plant natural products. Those enzymes have been applied to produce cannabinoid glycosides (Hardman et al., 2017), rebaudioside D (L. Chen et al., 2020), and so on. Rebaudioside D was formed by a multiple enzyme system including UGT76G1, UGTSL2, and StSUS1 (L. Chen et al., 2020). In this case, UDP-Glc as a sugar donor was synthesized by *Solanum tuberosum* sucrose synthase (StSuSy1) from UDP and sucrose (Schmölzer et al., 2016). The cost of production was reduced due to the recycling of UDP to UDP-Glc by StSuSy1. Another example is *Arabidopsis thaliana* UGT73C6, which catalyzes the 23-O-glucosylation of brassinosteroids, so it has potential for glycosylation of steroids and other hydrophobic drugs. Brassinosteroids are steroid hormones of plants that play important roles in plant growth and development (Gan et al., 2021). Some other enzymes were mentioned in previous reviews (Wang, 2009), such as UGT71G1 from *Medicago truncatula* for saponin biosynthesis and UGT72L1 from *Medicago* for epicatechin 3'-O-glucoside synthesis.

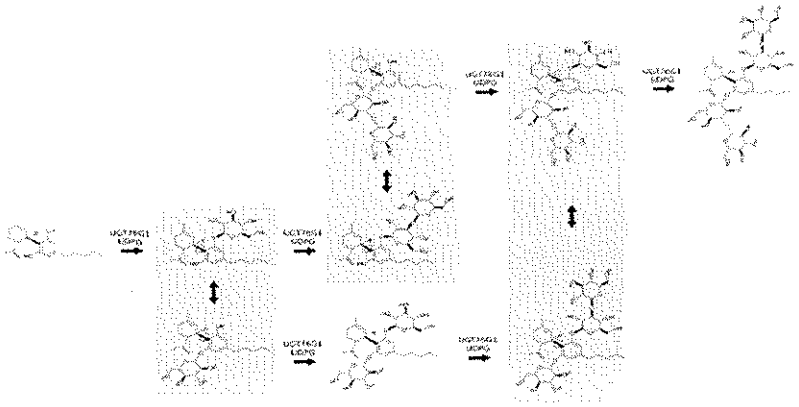

Figure 2.10 The pathway of CBD glycosides using UGT76G1 enzyme (Hardman et al., 2017).

2.5 Advantage of CBD glycosides prodrug

2.5.1 Targeting and the role of carbohydrate in cellular interactions

Previous studies have shown that carbohydrates play a significant role in cellular interactions, such as cellular signaling, recognition and interaction of cells with each other and the extracellular environment (Martin et al., 2022, Brandley and Schnaar, 1986, Shchegravina et al., 2021). That is a reason for the application of carbohydrates to drug delivery systems. It can gain many advantages, such as remarkable selectivity for protein receptors, simple structure for determination, being biocompatible and biodegradable materials, there being many different natural carbohydrate sources, shielding therapeutic agents or nanoparticles from undesirable interactions with proteins, and being highly soluble, leading to improved drug administration (Shchegravina et al., 2021). The most prominent are targeting delivery systems based on monosaccharide ligands such as D-glucose, D-galactose, D-quinovose, D-xylose, D-fucose, L-arabinose, and so on (Elferink et al., 2022) and carbohydrate nanoparticles. The prodrugs targeting the organ depend on the kind of monosaccharide, which uses the SLC2A family of transporters (Shchegravina et al., 2021). For example, the brain is targeted by glucose due to GLUT1, which is highly expressed on the surface of the cerebral capillary lumen; the liver is targeted by mannose or galactose due to the asialoglycoprotein receptor (ASGP-R), the lung is targeted by mannose or glucose due to macrophages which are abundant in lung

tissues, that have a mannose receptor on the surface; and GLUT1 is highly expressed in lung cancer issues (Chen et al., 2020). By the same principle of receptor binding, CBD glycosides are prodrugs with many advantages thanks to monosaccharides.

2.5.2 Enhanced Pharmacokinetic properties

Pharmacokinetic properties are presented in four parts: absorption, distribution, metabolism, and excretion.

2.5.2.1 Absorption

In oral administration, absorption of CBD glycosides involves transport across the membranes of epithelial cells in the gastrointestinal tract. The stomach is the first organ, with a comparatively large epithelial surface area; yet, absorption of CBD glycosides is limited by its thick mucous layer and fast transit time. Then, the CBD glycosides are sent to the small intestine, where they can be absorbed into the small intestine or large intestine. Addition of the carbohydrate group of glucose in CBD glycosides can increase the solubility of CBD due to the OH groups of sugar, which can increase the bioavailability of drugs. In the case of cannabidiol (CBD), which is a hydrophobic molecule with low bioavailability in oral administration. CBD has been glycosylated with glucose by UGT76G1, and based on the amount of glycosylation, the aqueous solubility of CBD glycoside increases, leading to an increase in the bioavailability of CBD glycoside (Hardman et al., 2017). In other research, they tested with high bioavailability assay of CBD glycoside (VB110-two glycoside of two-side OH group) on eight-week-old male Swiss mice. The results were found CBD and CBD-glycosides in the large intestinal at 60 min and 90 min time points. It was hydrolyzed by beta-glycosidases from the large intestinal microflora (Zipp et al., 2017). In addition, the highly aqueous solubility of CBD glycosides also enables new formulations for delivery in transdermal or aqueous formulations. In patents, CBD glycoside was used in numerous formulations, including gel, gel-like compositions, ointments, creams, patches, lotions, sprays, foam, and oils (Stinchcomb et al., 2010). Therefore, there is beginning to show promise for the use of CBD glycosides in improving human health.

2.5.2.2 Distribution

After CBD glycosides absorb into the bloodstream, they are distributed everywhere in our body. Based on the aqueous solubility of CBD glycosides, they can easily move in the circulatory system and target tissues with

increased expression of glycosidase. Especially, various glycosidase enzymes are also overexpressed in different cancer types, such as β-glucosidase (breast, gastric, and liver); α-fucosidase (ovarian, gliomas, colon, pancreatic), and so on (Martin et al., 2022). In addition, in cancer cells, the glucose transporters (GLUTs) are overexpressed due to the higher uptake of glucose than in normal cells. Therefore, CBD glycoside constitute a promising design for supporting cancer treatment.

In a previous study, 97% of the cannabinoid was bound to the plasma protein and distributed to the circulatory system due to its hydrophobic properties, which led to low bioavailability (Millar et al., 2018). With glucose moieties, CBD glycosides can also cross through some barriers in our body by intranasal, stereotactic, or intrathecal delivery and can also pass the blood-brain barrier with the sugar facilitating the transport (Zipp et al., 2017). After glucose moieties support crossing the blood-brain barrier, the glycosidase in the brain can break the glycosidic bond to release CBD (Zipp et al., 2017).

2.5.2.3 Metabolism and excretion

CBD glycosides are prodrugs with low degradation or metabolism in the stomach and small intestine, which leads to higher total bioavailability of CBD glycoside upon oral delivery. It can be found in the small and large intestines, where some molecules were degraded by beta-glycosidases from microflora [17, 22]. However, in first-pass metabolism CBD glycosides pass through the liver and react with CYP450 for detoxification and targeting them for excretion. Nevertheless, glycosylation of acceptor hydroxyl groups may afford protection, preventing CBD glycosides from binding to the CYP450 active site (Zipp et al., 2017). Therefore, long-term release of CBD formulation from CBD glycosides supports reduced toxicity in the liver and slow excretion from the body. In addition, the glucose moiety with several possible numbers of glucose moieties on both OH groups becomes more varied and complex, and when CBD glycosides are administered, the CBD glycosides prodrug delivery kinetics are altered, resulting in a prolonged-release drug formulation.

2.5.3 Reduced toxicity and side effects

This property of low toxicity is also related to targeting cells because CBD glycosides are a kind of inactive drug if their parent drugs are not released, so

target cells overexpressing the appropriate glycosidase are most affected. After release from the parent drug, the glucose moiety has many advantages, such as nontoxicity, no immunogenicity, good biocompatibility, and biodegradation, as mentioned in a previous paper (Chen et al., 2020).

Based on the low toxicity and availability of targeting cancer cells by glycosidase and properties of high GLUTs expression in cancer cells, CBD glycosides are a promising modern medicine for cancer cell treatment. Besides that, the improved solubility of CBD glycoside leads to high bioavailability. The amount of drug dose can be reduced, and there are diverse routes of medication administration when compared with traditional drugs.

In addition, conventional cancer drugs affect not only cancer cells but also normal cells. Thus, lack of specificity to tumor cells and high toxicity still exist in conventional drugs. Therefore, the new drug delivery is very necessary and challenging for scientists to improve the properties of conventional drugs. In this case, glycoside prodrugs not only significantly improved pharmacokinetics but also further enhanced the permeability, solubility, stability, specificity, and selectivity of GDs to target cells. With GDs, the following benefits can be gained: cell targeting based on sugar; high solubility leading to high bioavailability; low toxicity due to the sugar group; and high biocompatibility (Martin et al., 2022) (Chen et al., 2020). More applications of glycosylation in pharmacy, food/dietary supplements, cosmetics are summarized in Table 2.3.

Table 2.3 Glycoside prodrugs for modern medicine and other applications.

Glycoside prodrugs	Carbohydrate group(s)	Catalyst used for synthesis or source	Activating enzyme	Function of GD	References
CBD glycosides	Glucose and glucooligosaccharides	Enzymes catalyst	Beta-glycosidase	Anti-psychotic, a neuroprotectant, and other maladies	(Zipp et al., 2017)
Curcumin glycosides	Gluco-oligosaccharide	Enzymes catalyst	Glycosidase	Anticancer, anti-inflammatory, neuroprotective (Alzheimer's disease anti-oxidative affection)	(Hamada et al., 2020)
Digoxin and lanatoside C	Glycone	Medicinal plant		Anti-neuroinflammation	(Jansson et al., 2021)
Glycosylated Paclitaxel	Glucose	Chemical catalyst	β-glucuronidase	Anticancer for breast cancer and ovarian cancer cell	(Mao et al., 2018)
ETP, a topoisomerase II inhibitor	Glucosyl acetone-based ketel-linked glycoside prodrugs	Chemical catalyst	β-glucuronidase and acid-triggered ketal hydrolysis	Cancer therapy	(Yu et al., 2020)

Table 2.3 Glycoside prodrugs for modern medicine and other applications (Continuous)

Glycoside prodrugs	Carbohydrate group(s)	Catalyst used for synthesis or source	Activating enzyme	Function of GD	References
Glycosyloxymethyl prodrugs with 5-fluorouracil, thioguanine, propofol and losartan.	Monosaccharides (β-D-glucose, β-D-quinovose, β-D-xylose, β-D-galactose, β-D-fucose, α-L-arabinose	Chemical catalyst	β-glycosidases in the GI-tract	Anticancer for acute myeloid leukemia, acute lymphocytic leukemia, and chronic myeloid leukemia; Treatment of irregular heart rate and high blood pressure	(Elferink et al., 2022)
Glycoside prodrugs of daunorubicin	Glucose and galactose	Chemical catalyst	β - glycosidases	Cancer therapy	(De Graaf et al., 2003)(Ghosh et al., 2000)
Rebaudioside D	Glucose	Enzyme catalyst	-	Diabetics (food supplement)	(L. Chen et al., 2020)
Myricitrin glycosides	Galactose	Enzyme catalyst	-	Anti-oxidative activity	(Shimizu et al., 2006)

Table 2.3 Glycoside prodrugs for modern medicine and other applications (Continuous)

Glycoside prodrugs	Carbohydrate group(s)	Catalyst used for synthesis or source	Activating enzyme	Function of GD	References
Glycosylated antioxidants, Mangiferin glucosides	Glucose, maltose	Enzyme catalyst	-	Antioxidants	(De Winter et al., 2015), (Wu et al., 2021)
Quercetin glucosides	α- Oligoglucosylation	Enzyme catalyst	α – glucosidase	Flavonoid as antioxidant	(Murota et al., 2010)
Menthol glucoside	Glucose	Enzyme catalyst	-	Hair lotions, oral hygiene, dental, skin care product, skin irritation, so on.	(Kurze et al., 2021)
Glycosylated-chitosan derivaties	oligosaccharides	Chemical catalyst	-	Apply in different sectors such as food supplement, biomedical, so on.	(Sacco et al., 2020)

2.6 *Stevia rebaudiana*

Figure 2.11 *Stevia rebaudiana* (Madan et al., 2010).

Stevia rebaudiana (Figure 2.11) is a plant with sweet taste. It can also be called honey leaf or sweet leaf. It produces sweet taste but no energy values. Normally, it can be used instead of sugar for reducing dental caries in children and reducing digestible sugar in the diet. In addition, the compounds of *S. rebaudianna* have many advantages, including anti-hyperglycemic, anti-hypertensive, anti-inflammatory, anti-tumor, etc, (Ferrazzano et al., 2016). The biosynthesis pathway is shown in Figure 2.12. The *S. rebaudiana* has been investigated and found to have 44 UDP-glucosyltransferase (UGTs), which are displayed in the phylogeny tree in Figure 2.13. There are many UGTs, three of which have been identified and characterized (srUGT85C2, srUGT74G1 and SrUGT76G1) (Richman et al., 2005). Of the 44 UGT enzymes, the SrUGT76G1 enzyme with favorable characteristics has been applied to generate several products, such as sweeteners with good taste which replace sugar while providing low energy (rebaudioside A, rebaudioside C), curcumin glycosides and cannabinoid glycosides with improved properties compared to the original molecules, as shown in Table 2.4.

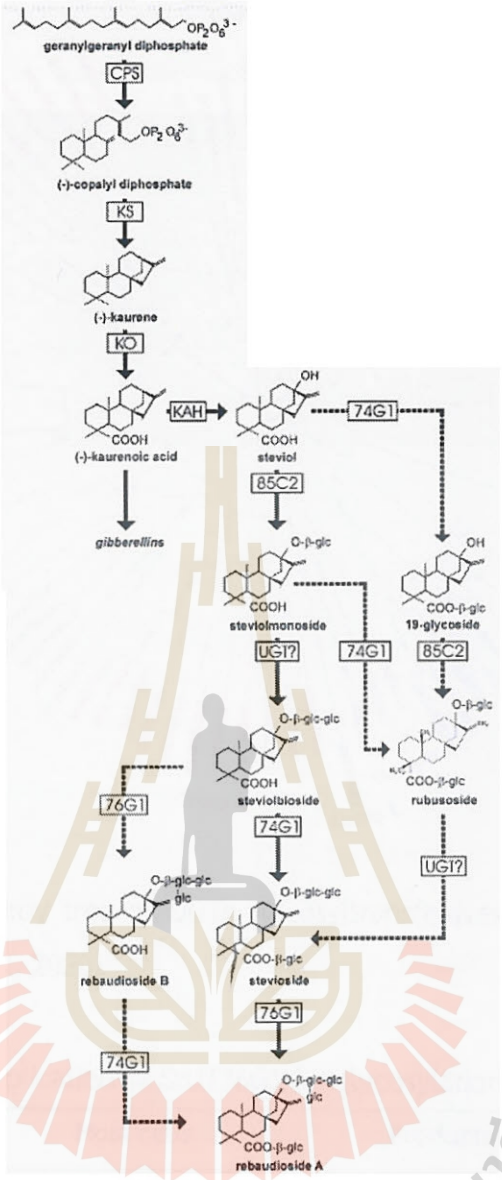

Figure 2.12 Biosynthesis pathway of the steviol glycosides. Abbreviations: CPS, copalyl diphosphate synthase; KS, kaurene synthase; KO, kaurene oxidase; KAH, kaurenoic acid oxidase; UGTs are abbreviated to their numerical identifiers (Humphrey et al., 2006).

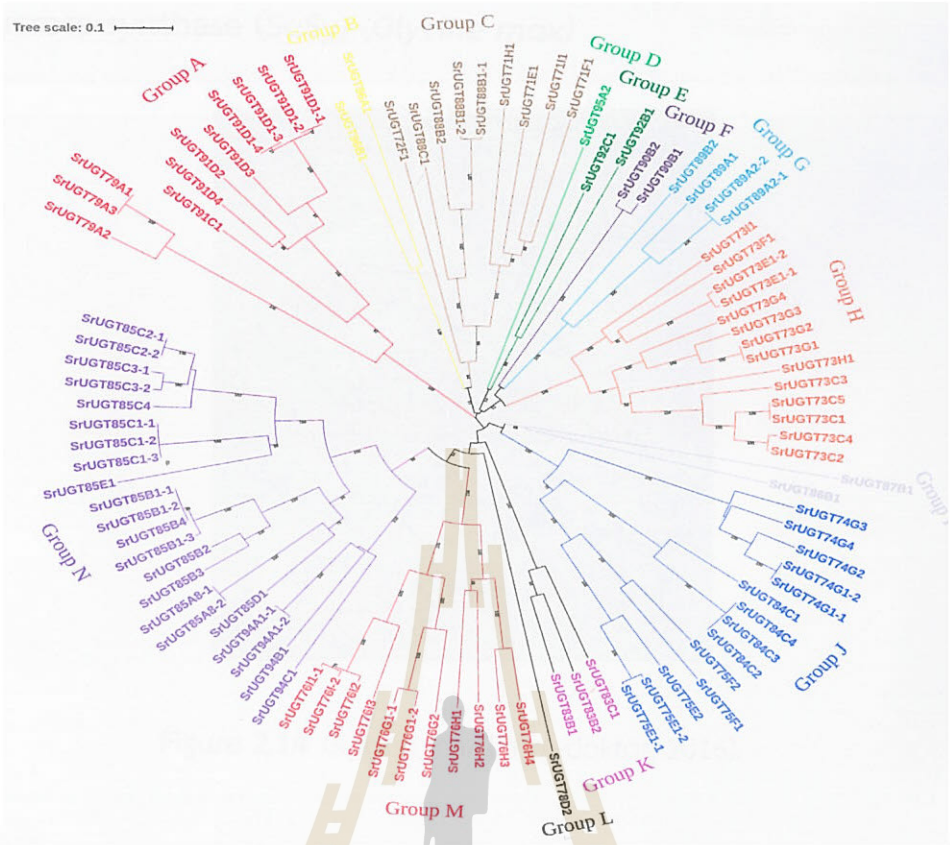

Figure 2.13 The phylogeny tree of UGTs glycosyltransferases in *Stevia rebaudiana* (Zhang et al., 2020).

Table 2.4 Summary application of SrUT76G1 for glycosylation.

Enzymes	Host cells	Products	References
SrUGT76G1 (*Stevia rebaudianna*) and Os03g0702000p (*Oryza sativa*)	*E. coli* BL21(DE3)	Cannabinoid glycoside	(Hardman et al., 2017)
SrUGT76G1, UGT74G1, and UGT85C2	*BL21-CodonPlus(DE3) E.coli* (Stratagene)	Rebaudioside A	(Richman et al., 2005)
UGT-76G1*Sr*	*E. coli* BL21(DE3) cells (Novagen)	Curcumin glycoside	(Dewitte et al., 2016)
SrUGT76G1	*E. coli* BL21(DE3)-derived Rosetta strain	Rebaudioside C	(Kim et al., 2019)
SrUGT76G1	*E. coli* BL21(DE3) pLysS	Rebaudioside A	(Madhav et al., 2013)

2.7 Sucrose synthase (SuSy) *(Glycine max)*

Figure 2.14 Glycine max (Fraw-doktor, 2016).

Due to expense of UDP-glucose, sucrose synthase (SuSy) has been applied to catalyze the reversible transfer of a glucosyl moiety between fructose and uridine diphosphate (UDP) (sucrose + NDP <-> UDP-Glc + fructose). *Glycine max* (Figure 2.14) is commonly called soybean and has many interesting enzymes that can be applied in production of glycosides. Of these, sucrose synthase is of interest in the synthesis of glycosides. The coupled enzymes system with sucrose synthase has been applied in many reports to produce glycosides, such as hyperoside (Pei et al., 2017), ginsenoside (Dai et al., 2018), and calycosin-7-O-β-D-glucoside (Hu et al., 2020). Based on pH values between 5.5 and 7.5, the reaction can be controlled to produce UDP-Glc. For UDP recycling, the concentration of UDP could be lower than 0.5 mM and UDP inhibited the reaction when it was higher than 4 mM (Schmölzer et al., 2016). Coupled UGT and SuSy for regeneration of UDP-Glc can maximize glycoside production by raising the acceptor concentration instead of a further reduction of UDP.

2.8 Fermentor

Figure 2.15 5 L fermentor and 50 L fermentor systems.

The fermentor (Figure 2.15) is a kind of equipment used for cell cultivation with probes and sensors to monitor cell cultivation conditions. Several parameters can be controlled in fermenters, such as the rate of rotation of stirring paddles which provides homogenization of the medium with cells and distributes heat and air for cells; the flow of compressed air into the chamber via the aerator, the use of a defoamer to prevent the formation of foam; and the pH, DO, and temperature which are monitored with probes to provide good conditions for cell growth. In the case of recombinant protein production such as in *E. coli*, the two periods that are used for the optimal generation of recombinant protein are when biomass is rapidly accumulated during the non-inducing period and when protein production is achieved during the inducing period. Nevertheless, a high cell density can frequently result in a number of serious issues, such as plasmid loss from *E. coli*, a large pH drops due to cell metabolites, and limited dissolved oxygen availability. These issues frequently lead to minimal or even no protein production while maintaining a high cell density (Sivashanmugam et al., 2009). Therefore, the cell density should be controlled to a level which is optimal for the protein expression period.

2.9 High Pressure Homogenizer or Microfluidics

To reduce particle size and enhance homogeneity, high-pressure homogenization (HPH) (Figure 2.16) is done with equipment that results in highly efficient generation of emulsions or suspensions. The principle of HPH is the application of high pressure to push sample fluids through a narrow gap over a very short distance. This machine can be applied in various areas, including nano-emulsions or suspensions, enzyme extraction. In a previous study, the HPH was used to breakdown the *E. coli* for enzyme extraction with conditions of 46 Mpa pressure, feed cell concentration of 100 g/L, and 10 homogenizer passes, resulting in a disruption efficiency of 99.5% (Kleinig et al., 1995). In the case of enzyme extraction, the disruption efficiency of HPH is based on pressure, cell concentration, and time of homogenizer passes (Middelberg, 2000). The advantages of HPH for enzyme extraction are its low temperature to reduce inactivation of enzymes, the ability to breakdown cell wall and reduce viscosity without the enzymes DNase and lysozyme to reduce the cost of extraction, and its ease in applying for large scale for enzymes in industry.

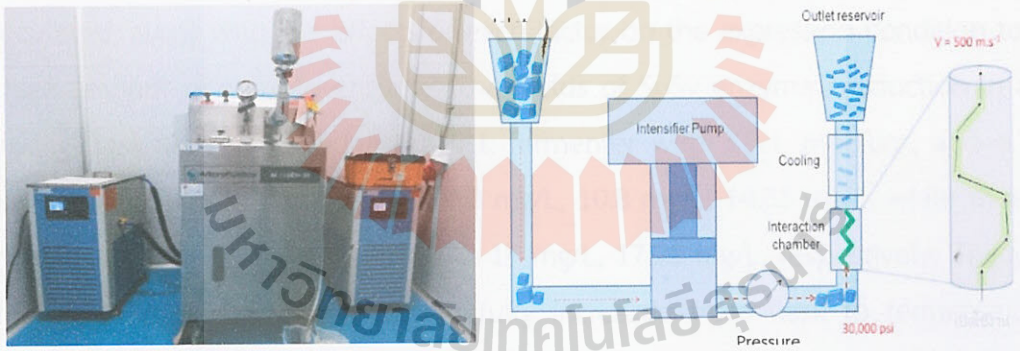

Figure 2.16 The high-pressure homogenizer.

CHAPTER III

SCREENING MEDIA AND SUITABLE EXPRESSION CONDITIONS FOR SUSY AND SrUGT76G1 ENZYMES PRODUCTION

3.1 Abstract

The objective of this chapter was to screen for an appropriate medium and suitable expression conditions for SuSy and SrUGT76G1 production in shaking flask, 5 L fermenter, and 50 L fermenter cultures. This would support for the preparation of enzymes for CBD glycoside production. After the good medium was identified, the box-Benhken design was used to optimize the suitable expression conditions for SuSy and SrUGT76G1 enzymes in terms of three factors, including temperature, lactose, and time. For this, the suitable expression conditions were successfully applied in the shaking flask, 5 L fermenter, and 50 L fermenter. In addition, the contour plots of the combined effects of temperature, time, and lactose were calculated, along with the effects of each factor on the expression condition to gain a high amount of soluble enzyme. The yields of SuSy enzyme production in a 2 L shaking flask with 1 L medium, a 5 L fermenter with 3.5 L medium, and a 50 L fermenter with 35 L medium were 7.3 mg/L, 10.8 mg/L, 14.85 mg/L, while those for SrUGT76G1 production were 14 mg/L, 15 mg/L, 17.25 mg/L, respectively. The yields of enzyme production were successfully increased from flask to fermenter. The specific activities of the enzymes were also not significantly different.

3.2 Introduction

Cannabis is a kind of plant that is a psychoactive drug used primarily for medical and recreational purposes. Cannabis contains over 400 compounds and 60 derivative cannabinoids (Ashton, 2001), such as cannabidiol (CBD) and tetrahydrocannabinol (THC). However, THC is the main psychoactive constituent of cannabis. On the other hand, the CBD is being developed as an influential drug for use in the modern medicine, including for treatment of schizophrenia, post-traumatic

stress disorder, anxiety, graft-versus- host disease, addiction, cancer and inflammatory bowel disease (Millar et al., 2020). In addition, CBD was also warranted by FDA (Food and Drug Administration) for adding to food, beverages and dietary supplements (Corroon et al., 2020). With many advantages of CBD, nevertheless, it has some problematic intrinsic features, such as low solubility in water, low bioavailability and changeable pharmacokinetic profiles (Millar et al., 2020). The solubility of CBD is low and that reduces its bioavailability and limits transmission to target cells. Several methods have been found to improve the hydrophobic property including encapsulation in liposomes, and nanoparticles, and drug glycosylation, etc. However, a traditional nano-drug carrier such as liposomes present a few disadvantages: poor stability, poor reproducibility, and low drug encapsulation efficiency (Idrees et al., 2020). In the current techniques, glycosylation is a good strategy to improve the solubility of CBD with carbohydrate moieties which gain more advantages for CBD glycoside. CBD glycosides acts as a prodrug that has many advantages including targeting due to the role of carbohydrate in cellular interactions, enhanced pharmacokinetics, and reduced toxicity and side effects. The SrUGT76G1 enzyme from *Stevia rebaudiana* has been used for the glycosylation of CBD using UDP-Glc as the glucosyl donor (Hardman et al., 2017). Sucrose synthase (SuSy) can facilitate this glycosylation because it, catalyzes release of fructose from sucrose and attachment of glucose to urindine diphosphate to synthesize uridine diphosphate glucose (UDP-Glc) (Stein and Granot, 2019) (Chen et al., 2020). Based on this characteristic of SuSy enzyme, the coupled enzymes reaction including SrUTG76G1 and SuSy can be applied to decrease the cost production of CBD glycosides by generating the UDP-Glc donor substrate in situ.

In this study, SrUGT76G1 and SuSy enzymes were produced from recombinant protein expression in *Escherichia coli* BL21(DE3) with pET32a(+) and pET30a(+) expression vectors, respectively. Media were screened to choose the best medium for expression of both enzymes. In addition, the suitable expression condition was evaluated by Box-Behnken design with three factors (lactose as inducer, temperature, and time), and five center points. The medium and expression condition was applied in shaking flask, 5 L fermenter, and 50 L fermenter cultures to produce SrUTG76G1 and SuSy for CBD glycoside production.

3.3 Materials and methods

3.3.1 Strains, chemicals

Cannabidiol was purified from Suranaree University of Technology (SUT) Cannabis farm AB Laboratory. UDP sodium salt was purchased from Nanjing Duly Biotech Co., Ltd (Nanjing, China). UDP-Glo™ Glycosyltransferase Assay was purchased from Promega (Madison, WI, USA). The Amicon® Ultra -15 Centrifugal filter 30K was acquired from Sigma-Millipore (Burlington, USA). IMAC Sepharose™ 6 fast flow was purchased from GE Healthcare (Cytiva, Chicago, Illinois, USA). A gene encoding *Glycine max* sucrose synthase (SuSy) optimized for expression in *E. coli* was synthesized by (Gene Universal Inc) and cloned in the ncoI and xhoI sites of pET30a(+). A synthetic gene of SrUGT76G1 was constructed by Twist company flanked by 5' NcoI and 3' XhoI sites and company linkers. All chemicals used in this study were of analytical grade.

3.3.2 Cloning, expression, and purification of SrUGT76G1 enzyme from recombinant protein in *E. coli* strain BL21(DE3)

3.3.2.1 Cloning of SrUGT76G1

The SrUGT76G1 encoding gene fragment obtained from Twist Bioscience company, was amplified by PCR with the forward 5' GGAGGTACTGTTTCAGGGTC 3' and reverse 5' ATTGGAACGATCTCGAGTCAC3' primers. *Pfu polymerase* was used to amplify the gene with the temperature cycling parameters shown in Table 3.1. The reaction contained 0.5 µL 1 ng/µL gene, 0.5 µL forward primer, 0.5 µL reverse primer, 0.5 µL 10 mM dNTP mix, 20 µL H_2O, 2.5 µL 10X PCR buffer, and 0.5 µL *Pfu* enzyme. The annealing temperature for PCR was screened to choose the temperature to scale up the reaction volume 10 times for cloning. Electrophoresis on a 1% agarose gel was used to check the PCR product band (1,465 bp). The SrUGT76G1 gene and both plasmids pET30a(+) and pET32a(+), were cut with the *NcoI* and *XhoI* restriction endonucleases (10,000 units/ml, 1 µl for gene, 1.5 µl for plasmid), in CutSmart™ buffer. The reactions were incubated at 37°C overnight. After that, agarose gel electrophoresis was used to evaluate the product. The target band was collected and then the DNA was extracted and purified with the GF-1 Ambiclean kit (PCR&Gel) according to the instructions of the manufacturer. The SrUGT76G1 gene was directly purified due to short band cutting. The DNA

concentration of the purified samples were measured by a Nanodrop spectrophotometer. Then, T4 ligase was used to ligate the linear gene DNA with the plasmids. The ligation mixtures were transformed into competent *E. coli XL-1 Blue* $CaCl_2$ treated cells by heat shock at 42°C for 45 seconds.

Table 3.1 PCR condition for amplification of SrUGT76G1.

Segment	Cycles	Temperature (°C)	Time (minute)
1	1	95	2
		95	0.5
2	30	55 or 60	0.5
		72	3.3
3	1	72	10

Cultivation on agar with LB broth and 50 µg/mL ampicillin was used to isolate the colonies. A single colony was picked up and cultured in LB medium with 50 µg/mL ampicillin for pET32a overnight and 30 µg/mL kanamycin for pET30a. The bacterial culture was collected and then the plasmid DNA was extracted by the alkaline lysis method. In the alkaline lysis procedure, the colony of *E. coli* cells containing the plasmid was collected and inoculated into 5 mL of LB broth with appropriate antibiotic and incubated at 37°C, 200 rpm, 16-18 hours. Subsequently, the cells pellet was obtained by centrifugation at 4720×g for 15 minutes. The pellet was re-suspended in 100 µl of lysis buffer I (50 mM glucose, 10 mM EDTA, 50 mM Tris-HCl, pH 8.0). Then, 200 µl of lysis buffer II (0.2 N NaOH, 1% (w/v) SDS) was added, and the tube was inverted 4 - 6 times and chilled on ice for 5 min. Finally, 150 µl of ice-cold lysis buffer III (3 M potassium acetate, pH 4.8) was added after that. The tube was mixed by inverting 4 - 6 times. It was incubated on ice for 5 minutes and the pellet was removed by centrifugation at 20,900×g for 10 minutes. The supernatant containing the plasmid was collected and transferred into a new tube and one volume of phenol: chloroform: iso-amyl alcohol (25:24:1) was supplemented into the tube and vortexed or shaken by hand thoroughly for approximately 20 seconds. The mixture solution was centrifuged at room temperature for 5 minutes at 20,900×g. The upper aqueous phase was carefully

removed into a fresh tube and precipitated with 2 volumes absolute ethanol for 10 minutes at 4°C. Centrifugation at 20,900×g for 10 min was used again to collect the precipitated DNA. The speed vacuum was used to remove left over ethanol. Then, the DNA was re-suspended in 100 µl TE buffer containing 2 µg RNase A and incubated at 37°C for 10 minutes. Then, 70 µl of ice-cold precipitation solution (20% PEG 6000, 2.5 M NaCl) was used to precipitate the RNase A-treated plasmids while then chilling on ice for 1 hour. After that, centrifugation at 20929×g for 10 minutes was done to obtain the precipitated DNA. The supernatant was removed and the pellet was washed by adding 0.5 ml of 70% ethanol and inverting the tube twice, after which the ethanol solution was removed and the tube dried by speed vacuum. Finally, the DNA was re-dissolved with 30 µl sterile water. And then, the absorbance of the plasmid DNA solution was determined and used to estimate the concentration and an aliquot was checked for the SrUGT76G1 gene by digestion with *NcoI* and *XhoI* restriction enzymes followed by agarose gel electrophoresis. Clones apparently containing the SrUGT76G1 gene were sent to sequence at Macrogen Company (Seoul, Korea).

3.3.2.2 Protein expression of E. coli BL21(DE3) and purification of SrUGT76G1

The recombinant pET30a(+), and pET32a(+) plasmids were transformed into *E. coli BL21(DE3)* as host cell and spread onto LB-agar containing 15 µg/ml kanamycin and 50 µg/ml ampicillin, respectively. The growing colonies were picked and inoculated into LB medium containing the appropriate antibiotics to make a starter culture. The expression culture of SrUGT76G1 was started by innoculating 1% final concentration of starter culture into the medium. It was cultured at 37°C with rotary shaking at 200 rpm. When the optical density at 600 (OD_{600}) of the culture reached 0.4 - 0.6, the protein expression was ready to induce. The IPTG (isopropyl β-D-thiogalactopyranoside) concentration was varied from 0 to 0.4 mM to obtain the optimum expression condition. When the IPTG was added into medium, the temperature was decreased to 20°C for 18 hours. The cells were collected by centrifugation at 4,720×g for 20 minutes at 4°C. The cell pellets were kept at -80°C for overnight. The cell pellets were melted on ice and then re-suspended in freshly preprared extraction buffer (20 mM phosphate buffer, pH 7.5,

0.200 µg/ml lysozymes, 1% Triton-X 100, 1 mM PMSF, 25 µg/ml DNase I and 0.1 mg/ml soy bean trypsin inhibitor). The re-suspended cells were incubated at room temperature for 30 minutes. Then, the soluble protein in supernatant was separated by centrifugation at 20,900×g for 15 min. Immobilized metal ion affinity chromatography (IMAC) was used to purify protein. After preparing the IMAC resin, the supernatant containing soluble protein was loaded on to the column. Then, the column was washed with 5 column volumes (CV) of equilibration/wash buffer (20 mM Phosphate buffer, pH 7.5, 150 mM NaCl), 10 CV of equilibration/wash buffer containing 5 mM imidazole or 10 mM imidazole to wash out the unbound protein. The bound protein was mostly eluted with 5 CV of elution buffer (20 mM phosphate buffer, pH 7.5, containing 500 mM imidazole). The activities of the enzyme after purification was checked with UDP-Glc and CBD. Samples of all steps were collected and checked for the appropriate size by SDS-PAGE (pellet, crude, flow through, EQ buffer, 5 or 10 mM imidazole, 500 mM imidazole). An ultracell-30K centrifugal filtration device was used to concentrate the protein at 3,940×g for 30 minutes. Then, 20 mM Tris-HCl, 150 mM NaCl, pH 7.5 buffer was used to wash 3 times. The protein was collected and diluted for measuring the absorbance at 280 nm with a nano-drop spectrophotometer.

3.3.2.3 Comparison SrUGT76G1 expression in pET30a(+) and pET32a(+)

The bacterial clones containing the SrUGT76G1 enzyme gene in pET30a(+) and pET32a(+) were tested for protein expression. The best clone was chosen to produce SrUGT76G1. The expression was checked expression with IPTG (0 mM, 0.2 mM, and 0.4 mM).

3.3.3 Expression and purification of *Glycine max* sucrose synthase (Susy) enzyme from recombinant protein in *E. coli* BL21(DE3)

The gene encoding *Glycine max* sucrose synthase (SuSy) optimized for expression in *E. coli* was synthesized and cloned in the *Nco*I and *Xho*I sites in pET30a(+) by Gene Universal Corp (Newark, DE, USA). *E. Coli* strain BL21(DE3) containing in pET30a/GmSuSy were obtained from JKC lab. The growing colonies were picked and inoculated into LB medium containing the appropriate antibiotics to make a starter culture. The expression culture of SuSy was started by innoculating 1%

final concentration of starter culture into the medium. It was cultured at 37°C with rotary shaking at 200 rpm. When the optical density at 600 (OD_{600}) of the culture reached 0.4 - 0.6, the protein expression was ready to induce. The IPTG (isopropyl β-D-thiogalactopyranoside) concentration used to induce expression was 0.2 mM to expression. When the IPTG was added into medium, the temperature was decreased to 20°C for 18 hours. The cells were collected by centrifugation at 4720×g for 20 minutes at 4°C. The cell pellets were kept at -80°C for overnight. For purification, the procedure was the same as that for SrUGT76G1 protein expression.

3.3.4 Screening media for expression of SuSy and SrUGT76G1 enzymes

Five media (FM, M9 modified, SOB, TB, and LB (Table 3.2)) were screened to investigate the best medium for both enzymes production. The experiment was designed in 500 mL flasks with 200 mL medium volume cultivation in triplicate (n = 3). LB broth was used as the starter culture medium and this culture was grown at 37°C overnight. A 1% feed of the starter culture was added to media and cultured 7 h at 37°C, with 200 rpm shaking. Then, 0.2 mM IPTG final concentration was added to the media except FM auto-induction medium. The cultures were cultured overnight at 20°C, with 200 rpm shaking. After that, the cells were collected by Hitachi CR22GIII centrifuge at 4720×g for 20 min. The cell pellets were kept in -30°C before extraction. The SuSy and SrUGT76G1 enzymes were purified by IMAC on a 1 mL cobalt-charged IMAC resin column according to the purification protocol described above. During the experiment, the parameters as OD_{600} final, weight of wet cells (WWC), amount of enzymes, and enzymes activities were determined. TotalLab TL120 software was used to measure the relative amounts of the SrUGT76G1 (69kD) and SuSy (97kD) bands on SDS-PAGE Gels loaded with 5 µg purified enzymes after one round of IMAC. The One-Way Anova Test was used to analyzed the results by using SPSS software.

Table 3.2 Initial composition of media for *E. coli* strain BL21(DE3) cultivation.

Substance	Unit	M9 modified (Sarkandy et al., 2010)	FM auto-induction (Duman-Özdamar et al., 2021)	SOB (Wang et al., 2011)	TB (Wang et al., 2011)	LB
Tryptone	g/L	-	10	20	12	-
Yeast extract	g/L	10	5	5	24	5
Peptone	g/L	-	-	-	-	10
Glycerol	mL	-	6	-	4	-
Glucose	g/L	10	1.5	3.6	-	-
NaCl	g/L	-	-	0.5	-	5
KH_2PO_4	g/L	7.5	6.8	-	2.31	-
K_2HPO_4	g/L	15	-	-	12.54	-
KCl	mM	-	-	2.5	-	-
$MgCl_2$	mM	-	-	10	-	-
$Na_2HPO_4.7H_2O$	g/L	-	10	-	-	-
$MgSO_4$	g/L	-	0.15	-	-	-
$(NH_4)_2SO_4$	g/L	2.5	3.3	-	-	-
$MgSO_4.7H_2O$	g/L	2	-	-	-	-
Citric acid	g/L	2	-	-	-	-
Lactose	g/L	-	20	-	-	-
Trace-element salts	mL	1	-	-	-	-

3.3.5 Investigating suitable expression conditions for SuSy and SrUGT76G1 enzymes

The experiment was done in 50 mL tubes with 10 mL culture medium and triplication (n = 3). The experiment was designed based on Box-Behnken Design and run with 17 runs (Table 3.3). The response was the amount of enzymes (relative density of bands in SDS-PAGE) per 5 µg total protein each supernatant. That was based on the results of TotalLab TL120 software of 5 µg protein from each supernatant run in SDS-PAGE results. Besides that, the protein concentrations of each extract were determined by Bio-rad assay.

3.3.6 Application of medium and suitable expression condition in 2 L flask, 5 L fermenter, and 50 L fermenter for enzymes production

The medium, which was the best medium from media screening experiments for each enzyme, was used as medium for that enzyme is production. The antibiotics 50 µg/mL ampicillin and 30 µg/mL kanamycin were used for pET32a(+) SrUGT76G1 and pET30a(+) SuSy, respectively. A 1% volume of LB broth feed starter culture was grown at on 37°C, with 200 rpm shaking for 16 h and then transferred to the fermenter. After that, the cells were cultured at 37°C with 200 rpm to reach OD_{600} to 1 and then expression was induced according to the best condition of the expression of the expression condition experiment. The air flow was controlled around 2 to 5 vvm. The sample was collected to determine OD, pH, DO% (only in 5 L fermenter), and sample collection for SDS-PAGE checking enzyme expression. And then, the cells were collected by Hitachi CR22GIII centrifuge at 4720xg for 20 min. Enzyme purification was done by the procedure described above.

Table 3.3 Box-Behnken design to identify suitable expression conditionsl.

Run	Factor 1 A: Temperature (°C)	Factor 2 B: Lactose (g/L)	Factor 3 C: Time (h)	Response Enzymes (μg/5 μg)			
				SuSy		SrUGT76G1	
				Experimental	Predicted	Experimental	Predicted
1	28.5	20	24	0.306	0.299	0.452	0.456
2	37	10	4	0.193	0.219	0.237	0.254
3	37	0	14	0.044	0.011	0.141	0.128
4	28.5	10	14	0.391	0.422	0.415	0.483
5	28.5	10	14	0.436	0.422	0.463	0.483
6	20	0	14	0.086	0.089	0.184	0.186
7	28.5	10	14	0.433	0.422	0.470	0.483
8	37	20	14	0.089	0.086	0.245	0.243
9	28.5	20	4	0.242	0.219	0.272	0.257
10	20	20	14	0.292	0.325	0.522	0.535
11	28.5	0	24	0.109	0.132	0.153	0.168
12	37	10	24	0.069	0.077	0.213	0.210
13	28.5	10	14	0.438	0.422	0.517	0.483
14	28.5	0	4	0.068	0.075	0.087	0.082
15	20	10	4	0.177	0.167	0.240	0.242
16	28.5	10	14	0.411	0.422	0.551	0.483
17	20	10	24	0.481	0.447	0.589	0.572

3.3.7 Enzymes activity assay

DNS assay for SuSy enzyme

The SuSy reaction was set up with 20 mM sucrose, 2 mM UDP, 8 mM $MgCl_2$, 50 mM potassium phosphate buffer pH 7.2, and 30 µg/ 50 µL reaction. The reaction was incubated in 37°C for 18 hours. To a 50 µL reaction, 50 µL DNS reagent was added and the mixture was boiled in boiling water for 5 min. After that, the centrifuge was used to centrifuge the samples at 10,625×g for 10 min. Then, 90 µL sample was mixed with 360 µL water. Two hundred microliters of the mixture were taken to measure the absorbance at 540 nm. The A_{540} values was used to analysis specific enzyme activity A_{540} /slope/mg Susy/min. The slope was 0.0012 from a fructose standard curve (0 µM, 12.5 µM, 25 µM, 50 µM, 75 µM, 100 µM, 125 µM, 150 µM, 175 µM, 200 µM, 225 µM, and 250 µM concentrations) (Figure 3.1). The blank was the reaction without enzyme.

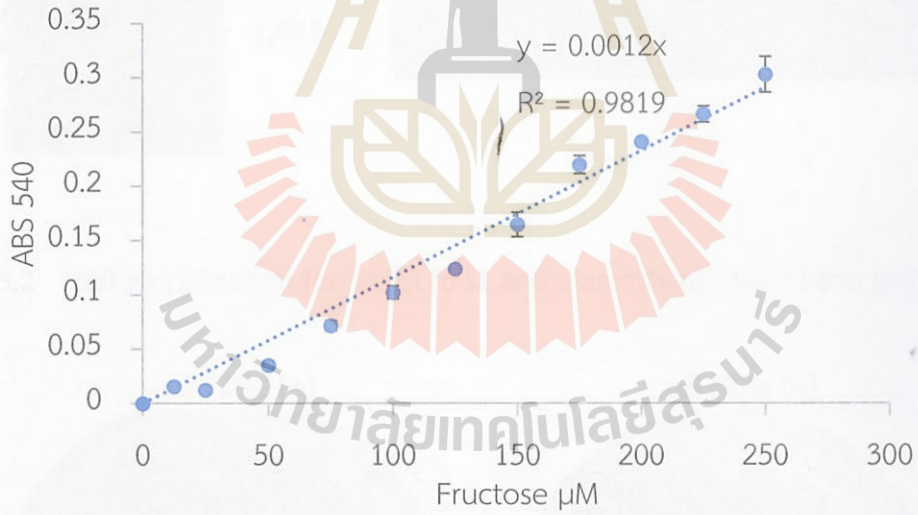

Figure 3.1 Fructose standard of DNS assay with SuSy enzyme.

UDP-Glo™ glycosyltransferase assay for SrUGT76G1 enzyme

The UDP-Glo™ glycosyltransferase Assay Kit from Promega company was used. SrUGT76G1 (5 µg /25 µL reaction) in 50 mM potassium phosphate buffer pH 7.2, 1 mM UDP-Glc, 9 mM $MgCl_2$, 1 mM CBD. The reaction was incubated at room temperature for 20 min. To the 25µL reaction, was added 25 µL reagent kit and it was

incubated at room temperature for 1 hour and after that the luminescence signals were measured by using a Varioskan™ LUX multimode microplate reader (Thermo Scientific, USA).

3.4 Results and discussion

3.4.1 Cloning, expression, and purification of SrUGT76G1 enzyme from recombinant protein in *E. coli* BL21(DE3)

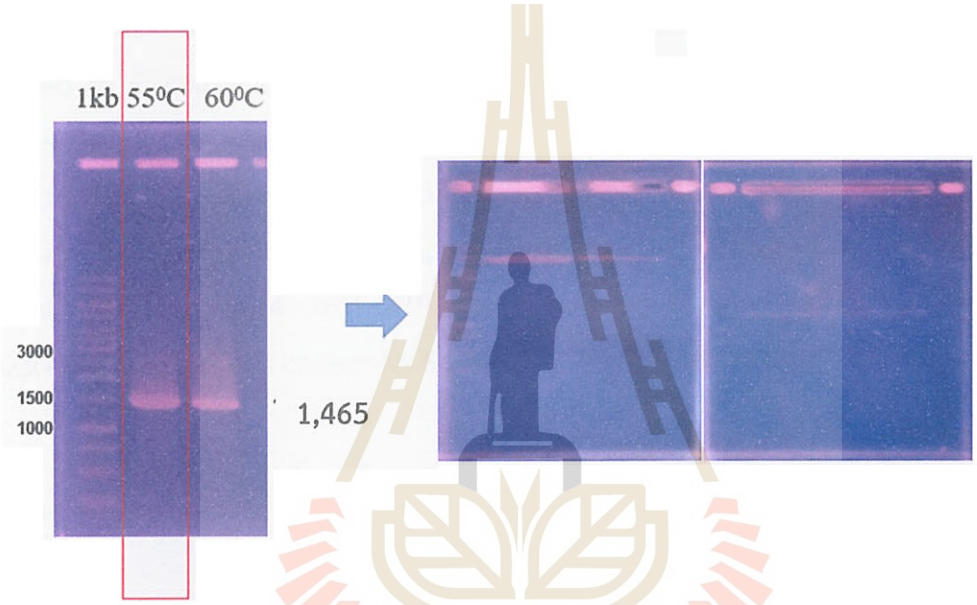

Figure 3.2 PCR amplification for SrUGT76G1 and plasmids pET30a(+) and pET32a(+).

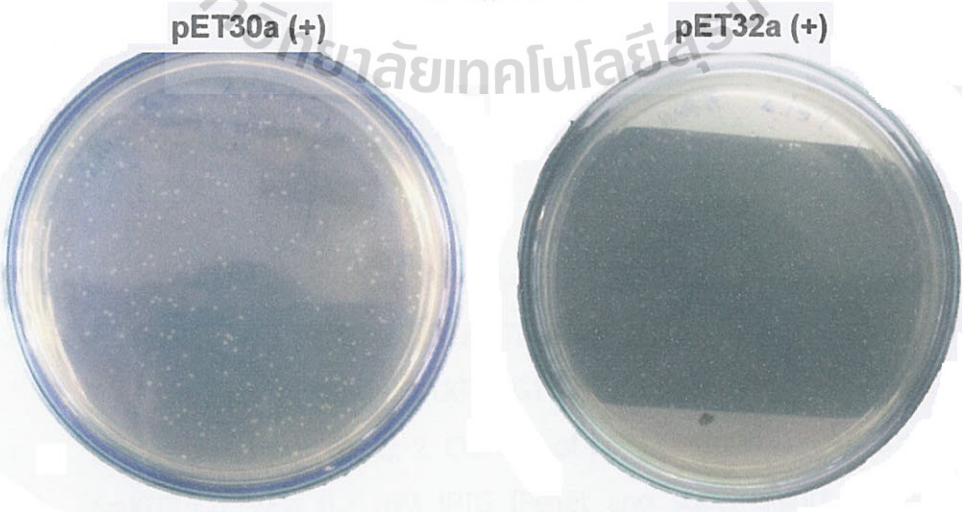

Figure 3.3 Colonies of SrUGT76G1 enzyme in XL1 blue competent cells.

The PCR condition for amplifying the SrUGT76G1 gene was successfully determined and had an annealing temperature of 55°C (Figure 3.2). So this was used in a scale of 250µL (Figure 3.2). After purification by PCR clean-up kit, the SrUGT76G1, 1000ng DNA was obtained. The gene and the plasmids were cut again with the restriction enzymes *NcoI* and *XhoI*. After being cut by restriction enzymes, the PCR clean-up kit was used for purification. And then, the T4 ligase was used to ligate plasmids and genes at 17° C overnight. The cloning was transferred to NEB5α and XL1-Blue competent cells. The six colonies (Figure 3.3) were picked and cultured overnight and plasmids extracted to check the insert again. The insert was checked by sequencing and the correct plasmid was transferred to *E. coli* BL21(DE3) as a host cell for enzyme production. One clone of pET32a(+) and pET30a(+) were chosen to vary the IPTG. From Figure 3.4, the results indicated that the clone of pET32a(+)/SrUGT76G1 had higher expression than pET30a(+)/SrUGT76G1 at 0.2 mM IPTG, and the amount of protein upon induction with 0.2 mM IPTG and 0.4 mM IPTG was not significantly different. Therefore, pET32a(+)/SrUGT67G1 was chosen for SrUGT76G1 enzyme production.

Figure 3.4 The SDS-PAGE analysis when varying the IPTG for induction of SrUGT76G1 expression from pET32a(+)/SrUGT76G1 and pET30a(+)/SrUGT76G1. (M. Marker; 1. Clone 1 of pET32a(+)/SrUGT76G1 or pET30a(+)/SrUGT76G1 without IPTG (Pellet and supernatant); 2. Clone 1 of pET32a(+)/SrUGT76G1 or pET30a(+)/ SrUGT76G1 with 0.2 mM IPTG (Pellet and supernatant); 3. Clone 1 of pET32a(+)/SrUGT76G1 or pET30a(+)/ SrUGT76G1 with 0.4 mM IPTG (Pellet

and supernatant); 4. Clone 2 of pET32a(+)/SrUGT76G1 or pET30a(+)/ SrUGT76G1 with without IPTG (Pellet and supernatant); 5. Clone 2 of pET32a(+)/SrUGT76G1 or pET30a(+)/ SrUGT76G1 with 0.2 mM IPTG (Pellet and supernatant); 6. Clone 2 of pET32a(+)/SrUGT76G1 or pET30a(+)/ SrUGT76G1 with 0.4 mM IPTG (Pellet and supernatant)) and (M-Marker, P-Pellet, S-Supernatant).

The pET32a(+)/SrUGT76G1 enzyme was produced using three litters of culture and purified by IMAC resin-CO^{2+}. The results showed that 250 mM imidazole did not elute all the protein (Figure 3.5). Therefore, 500 mM imidazole was used to elute SrUGT76G1 and the 250 mM imidazole step was eliminated. From 3 L culture, the purification yielded 9.9 mg/L SrUGT76G1 protein. With the objective of reducing the cost of enzyme production, lactose was tried as an inducer in place of IPTG. Therefore, the screening media and suitable expression conditions were investigated in the next experiment.

Figure 3.5 The SDS-PAGE of SrUGT76G1 purification after of IPTG for induction of expression and IMAC with $CoCl_2$ for purification. (1. Marker; 2. Pellet; 3. Supernatant; 4. Flow through of supernatant; 5. EQ buffer wash; 6. 5 mM imidazole wash; 7. 10 mM imidazole wash; 8. 250 mM imidazole elution; 9. 500 mM imidazole elution).

3.4.2 Purification of Sucrose synthase (SuSy) enzyme from recombinant expression in *E. coli* strain BL21(DE3) with IPTG induction.

The Sucrose synthase enzyme was produced using four litters of culture. Up purification by IMAC, 250 mM imidazole did not elute all the protein (Figure 3.6). Therefore, 500 mM imidazole was used to elute SuSy and the 250 mM imidazole step was eliminated. From 4 L culture, the expression and purification yielded 3.75 mg/L SuSy protein. With the objective of reducing the cost of enzyme production, lactose was considered as an inducer in place of IPTG. Therefore, the screening media and suitable expression condition were investigated in the next experiment.

Figure 3.6 The SDS-PAGE of SuSy purification after of IPTG for induction of expression and IMAC with $CoCl_2$ for purification. (1. Marker; 2. Pellet; 3. Supernatant; 4 - Flow through of supernatant; 5. EQ buffer wash; 6. 5 mM imidazole wash; 7. 10 mM imidazole wash; 8. 250 mM imidazole elution; 9. 500 mM imidazole elution).

3.4.3 Screening media for enzymes production

Five media, including LB, TB, SOB, FM auto-induction, and modified M9 were used to screen the medium for SrUGT76G1 and SuSy enzyme production. Depending gene, expression plasmid, host cell, protein expression is different with different medium (Table 3.4). For example, interleukin-2 was expressed from pET21a

in *E. coli* BL21(DE3) in modified M9 medium (Sarkandy et al., 2010). When compared to the TB medium, the LB medium can occasionally produce higher enzyme expression, according to one study (Tripathi, 2016). In this experiment, according to the SDS-PAGE analysis of the pellet and supernatant (Figure 3.7 and Figure 3.8), the enzymes can express in LB, TB, and FM, and were expressed in lower amounts in SOB, and M9 modified media. For SOB medium, its viscosity (20 g/L tryptone) may be higher than the other media, which may lead to the dissolved oxygen being quite lower than in the other media (no data show). Therefore, SOB and M9 modified media were rejected to use as medium for production of the enzymes. In addition, Table 3.5 and Table 3.6 clearly showed the properties of enzymes in different media. The highest levels of SDS-PAGE band intensities and enzymes activities were recorded in LB medium. Higher numbers of culturable cells were abtained in all media containing simple carbon sources (glycerol or glucose) such as FM auto-medium, TB, modified M9, compared to LB medium. However, the higher protein expression was found in LB broth media. Yeast extract and tryptone, which are found in complex media like TB, LB, and FM auto-induction, are known to provide biosynthesis precursors, such as vitamins and amino acids that enhance protein production in *E. coli* (Kweon et al., 2001) (Goyal et al., 2009). Additionally, the cellular stress during the synthesis of recombinant proteins may be decreased by yeast extract (Yoon et al., 1994). Goyal et al. discovered that a synthetic medium comprising yeast extract and tryptone increased streptokinase protein content in *E. coli* without increasing cell density, which is similar to what was seen in the current work using LB. Therefore, inthis experiment, the LB broth medium was the best medium for SuSy and SrUGT76G1 enzyme production compared with TB, SOB, FM auto-induction, and M9 modified. In previous studies, FM auto-induction medium was successfully used for high enzyme expression (Ashton, 2001) (Chen et al., 2020) but, in our case, the activity recovered from FM-auto induction medium expression is really lower than from expression in LB broth. Therefore, FM auto-industion medium was not considered to use for SuSy and SrUGT76G1 enzyme production. However, in FM auto-induction medium, the enzymes can be expressed with lactose induction condition. This suggested the idea for investigation of the suitable expression condition with lactose as an inducer in place of IPTG.

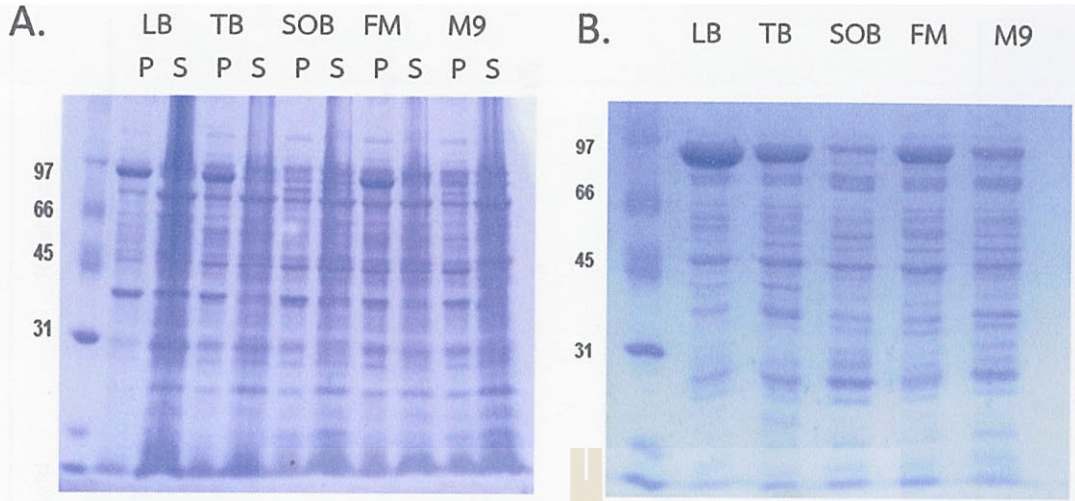

Figure 3.7 SDS-PAGE of pellet and supernatant after cell lysis and 5 µg protein after first IMAC from SuSy expression in different media.

Figure 3.8 SDS-PAGE of pellet and supernatant after cell lysis and 5 µg protein after first IMAC from SrUGT76G1 expression in different media.

Table 3.4 Recently published recombinant protein production in *E. coli*.

Enzymes	Vector	Medium	Expression condition	Purification	Yield (mg/L)	References
GmSuSy-*Glycine max*	pET-STRP3	LB	25°C, OD 0.8-1.0, 0.5 mM IPTG, overnight	Cooled French press,100 bar IMAC 3 ml resin	12	(Kulmer et al., 2017)
GmSUS-*Glycine max*	pACYCDuet-GmSUS	LB	20°C, OD 0.7, 0.1 mM IPTG, 20h	French press 3 times IMAC	-	(Dai et al., 2018)
GmSuSy-*Glycine max*	pXUN-SS	TB	25°C, OD ≈ 0.8, 0.1 mM IPTG, overnight	HIC, AEX	11.6 (22.7)	(Schmölzer et al., 2016)(Zhang et al., 1999)
GmSuSy-*Glycine max*	pET-STRP3-GmSuSy	LB	25°C, OD ≈ 0.8-1, 0.2 mM IPTG ,overnight	Cooled French press at 100bar Affinity (strep-Tactin®)	12	(Schmölzer et al., 2016)(Bungaruang et al., 2013)
GmSuSy-*Glycine max*	pET30a(+)GmSuSy	LB	27°C, OD ≈ 1, 12 g/L lactose, 16h	Lysozyme extraction IMAC-Co-charged resin	14.14	In this study
UGT76G1-*Stevia rebaudiana*	pRSFDuet-1-UGT76G1	LB	20°C, OD ≈ 0.6-0.8, 0.1 mM IPTG, 36h	Ultrasonic Cell Disruptor IMAC-Ni-charged resin	-	(Yu et al., 2022)

Table 3.4 Recently published recombinant protein production in *E. coli* (Continued).

Enzymes	Vector	Medium	Expression condition	Purification	Yield (mg/L)	References
UGT76G1- Stevia rebaudiana	*E. coli* BL21(DE3) M/P-3-S32U-Stm3-UGT76G1 (Co-expression with *malK* and *prpD* gene)	LB – flask synthetic medium-fed-batch	25°C, OD ≈ 0.6-0.8, 0.01 mM IPTG, 24 h	Ultrasonication at 50 Hz for 5 min and IMAC-Ni-charged resin	1.97 –flask 61.6 mg/L/h –fed-batch	(Shu et al., 2020)
UGT76G1- Stevia rebaudiana	pET28a-CysQ-UGT, pET28a-EDA-UGT and pET28a-NusA-UGT	LB	30°C, OD ≈ 0.5-0.6, 0.5 mM IPTG, 16 h	Sonifier and IMAC-Ni-charged resin	Increase 40% soluble	(Chen et al., 2017)
Glucose isomerase-*Actinoplanes missouriensis CICIM B0118(A)*	pET-28a-xylA118	10.0 g/L NaCl, 5.0 g/L yeast extract, 10.0 g/L tryptone, 1.8 g/L xylose, 0.25 g/L glucose, and 180 μM $CoCl_2$-$6H_2O$	30°C, OD ≈ 0.8, 0.6 mM IPTG, 10 h	Sonicate and IMAC-Ni-charged resin	31.62	(Wang et al., 2011)
Interleukin-2	pET21a-hil2	M9 modified + Amino acid solutions	IPTG		81 to 195-flask, 403 to 594 fermenter and 5.15 to 10.01 fed-batch	(Sarkandy et al., 2010)

Table 3.4 Recently published recombinant protein production in *E. coli* (Continued).

Enzymes	Vector	Medium	Expression condition	Purification	Yield (mg/L)	References
Lysostaphin-Staphylococcus simulans	pBADLys – *E. coli* Top 10	yeast extract 5 g/L, tryptone 10 g/L, $Na_2HPO_4 \cdot 7H_2O$ 7.10 g/L, KH_2PO_4 6.8 g/L, $MgSO_4$ 0.15 g/L, $(NH_4)_2SO_4$ 3.3 g/L, glucose 0.5 g/L) with 0.1% (v/v) filter-sterilized arabinose solution	30°C, 48 h, 0.1% (v/v) filter-sterilized arabinose solution	Lysozyme + sonicator and cation exchange chromatography	184	(Duman-Özdamar et al., 2021)
SrUGT76G1 *(Stevia rebaudiana)*	pET32a (+) in *E. coli* BL21(DE3)	LB	0.2 mM IPTG at 20°C for overnight	Lysozyme extraction IMAC with $CoCl_2$	9.9	In this study
SrUGT76G1 *(Stevia rebaudiana)*	pET32a (+) in *E. coli* BL21(DE3)	LB	14 g/L lactose at 20°C for 22 h	Lysozyme extraction IMAC with $CoCl_2$	17.37	In this study
GmSuSy- Glycine max	pET30a (+) GmSuSy in *E. coli* BL21(DE3)	LB	0.2 mM IPTG at 20°C for overnight	Lysozyme extraction IMAC-Co-charged resin	3.73	

Table 3.5 Parameters of media screening for SuSy production.

Media	OD final, (OD600)	WWC, (g)	Enzyme, (mg)	Specific activity (A540/slope/mg enzyme/ min)
LB	$2.30^{a} \pm 0.097$	$0.86^{a} \pm 0.061$	$0.673^{d} \pm 0.023$	$3.086^{d} \pm 0.025$
TB	$6.64^{d} \pm 0.293$	$1.57^{c} \pm 0.217$	$0.627^{c} \pm 0.016$	$2.580^{c} \pm 0.119$
SOB	$3.58^{b} \pm 0.269$	$1.06^{ab} \pm 0.021$	$0.047^{a} \pm 0.007$	$0.034^{a} \pm 0.029$
FM-auto	$7.31^{e} \pm 0.074$	$1.29^{bc} \pm 0.170$	$0.277^{b} \pm 0.015$	$1.603^{c} \pm 0.029$
M9 modified	$4.53^{c} \pm 0.323$	$1.60^{c} \pm 0.091$	$0.128^{b} \pm 0.015$	$0.214^{b} \pm 0.083$

All values were presented as the mean ± SD (n=3), ^{a,b,c,d,e} means in the same column sharing different superscripts are significantly different ($P<0.05$) as determined by Turkey's range test. LB (Lysogeny Broth), SOB (Super Optimal Broth), TB (Terrific Broth), M9 modified (M9 minimal medium modified), and FM (For medium auto-induction).

Table 3.6 Parameters of media screening for SrUGT76G1 production.

Media	OD final, (OD600)	WWC, (g)	Enzyme, (mg)	Specific activity (μM UDP/mg enzyme/ min)
LB	$2.85^{a} \pm 0.12$	$0.787^{a} \pm 0.015$	$1.001^{c} \pm 0.054$	$19.2^{d} \pm 1.5$
TB	$5.30^{c} \pm 0.2$	$1.230^{b} \pm 0.070$	$0.605^{b} \pm 0.012$	$16.2^{c} \pm 1.7$
SOB	$2.538^{a} \pm 0.018$	$0.950^{a} \pm 0.061$	$0.181^{a} \pm 0.031$	$4.34^{b} \pm 0.46$
FM	$6.31^{d} \pm 0.33$	$1.37^{b} \pm 0.056$	$0.621^{b} \pm 0.019$	$1.88^{b} \pm 0.57$
M9	$4.29^{b} \pm 0.2$	$1.59^{c} \pm 0.86$	$0.197^{a} \pm 0.024$	ND^{a}

All values were presented as the mean ± SD (n=3), ^{a,b,c,d} means in the same column sharing different superscripts are significantly different ($P<0.05$) as determined by Turkey's range test. LB (Lysogeny Broth), SOB (Super Optimal Broth), TB (Terrific Broth), M9 modified (M9 minimal medium modified), and FM (For medium auto-induction).

3.4.4 Suitable expression conditions for production of SuSy and SrUGT76G1 enzymes

The discovery that lactose can be used for both enzymes expression came through screening media. Additionally, utilizing lactose as an inducer for protein expression has a number of advantages over IPTG, such as a hundredfold reduced cost, an impressive industrial advantage, non-toxicity (IPTG is toxic to cell growth (Lu et al., 2021)), and a higher efficiency for expressing the target proteins (Rosano and Ceccarelli, 2014). Lactose cannot penetrate the bacterial body. to be carried into the host bacterium, it needs the assistance of a unique enzyme known as primase. To initiate the T7 Lac promotor, galactosidase must convert the lactose present in the bacterial cell into allolactose. Therefore, lactose's inducing characteristics, such as dosage, temperature, time, and original bacterial concentration, must be clarified if it is used as an effective inducer. In order to produce SrUGT76G1 and SuSy, the high enzyme expression condition was optimized in order to determine the ideal values of three independent variables (temperature, lactose, and expression time). With the results from each experimental run being described in the design matrix, RSM based on the use of Box-Behnken design was carried out. According to the Table 3.3, experimental runs 4,5,7,13,16,17 for SuSy and 1,4,5,7,10,13,16,17 for SrUGT76G1 demonstrated high expression, with values ranging from 0.415 to 0.589 µg/ 5 µg total protein for SuSy and 0.391 to 0.481 µg/ 5 µg total protein SrUGT76G1, respectively. The results were showing close similarity with the predicted results.

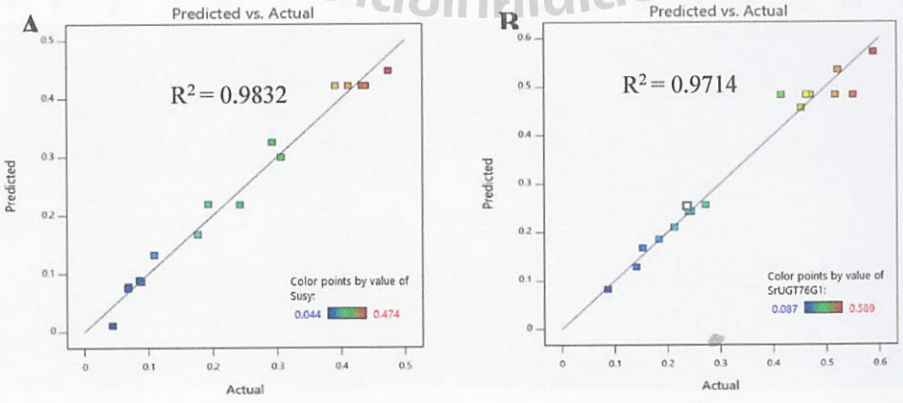

Figure 3.9 Plot indicating the predicted values against experimental values for enzymes expression of SuSy (A) and SrUGT76G1 (B).

The second order-model equation was fitted to the independent variables, and the goodness of fit was assessed. The applied equation's anticipated optimal values and the experimental amount of protein expression per 5 µg of total protein in the cell lysate supernatant were used to validate model's relevance. The derived regression equation showed that SrUGT76G1 and SuSy had a R^2 value of 0.9714 and 0.9832, respectively (more than 0.75 shows that suitability of the model) (Figure 3.9). It demonstrated that theoretical values as predicted by the models suited the experimental data well and ensured a suitable adjustment of the quadratic model to the experimental data (Figure 3.9). The SDS-PAGE of protein expression per 5µg of total protein after lysis cells showed in Figure 3.10 and 3.11.

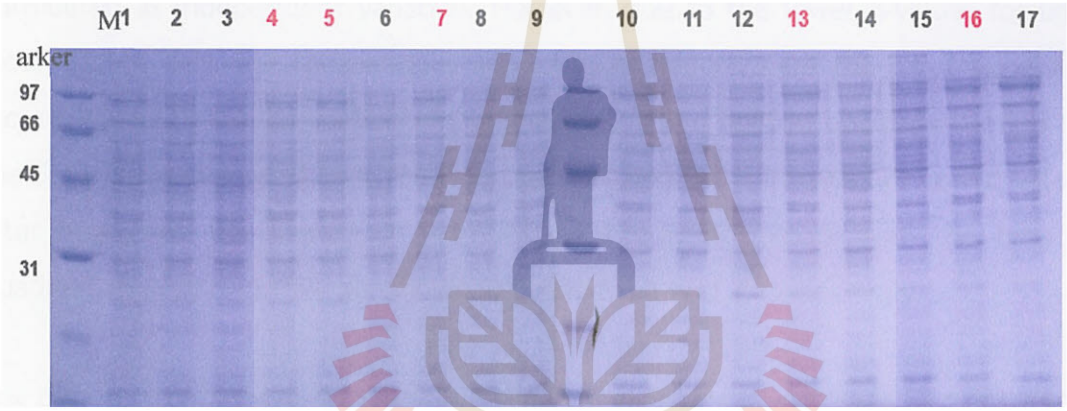

Figure 3.10 SDS-PAGE of 5 µg SuSy from 17 runs (Table 3.3) of RSM experiment.

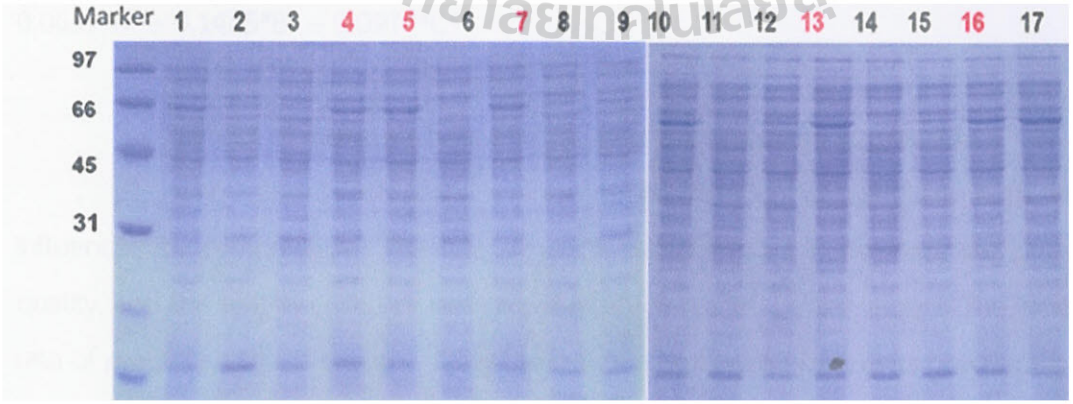

Figure 3.11 SDS-PAGE of 5 µg SrUGT76G1 from 17 runs (Table 3.3) of RSM experiment.

Table 3.7 presents the findings of the second order response surface model as an analysis of variance (ANOVA). The significance of the regression is shown by Fisher's F- test and p-values. The F computer higher than F table and ANOVA tables show the overall significant effect of interaction terms on enzyme expression at the 5% level of significance ($p < 0.05$). Low pure errors for SuSy expression (0.0017) and SrUGT76G1 expression (0.0110) suggest that the experimental data are well reproducible. The model is significant, as shown by the F-values for SrUGT76G1 expression (26.45) and SuSy expression (45.48). The likelihood of the model F-value being this high due to noise in the expression of both enzymes is 0.01% at most.

According to the calculated parameters and the accompanying p-values, all the factors had significant effects on the expression of both SuSy and SrUGT76G1 when considered as independent variables. However, due to the lower p-values for time factor (Table 3.7), the temperature and lactose inducer were the most significant factors impacting the expression of the enzymes. The simplified quadratic models for the SuSy expression and SrUGT76G1 expression were built in terms of coded values after neglecting the impact of unimportant interacting factors from the broader quadratic model, and they are shown in Equations 1 and 2, respectively.

$$Y = 0.4218 - 0.0793*A + 0.0778*B + 0.0348*C - 0.0403*AB - 0.1053AC + 0.0058*BC - 0.1235*A^2 - 0.1705*B^2 - 0.07*C^2 \quad (1)$$

$$Y = 0.4832 - 0.0874*A + 0.1158*B + 0.0714*C - 0.0585*AB - 0.0933*AC + 0.0285*BC - 0.0657*A^2 - 0.1445*B^2 - 0.0977*C^2 \quad (2)$$

Effect of temperature and lactose on enzymes expression

The creation of proteins and the proliferation of cells are both greatly influenced by temperature. The rate at which substrates are consumed, the product's quality, and the length of the process are similarly impacted by this aspect. The increased rate of protein synthesis brought on by the use of a prokaryotic host at its optimum growth temperature may not allow enough time for proper protein folding (Rezaei et al., 2020). To enhance folding and solubility during the expression, temperature from 20 to 37 degrees Celsius were screened to identify the good condition for each protein (SrUGT76G1 and

SuSy). Besides that, to assess the gene expression system's sensitivity to variations in inducer level, the amount of lactose added for induction was screened. Rising lactose concentrations led to an increase in the amount of recovered recombinant protein, however at high concentration of lactose, for instance at over 0.8 mM lactose, the system was fully active, indicating that the protein expression was constant (Menzella et al., 2003). In other study, the optimal lactose dosage used for pET32a-hpaA-*E.coli* BL21 expression was 50 g/L; pET32a-ureB-E.coli BL21, pET32a-LTKA63-E.coli BL21 and pET32a-LTB-E.coli BL21 expression were 100 g/L. Therefore, the testing experiment of lactose as inducer was done with a range 0g/L to 20g/L for pET32a(+)/SrUGT76G1 and pET30a(+)/SuSy expression (data not show). That is a reason the lactose was investigated at 0 to 20 g/L culture for SuSy and SrUGT76G1 enzymes expression. From the contour of its RSM (Figure 3.12 and 3.13), the expression of SuSy can get high expression with higher temperature more than SrUGT76G1. Additional, the amount of lactose 10 to 15 g/L and 12 to 20 g/L can gain high expression for SuSy, and SrUGT76G1, respectively.

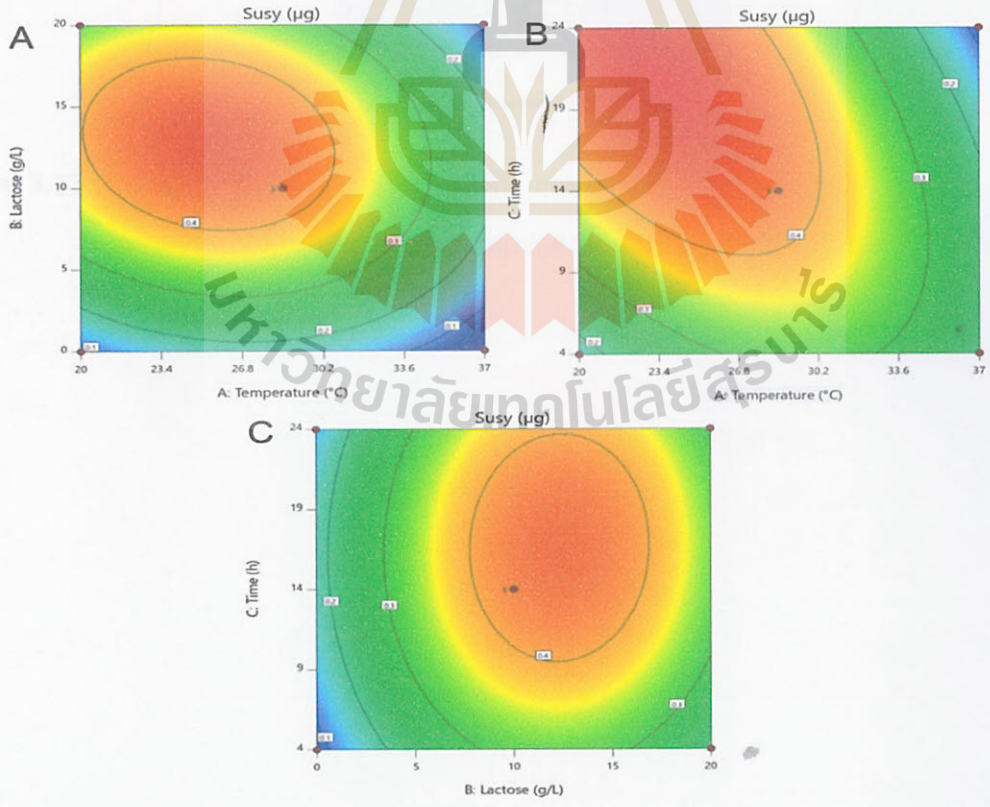

Figure 3.12 Contour plots of SuSy combined effects of A. lactose and temperature, B. Time and temperature, C. Time and lactose.

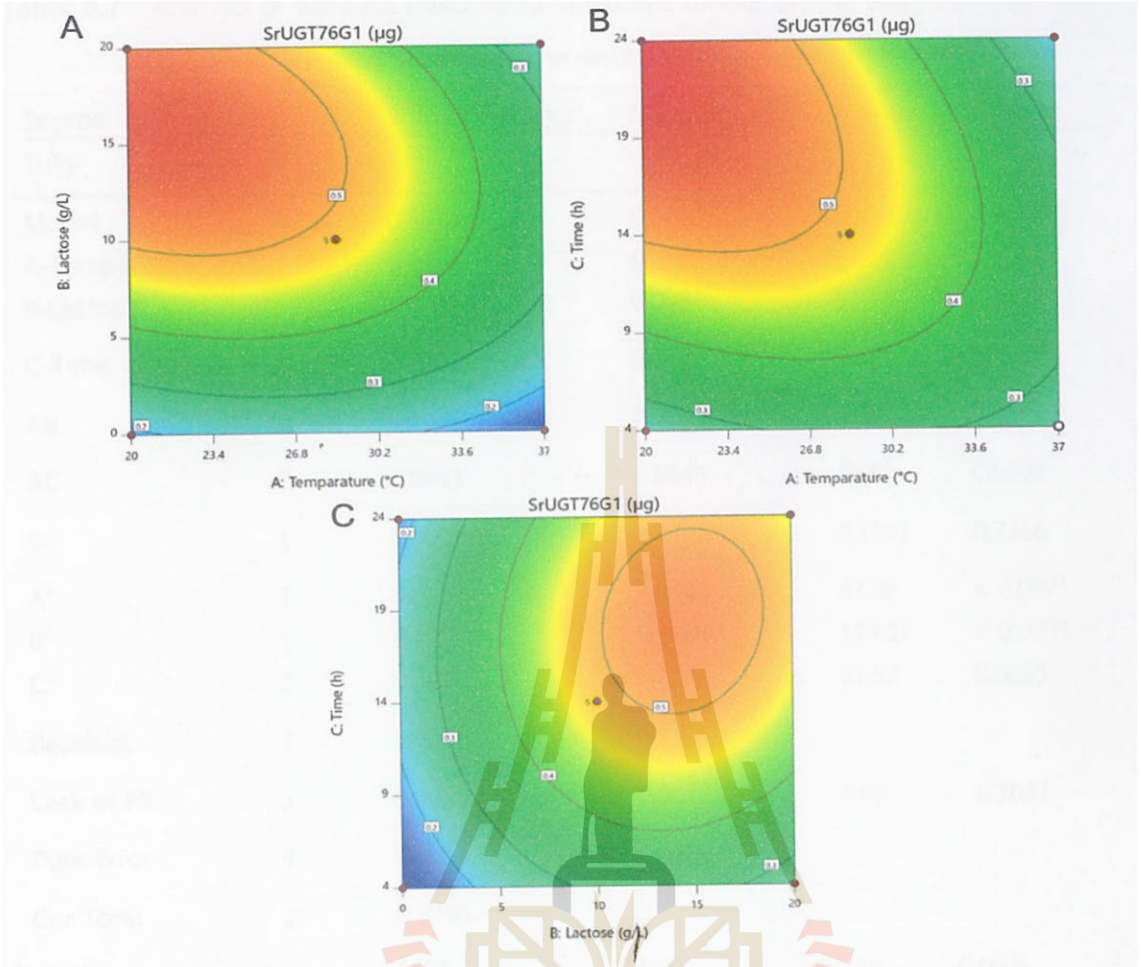

Figure 3.13 Contour plots of SrUGT76G1 combined effects of A. lactose and temperature, B. Time and temperature, C. Time and lactose.

Table 3.7 Analysis of variance (ANOVA) for quadratic model on the enzymes expression of SrUGT76G1 and SuSy from the results of Box-Behnken design.

Source	DF	Sum of Squares	Mean Square	F-value	*p-value*
SuSy					
Model	9	0.3873	0.0430	45.48	< 0.0001
A-Temperature	1	0.0502	0.0502	53.09	0.0002
B-Lactose	1	0.0484	0.0484	51.10	0.0002
C-Time	1	0.0097	0.0097	10.21	0.0152
AB	1	0.0065	0.0065	6.85	0.0346
AC	1	0.0443	0.0443	46.82	0.0002
BC	1	0.0001	0.0001	0.1397	0.7196
A^2	1	0.0642	0.0642	67.88	< 0.0001
B^2	1	0.1224	0.1224	129.37	< 0.0001
C^2	1	0.0206	0.0206	21.82	0.0023
Residual	7	0.0066	0.0009		
Lack of Fit	3	0.0050	0.0017	4.00	0.1067
Pure Error	4	0.0017	0.0004		
Cor Total	16	0.3940			
Model	9	0.4220	0.0469	26.45	0.0001
A-Temperature	1	0.0611	0.0611	34.45	0.0006
B-Lactose	1	0.1072	0.1072	60.47	0.0001
C-Time	1	0.0408	0.0408	22.99	0.0020
AB	1	0.0137	0.0137	7.72	0.0273
AC	1	0.0348	0.0348	19.62	0.0030
BC	1	0.0032	0.0032	1.83	0.2179
A^2	1	0.0182	0.0182	10.26	0.0150
B^2	1	0.0879	0.0879	49.58	0.0002
C^2	1	0.0402	0.0402	22.68	0.0021
Residual	7	0.0124	0.0018		
Lack of Fit	3	0.0014	0.0005	0.1745	0.9084
Pure Error	4	0.0110	0.0027		
Cor Total	16	0.4344			

Effect of time and lactose to enzymes expression

Lactose is an inducer for protein expression, however, doges of lactose could be based on gene, expression plasmid, protein expression, expression condition and host cell; for example, *E. coli* strain MP101 in batch culture with pH20 plasmid was constants protein production over 0.8 mM lactose (Menzella et al., 2003). In this study, the range of lactose 10 -15 g/L and expression time 13 - 20 h was considered to give strong expression for SuSy. In addition, in the case of SrUGT76G1 expression, 12 - 16 g/L lactose and 18 – 22 h of expression time were ideal for it.

Effect of temperature and time on enzymes expression

Similar to the relationship between temperature and lactose, the relationship between temperature and time also involves the substrate consumption rate, proper protein folding, and particular growth rates. The red zone with high SuSy expression is where the temperature is between 23 and 27 degrees Celsius and between 14 and 24 hours, and 20 to 24 degrees Celsius and 16 to 24 hours are red areas of strong expression for SrUGT76G1, according to the response surface contour (Figure 3.12, and 3.13).

Optimization of SuSy and SrUGT76G1 expression conditions

Temperature, lactose, and time were all equally important factors in the numerical optimization technique used to optimize the process conditions for the SuSy and SrUGT76G1 synthesis of *E. coli* strain BL21(DE3) for appropriate expression conditions. Targeting high soluble enzyme expression was the major criterion for limitations optimization. The ideal operating parameters for SuSy expression were 27 degrees Celsius, 12 g/L lactose, and a 16 h expression period in order to attain the desired 0.45 µg per 5 µg total protein. The expression settings for SrUGT76G1 were 20 degrees Celsius, 14 g/L lactose, and 20 h expression time, to targeted 0.62 µg per 5 µg total protein. The experiment was run in 2 L flasks with 1 L medium, a 5 L fermenter with 3.5 L medium, and a 50 L fermenter with 35 L medium to validate the outcomes of optimization.

3.4.5 Application of suitable expression condition in 2L flask, 5L fermenter, 50L fermenter for SuSy and SrUGT76G1 production.

The two periods that make up the optimal generation of recombinant protein by *E. coli* strain BL21(DE3) are when biomass is rapidly accumulated during non-inducing period and when protein production is achieved during the inducing

period. Nevertheless, a high cell density can frequently result in a number of serious issues, such as plasmid loss from *E. coli*, a large decrease pH due to cell metabolites, and limited dissolved oxygen availability. These issues frequently lead to minimal or even no protein production while maintaining a high cell density (Sivashanmugam et al., 2009). Therefore, lactose was added for the inducing period when the cell density reached an OD_{600} of 1. The expression conditions of SrUGT76G1 and SuSy were applied in 2L flask to examine the expression and activity of the enzymes. Then, the conditions for the expression of the enzymes were also verified in the 5 L and 50 L fermenters once more. The outcomes showed that SuSy and SrUGT76G1 production could be successfully carried out under the right expression circumstances. The findings showed that the expression conditions were successful in flask and fermenter, and the concentrations of SrUGT76G1 and SuSy were from 14 to 17 mg/L and 7.3 to 14.9 mg/L, respectively. Table 3.8 displays the results of the determination of both yields and enzymes's activities as well. The specific activity of SrUGT76G1 and SuSy was not significantly different from between flask and fermenter cultures. Due to using a single IMAC in purification, the enzyme activities are affected by the ratio of expressed protein to impurity. Finally, the enzyme expression in the 50 L fermenter for SuSy and SrUGT76G1 was higher than in the flask and 5 L fermenter. In the fermenters, SuSy's cell density was comparable, peaking at 3.16 ± 0.102 (Figure 3.14). However, the 50 L fermenter SrUGT76G1 cell density was higher by 1 OD unit when compared with 5 L fermenter. This was a reason why there was more SrUGT76G1 enzyme in 50 L than in 5 L cultivation. Moreover, the lactose serves as a carbon source for bacteria to encourage growth per volume in culture, as previously noted (Pan et al., 2008). This increases the amount of the target recombinant protein produced. However, lactose, on the other hand, remained unchanged over the expression period when it was measured by HPLC an Aminex® HPX-42A, 300 mm × 7.8 mm, column, RI detector. The condition was performed at flow rate of 0.6 ml/min, using as mobile phase a deionized water, 20 µl sample injection, column temperature 85°C, pressure 185 psi. The outcomes showed that lactose digestion did not happen in this case with low density of *E. coli* BL21(DE3). The pH of the culture for SuSy and SrUGT76G1 in the fermenters was around neutral 6 to 7.45 and 6 to 8.5 during cultivation time, respectively, because the cell density was controlled to 1

prior to the shift in the expression period. Therefore, acid formation during fermentation was not much effect to broth pH. Furthermore, the SDS-PAGE analysis of 5 µg of total protein in the supernatant demonstrated the potential of enzyme-expression to increase with time (Figures 3.15 and 3.16). When comparing with other studies, the yield of enzyme production was lower than some others such as 12 mg/L of SuSy (Dai et al., 2018) (Zhang et al., 1999) (Nidetzky et al., 2018) (Yu et al., 2022) that in flask cultivation with IPTG as inducer, and 61.6 mg/L/h of SrUGT76G1 that had fusion (*malK* and *prpD* (Shu et al., 2020), *CysQ, EDA, NusA* (Chen et al., 2017)) for increasing soluble enzyme and fed-batch fermentation condition (Chen et al., 2017) (Wang et al., 2011). However, this study was successful to screening an effective medium and suitable expression conditions appropriate to apply in flask and fermenter to produce SuSy and SrUGT76G1 using lactose as inducer. The yield was high in the case of 50 L fermenter culture, which will support enzyme production for glycoside synthesis.

Table 3.8 The yield and specific activity of SuSy and SrUGT76G1 from 2 L shake flask, 5 L fermenter, and 50 L fermenter cultures.

		2L flask	5L fermenter	50L fermenter
SuSy	Yield (mg/L)	7.3	10.8	14.85
	Specific activity	3.815 ± 0.011	3.76 ± 0.003	2.87 ± 0.003
SrUGT	Yield mg/L	14.1	15.0	17.3
76G1	Specific activity	20.03 ± 1.8	17.25 ± 0.25	17.7 ± 4.1

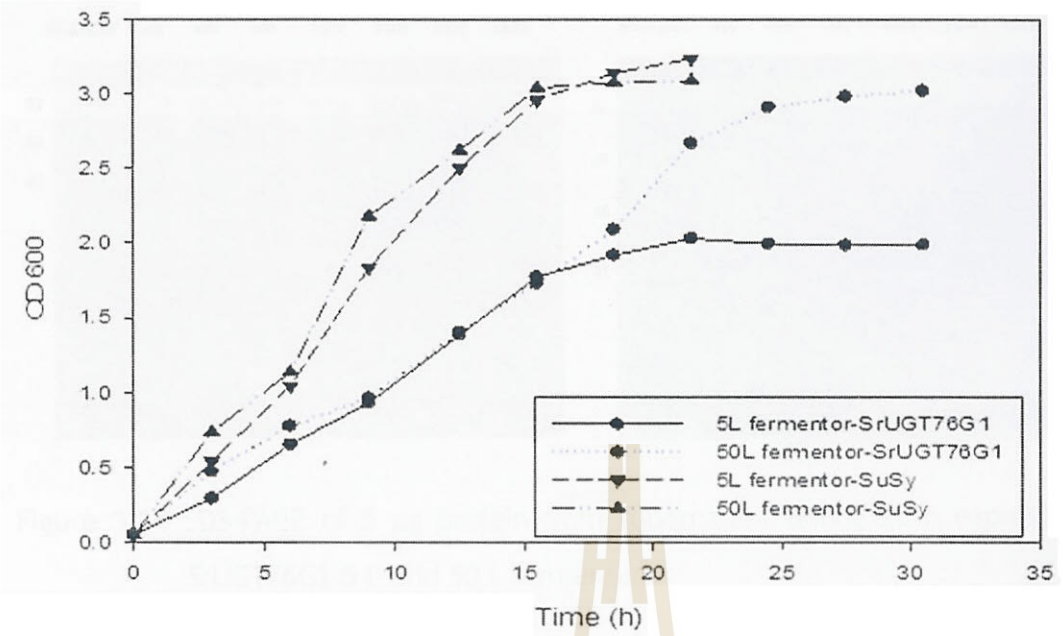

Figure 3.14 Growth curve of *E. coli* strain BL21(DE3) for enzyme production in 5 L and 50 L fermenters.

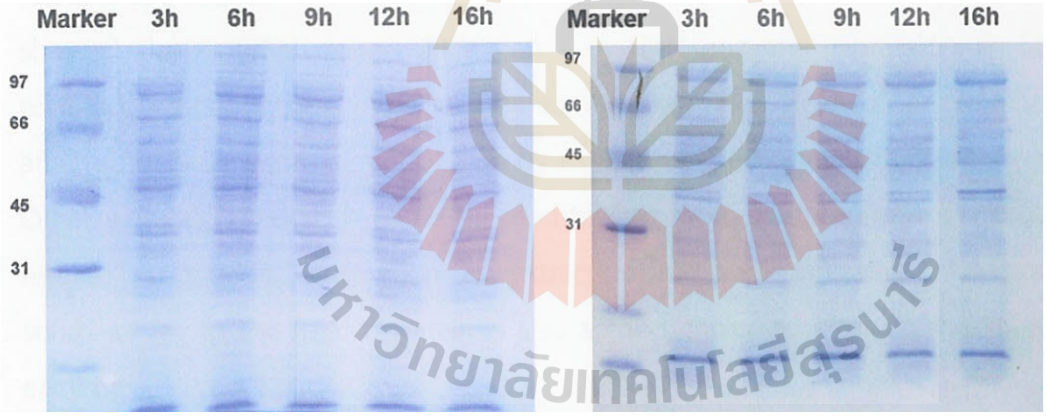

Figure 3.15 SDS-PAGE of 5 µg protein from supernatant during 16 h expression of SuSy in 5 L and 50 L fermenters.

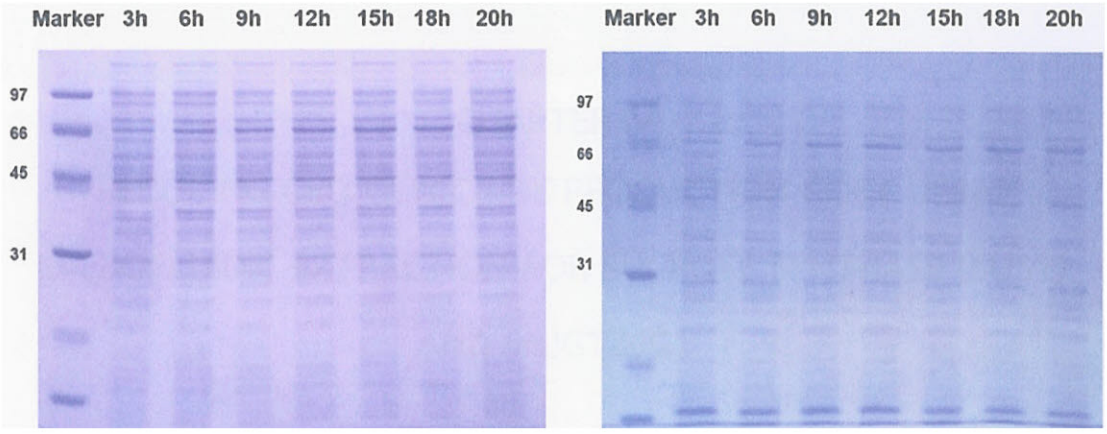

Figure 3.16 SDS-PAGE of 5 µg protein from supernatant during 20 h expression of SrUGT76G1 5 L and 50 L fermenters.

3.5 Conclusion

This chapter shows the effects of medium, temperature, inducer, time on expression of SuSy and SrUGT76G1 enzymes. The suitable expression condition was successfully applied in shake flask and 5 L and 50 L fermenter. These effects clearly showed the optimal zone which can gain high enzyme expression in response resurface methodology with Box-Behnken design. The yield of enzyme was not affected only by expression, but also by extraction, method and purification method. Other extraction methods could be tried to gain more soluble enzymes soluble and reduce production cost, such as extraction by homogenization. Addition of a solubility tag to the fusion protein is also a good choice to improve the solubility of enzymes.

CHAPTER IV
REDUCING CBD GLYCOSIDE PRODUCTION COST USING MICROFLUIDIC EXTRACTION FOR SUCROSE SYNTHASE (SUSY) AND SrUGT76G1

4.1 Abstract

In order to lower the cost of producing CBD glycoside by reducing the use of lysozyme and DNase, the goal of this chapter was to examine the microfluidic method of enzyme extraction as a substitute for the lysozyme extraction method. The SrUGT76G1 and SuSy enzymes were purified by the method using microfluidic extraction and IMAC over a column containing 5 mL of IMAC-resin-Co for purification, yielding 18.4 ± 1.2 mg/L, and 12.7 ± 1. 2 mg/L, respectively. The SrUGT76G1 and SuSy enzymes were produced with yields of 17.4 ± 1.4 mg/L and 14.1 ± 0.97 mg/L, respectively, by the method using lysozyme extraction. ANOVA analysis showed that there was no significant difference in the enzymes production yield. Furthermore, there was a notable similarity in the enzyme activity between the two extraction techniques. Microfluidic condition with 25g/L cell concentration, 69 Mpa, and a single pass at 86% disruption efficiency, can benefit the extraction of both enzymes. The cell concentration can be increased to 150 g/L at 69 Mpa and at least two passes with disruption efficiency of 91.33%. The low-cost manufacture of enzyme materials for the synthesis of glycosides was thus facilitated by microfluidic extraction.

4.2 Introduction

Escherichia coli grows quickly, is simple to work with, and maintains genetic stability in large cultures, traits which make it one of the best hosts for producing recombinant proteins. However, the production of recombinant protein intracellularly is a disadvantage when using *E. coli* on a large scale. Thus, in order to extract the desired protein, the cells must be lysed. Three layers make up the periphery of *E.*

coli: an inner membrane, a peptidoglycan cell wall, and an outer membrane. Since, *E. coli* is a Gram-negative bacteria it has a thinner wall that is protected from the environment by an outer membrane, compared to gram positive bacteria (Navarro et al., 2022). The thin peptidoglycan is made up of glycan chains that repeat N-acetylglucosamine (GlcNAc) and N-acetylmuramic acid (MurNac) disaccharide units. Based on the way to open cell envelope to release protein, cell extraction methods are divided into mechanical and non-mechanical (Tan and Yiap, 2009). Mechanical methods, including, bead milling, high pressure homogenization, and ultra-sonication cause cell lysis. Non-mechanical methods like chemical or enzymatic cause gentler changes in the cell envelope permeability leading in outflow of intracellular content. However, these methods still have drawbacks, such as being expensive and often using toxic chemicals. In addition, the viscosity during the lysis process is affected by host cell DNA (Haberl Meglič et al., 2020), leading to the addition of DNase I for reducing the viscosity during lysis process.

Currently, the enzyme extraction methods are widely used include lysozyme lysis, ultra-sonication, microfluidic or high-pressure homogenization, bead milling, and cooled French press (Kulmer et al., 2017) (Shu et al., 2020) (Chen et al., 2017) (Duman-Özdamar et al., 2021) . In the lysis solution, some protease inhibitor is also added to supporting and protecting enzyme activity. Nevertheless, for enzyme extraction in large scale, ultrasonication and microfluidization could be favored. Ultrasound sonication can cause inactivation of many enzymes due to cavitation events, in particular, collapsing cavitation bubbles (Mawson et al., 2011). However, microfluidization or homogenizer extraction have many advantages over ultrasound sonication such as decreased particle size and improved homogeneity, and low temperature leading to less loss of enzyme activity. Use of high pressure to force sample fluids through a small opening over a short distance is the foundation of microfluidization. The microfluidic extraction method can be applied without lysozyme and DNase I, leading to reduced enzyme extraction cost production.

In this study, microfluidization was investigated for SrUGT76G1 and SuSy enzymes extraction from *Escherichia coli* BL21(DE3) with pET32a (+) and pET30a (+) expression vectors, respectively. The microfluidic extraction was successfully applied in the enzymes extraction in place of the lysozyme extraction method. It can gain

more benefit such as lowering the cost of the enzymes production, and availability for large scale extraction. The microfluidic condition was used 25g/L cell concentration and 69 Mpa with a single pass that led to 86% disruption efficiency, benefited the extraction of both enzymes. The cell concentration can be increased to 150 g/L at 69 Mpa, and passing the suspension at least two times through the devise will lend to a disruption efficiency of 91.3%. The low-cost manufacture of enzyme materials for the synthesis of CBD glycoside will be facilitated by this approach.

4.3 Materials and Methods

4.3.1 Materials

The *E. coli* BL21(DE3) cells expressing SuSy and SrUGT76G1 enzymes were provided from the 50 L fermenter culture described in the previous study Chapter 3. The *E. coli* BL21 (DE3) cells were centrifuged at 4720×g for 20 min at 25°C for remove the medium. All chemicals used in this study were of analytical grade. All measurements were made in triplicate and standard deviations were calculated.

4.3.2 Enzyme extraction methods

Five grams of wet cells were weighted and used as sample to investigate the enzyme extraction methods. The experiment was repeated 3 times and analysed by ANOVA.

In the lysozyme method, the lysis buffer was prepared with 80 ml for a sample including 20 mM phosphate buffer pH 7.5, 150 mM NaCl (EQ buffer); 0.4 mg/ml lysozyme; 1% Triton-X 100; 1 mM PMSF; 5 µg/ml DNase I (Bio Basis Canada, Canada, USA); and 0.1 mg/ml soy bean trypsin inhibitor (Millipore-sigma, Burlington, MA, USA).

Microfluidization proceeded with a pressure of 69 Mpa at 10°C for 5 passes. The lysis buffer was prepared with 200 ml for a sample and contained 20 mM phosphate buffer, pH 7.5, 150 mM NaCl; 1% Triton-X 100; 1 mM PMSF and 0.1 mg/ml soy bean trypsin inhibitor.

4.3.3 Turbidity

The turbidity was determined by measuring the optical density of the sample at 750 nm with a UV-VIS spectrophotometer (Bernaerts et al., 2019). Turbidity measurements was determined based on Eq. (3)

$$RT_i = 1 - \frac{T_i - T_0}{T_5 - T_0} \quad (3)$$

With RT being the relative turbidity after i passes, T_0, the measured turbidity the cells that were re-suspensed with lysis buffer, T_i, the measured transmission for a suspension homogenized for i passes, and T_5 the measured turbidity of the suspension homogenized by a high-pressure homogenizer with pressure at 10000 psi (69 Mpa) for 5 passes.

4.3.4 Purification and enzymes assay activity

A 5 ml IMAC-Co-resin column was used to purify each sample. The method for purification was describe in chapter 3. The DNS and UDP-Glo™ glycosyltransferase assays were clone following the description in chapter 3.

4.3.5 Scanning electron microscopy

The *E. coli* BL21(DE3) cells expressing SuSy and SrUGT76G1 were observed after 0 pass, 1 pass, and 5 passes of the process microfluidization. The samples were fixed in 0.1 M phosphate buffer (pH 7.2) 2.5% glutaraldehyde (Electron Microscopy Sciences, Hatfield, USA) overnight at 4°C, and then washed three times in phosphate buffer (4°C, pH 7.2), fixed in 1% osmium tetroxide (Electron Microscopy Sciences) for 2 hours, washed three times in distilled water (room temperature), and dehydrated in a graded acetone series (20%, 40%, 60%, 80%, AND 100% three times each). The sample was dried with Critical Point Drying and covered with a layer of gold (Leica Sputter coater EM ACE600, Austria), before undergoing scanning electron microscope (Carl Zeiss Auriga, Germany) with an acceleration voltage of 3 kV for observations.

4.4 Results and discussions

4.4.1 Lysozyme extraction method for SuSy and SrUGT76G1 enzymes

In case of intracellular expression, the extraction approach aims to degrade and rupture the cell membranes of *E. coli* BL21(DE3), releasing all of the enzymes from the cytoplasm. *E. coli* BL21(DE3) cell evelopes are composed of three layers: an outer membrane, a peptidoglycan wall and an inner membrane. The thin peptidoglycan cell wall is made up of glycan chains that repeat N-acetylglucosamine

(GlcNAc) and N-acetylmuramic acid (MurNac) disaccharide units. The ability of lysozymes, hydrolytic enzymes, to cleave the β–(1,4)-glycosidic linkages in peptidoglycan, a significant structural element of the *E. coli* cell wall, defines them (Nawaz et al., 2022). The results for this hydrolysis process weakens the cell wall, supporting extraction of protein from cytosol. In addition, Triton X 100 was added to lyse cells in order to extract protein since its hydrophobic tail mixes the fatty acyl group, while its polar head group disrupts the hydrogen bonds found in the cell's lipid bilayer, causing the lipid membrane to become less compact and intact (Koley and Bard, 2010). According to Table 4.1's data, the yield production of SuSy and SrUGT76G1 enzymes were 14.1 ± 1.0 mg/L and 17.4 ± 1.4 mg/L, respectively. Figure 4.1 displays the fractions from the purification process on SDS-PAGE. On the other hand, the microfluidization extraction method was investigated as a potential replacement for the lysozyme extraction method in the event of large-scale enzyme extraction. Because lysozyme and DNase I were not included in the lysis solution, there is a greater benefit to lowering the cost of producing CBD glycosides.

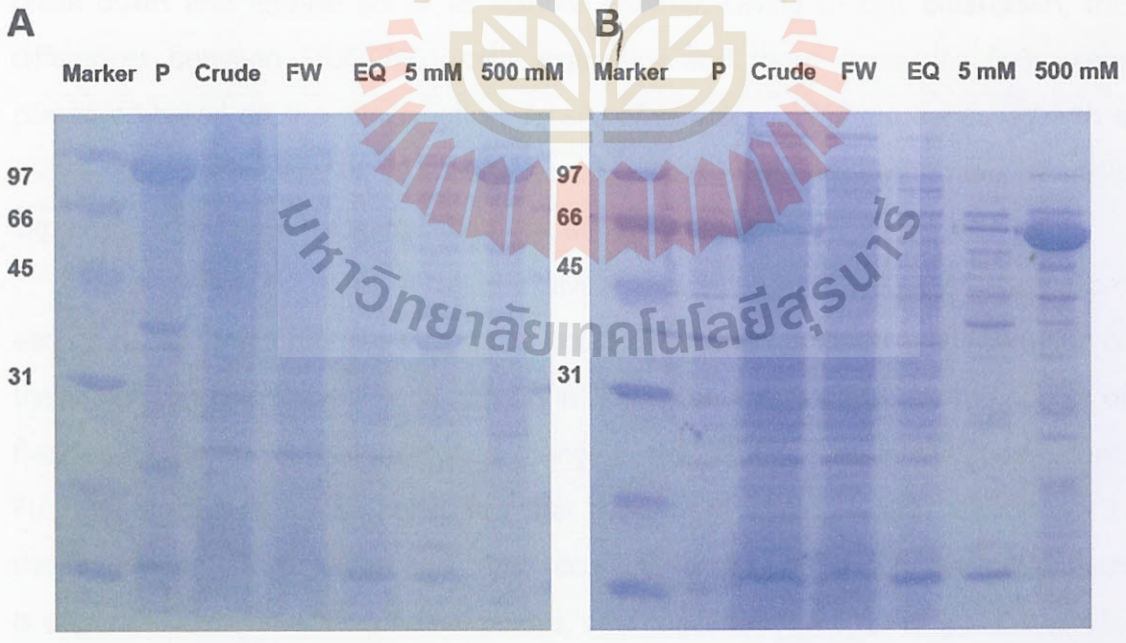

Figure 4.1 The SDS-PAGE of fractions from the SuSy (A), and SrUGT76G1 (B) purification by the lysozyme extraction method.

4.4.2 The microfluidization extraction method for SuSy and SrUGT76G1 enzymes

The processes could be described as producing emulsions or suspensions with high efficiency is high-press homogenization or microfluidization, which decrease particle size and improve homogeneity. Use of high pressure to force sample fluids through a small opening over a short distance is the foundation of microfluidization. A disruption efficiency of 99.5% was obtained in a prior work using a microfluidic process to break down the *E. coli* for enzyme extraction under the following conditions: 46 Mpa pressure, a feed cell concentration of 100g/L, and 10 microfluidic passes (Kleinig et al., 1995). Pressure, cell concentration, and the number of microfluidic passes determine the disruption efficiency of microfluidic processes in the context of enzyme extraction (Middelberg, 2000). In addition, the low temperature of microfluidic extraction reduces the possibility of inactivating enzymes; it breaks down cells without the need for DNase and lysozyme, which lowers extraction costs; and it is simple to use on a wide scale for enzyme production. The goal of this experiment was to determine the microfluidic extraction conditions under which *E. coli* BL21(DE3) would break down and release all of its soluble enzyme. Owing to cell breakdown, the differences between SrUGT76G1 cells expressing and those expressing SuSy were compared based on the intact optical density of samples at 750 nm measured with a UV-VIS spectrophotometer (Bernaerts et al., 2019). The homogenization of cells expressing SrUGT76G1 was faster than that of cell expressing SuSy (Figure 4.2)

After the cells were objectively broken down, the supernatant from each pass was measured to determine the total protein content and intensities of the target bands in 5 µg of total protein in SDS-PAGE (Figure 4.3). Over the course of five passes, there was no discernible change in the total protein in the supernatant. Furthermore, Figure 4.3 demonstrates that there were no appreciable differences in the soluble protein between each run. According to earlier research, cell breakdown is dependent on time microfluidic passes, cell concentration (g/L) (0 g/L ≤ X ≤ 150 g/L), and pressure (P) (30 Mpa ≤ P ≤ 70 Mpa) (Middelberg, 2000) (Kleinig et al., 1995). Equation (4) (Middelberg, 2000) can be used to determine the cell disruption:

$$\ln (1/1 - D) = (0.0149 - 2.75 \times 10^{-5} X)\, N^{0.71} P^{1.165} \qquad (4)$$

Figure 4.2 The turbidity of *E. coli* BL21(DE3) expressing SuSy and SrUGT76G1 in 5 passes of microfluidic extraction.

where N is the number of discrete homogenizer passes, P is the homogenizer operating pressure in Mpa, and D is the fractional release of protein (the release of protein at a given moment divided by the highest release achievable). The disruption efficiency increased from 86% for the first pass to 99.79% for the fifth pass followed equation 4. On the other hand, the enzymes 'solubility was necessary for their extraction. With SrUGT76G1 and SuSy enzymes, all of the soluble enzymes were extracted at 86% disruption efficiency. By using equation (4), it is possible to boost the cell concentration to 150 g/L at 69Mpa and achieve a disruption efficiency of 91.33% over a minimum of two passes of microfluidic extraction.

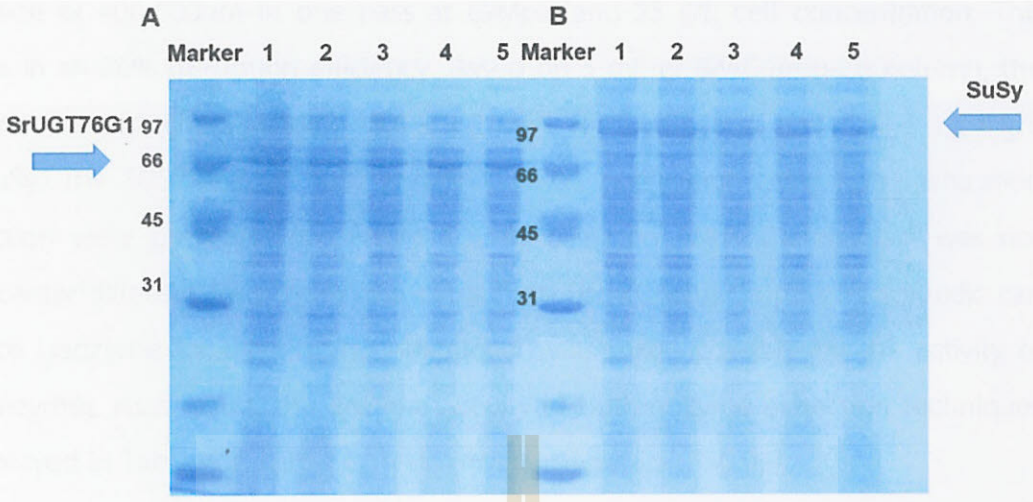

Figure 4.3 The 5µg total enzyme in supernatant in 5 times passes homogenizer, the numbers indicate the number of passes, SrUGT76G1 (69 kDa) (A), SuSy (97 kDa) (B).

SEM was used to observe clearly 5 samples, including untreated cells, cell after 1 pass, and cells after 5 passes of 2 clones, in order to learn more about the structure of the processed *E. coli* (Figure 4.4). Some *E. coli* BL21(DE3) cells were intact to shred without treatment SEM sample because Triton X 100 was used to extract protein it can start to disrupt the cell's lipid bilayer (Figure 4.4 A). Nevertheless, in the clones expressing SrUGT76G1 and SuSy, all of the *E. coli* BL21(DE3) cells were shredded to a size of 400-500nm during the initial microfluidic pass based on the SEM pictures (Figure 4.4 B and C). This may explain why the soluble enzymes were consistent over the course of five microfluidic passes. The only differences that separated the clones of cells were the plasmids that they contained pET32a(+)/SrUGT76G1, and pET30a(+)/SuSy and the proteins that they produced. The intact cells underwent the same treatment and differed. The cell expressing SrUGT76G1 can homogenized in the solution more easily than the SuSy clone. When compared to SuSy clone, the clone that expressed SrUGT76G1 could be homogenized in the lysis solution, as seen in Figure 4.4 D and E, the SEM of samples after the fifth microfluidic passes. However, this homogenization did not significantly affect the yield of enzyme extraction compare with lysozyme extraction (Table 4.1). Based on all data, the microfluidic device can shred 100% of *E. coli* BL21(DE3) cells

to a size of 400-500nm in one pass at 69Mpa, and 25 g/L cell concentration. This results in an 86% disruption efficiency. Based on 5 mL of IMAC-resin-Co column, the enzymes were purified, yielding 18.4 ± 1.2 mg/L for SrUGT76G1, and 12.7 ± 1.2 mg/L for SuSy. The SDS-PAGE of SuSy and SrUGT76G1 purification using homogenization extraction were presented on Figure 4.5. By using an ANOVA analysis, it was not significantly different from lysozyme extraction. The conclusion that microfluidic can replace lysozyme for the enzymes extraction was made possible by the activity of the enzymes. As a result, the enzyme activity of both enzyme eztraction techniques is displayed in Table 4.1, with a non-significant difference ($P>0.05$).

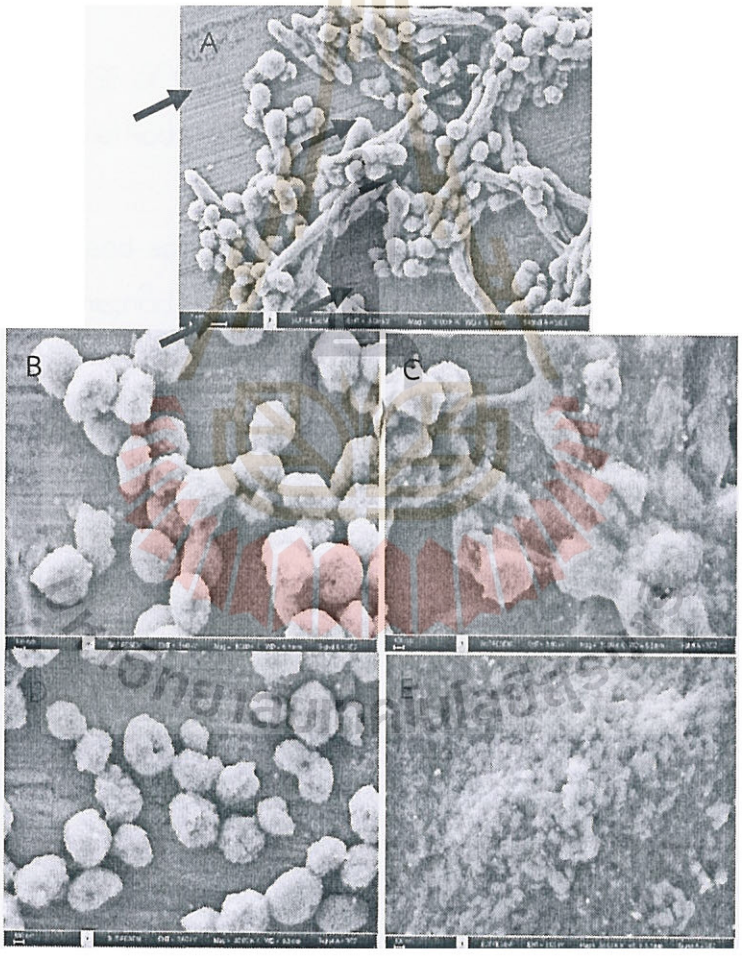

Figure 4.4 SEM of *E. coli* BL21(DE3) host cells after recombinant expression of SuSy (B: first pass of SuSy; D: fifth passes) and SrUGT76G1 (C: first pass of SrUGT76G1; D: fifth passes of SrUGT76G1) and A: untreated *E. coli* (in lysis solution).

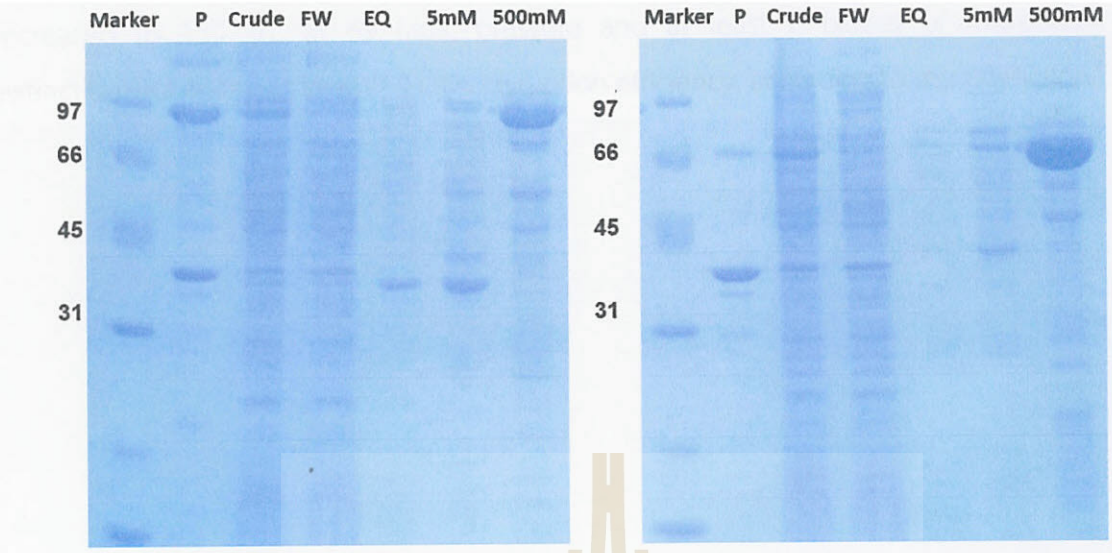

Figure 4.5 The SDS-PAGE of the enzymes purification in High-pressure homogenizer extraction method.

Table 4.1 The yields and specific activities of SuSy and SrUGT76G1 with different extraction methods.

		Homogenizer	Lysozyme
SrUGT76G1	Yield (mg/L)	$18.4^{b} \pm 1.2$	$17.4^{b} \pm 1.4$
	Specific activity (μM/min/mg)	$16.7^{b} \pm 2.6$	$17.7^{b} \pm 4.1$
Sucrose synthase (SuSy)	Yield (mg/L)	$12.72^{a} \pm 1.192$	$14.14^{a} \pm 0.97$
	Specific activity (mM/min/mg)	$2.67^{a} \pm 0.17$	$2.8^{a} \pm 0.09$

All values were presented as the mean ± SD (n=3), ^{a,b} means in the same row sharing different superscripts are significantly different ($P<0.05$) as determined by Turkey's range test.

4.5 Conclusions

The microfluidic extraction method can replace lysozyme enzyme extraction without affecting the yield and enzyme activity and reduces production cost due to not using lysozyme, and DNase. One pass with 25g/L cell concentration and 69Mpa pressure can achieve 86% disruption efficiency and 100% cell shredding to 400-500nm particles that were obtained by the microfluidics extraction method for both *E. coli* BL21(DE3) cells expressing SuSy and SrUGT76G1. The cell concentration can be

increased to 150 g/L at 69 Mpa, pressure and at least 2 passes of microfluidic extraction would result in with 91.3% disruption efficiency, according to my prediction.

CHAPTER V
SUITABLE CONDITION FOR CANNABIDIOL GLYCOSIDES PRODUCTION

5.1 Abstract

By enzymatic glycosylation, this chapter aimed to obtain optimal conditions for production of cannabidiol glycosides while reducing the cost of sugar donors by using sucrose synthase to regenerate uridine diphosphate glucose (UDP-Glc). Two conditions for generating less and more polar products, based on TLC position may be drawn from the results. Condition 1 (2 mM CBD, 50 mM potassium phosphate buffer pH 7.2, 20 mM sucrose, 8 µg SrUGT76G1, 4 µg Susy, 0.3 mM UDP, 15 mM $MgCl_2$ and incubated at 30°C for 5 days) was used to generate less polar products. Condition 2 (1 mM CBD, 50 mM potassium phosphate buffer pH 7.2, 100 mM sucrose, 14 µg SrUGT76G1, 8 µg Susy, 1 mM UDP, 6 mM $MgCl_2$ and incubated at 30°C for 5 days) was used to generate more polar products. LC/MS/MS was used to confirm the mass of CBD glycosides and determine their putative structure. As putative structure and mass, the CBD glycosides were identified with two to four glucose residue glycosylation

5.2 Introduction

The compound cannabidiol, or CBD, is present in cannabis and has been shown to have numerous health advantages, including treating conditions like anxiety, schizophrenia, addiction, post-traumatic stress disorder, cancer, graft-versus-host disease, and inflammatory bowel disease (Oberbarnscheidt et al., 2020, Cerino et al., 2021, Pamplona et al., 2018). CBD-containing medication formulations have received approval from the European Medicines Agency and the US Food and Drug Administration. On the other hand, CBD's poor water solubility after oral administration results in low bioavailability, inconsistent pharmacokinetic effectiveness, heightened adverse effects, and drug-drug interactions at larger dosages (Millar et al., 2020). The use of nanoencapsulated CBD, CBD in gelatin beads enclosed in gastro-resistant capsules,

resistant capsules, bi-sulphate derivatives of CBD (Millar et al., 2020), CBD glycosides (Hardman et al., 2017, Zipp et al., 2017), and other methods has been explored recently as ways to improve CBD delivery and efficacy. One of the most frequent modifications to CBD is glycosylation, which is carried out by uridine diphosphate-dependent glucosyltransferase (UGT). Following this process, CBD exhibits a great deal of structural variety (Hardman et al., 2017). The glucosyl moiety or moiety attached to the CBD glycosides improves their solubility, stability, bioavailability, and pharmacokinetic characteristics (Zipp et al., 2017). Nevertheless, UDP-Glc, a costly sugar donor, was employed as the sugar substrate in their study. Furthermore, numerous studies show that sucrose synthase (SuSy) and a UGT can be used in a one-pot reaction to recycle UDP-Glc from sucrose and UDP, offering an affordable method for the glycosylation of CBD. The CBD was glycosided to produce CBD glycosides in the prior study by the Stevia rebaudiana SrUGT76G1 enzyme (Zipp et al., 2017). Furthermore, Glycine max (soy bean) has sucrose synthase (SuSy), which is highly active in the synthesis of UDP-Glc (Bungaruang et al., 2013).

In this study, the SrUGT76G1 and SuSy enzymes were produced from recombinant proteins in *E. coli* strain BL21(DE3) from the pET32a (+) and pET30a (+) expression vectors, respectively. The multiple SrUGT76G1 and SuSy enzymes cascade reaction was developed to synthesize CBD glycosides using cheap sucrose as an expedient glucosyl donor. Thin layer chromatography was used to detect and optimize CBD glycosides conditions with many factors, including sucrose, UDP, CBD, $MgCl_2$, solvent for CBD stock solution, SuSy, and SrUGT76G1 concentration, and time for the glycosylation reaction. In addition, LC/MS/MS was used to confirm the mass of the CBD glycosides and led to a putative identification of the structures, based on Hardman et al. (2017) as a reference.

5.3 Materials and Methods

5.3.1 Materials

Cannabidiol was purified from the Suranaree University of Technology (SUT) Cannabis Farm, AB Laboratory, SUT. Uridine diphosphate (UDP) sodium salt and Uridine diphosphate glucose (UDP-Glc) were purchased from Nanjing Duly Biotech

Co., Ltd. (Nanjing, China). Sucrose synthase (SuSy) and SrUGT76G1 were provided from 50L fermenter culture described in Chapter 3. Thin-layer chromatography plates (Silica gel 60 F_{254}) purchased from Merck Chemical (Darmstadt, Germany). All chemicals used in this study were of analytical grade from various suppliers.

5.3.2 Varying conditions for CBD glycosides synthesis reaction with SrUGT76G1 enzyme

The suitable condition for synthesis of CBD glycosides was varied based on the effect of solvent, 0.5% to 2% v/v of acetone, and methanol in the reaction, 3 mM to 9 mM $MgCl_2$, 1 µg to 9 µg amount of enzyme for a reaction, 1 mM to 5 mM CBD and 1 h to 48 h incubation time of the reaction, respectively. The buffer potassium phosphate, pH 7.2, based on a previous study (Hardman et al., 2017). The whole volume for a reaction was 10 µl. The reaction was incubated at 30°C overnight to vary all factors, except time factor. The suitable condition for synthesis of CBD glycosides was used to vary time of reaction. Then, 10 µl of samples were collected and checked by TLC with butanol: acetic acid: water (3:1:1 (v/v/v)) as the mobile phase.

5.3.3 Varying conditions for CBD glycosides synthesis reaction with the SuSy and SrUGT76G1 coupled enzymes system.

The suitable conditions for synthesis of CBD glycosides was varied based on the effect of 2% to 20% v/v acetone in the reaction, 10 mM to 400 mM sucrose, 0.002 mM to 2 mM UDP, 6 µg to 18 µg SrUGT76G1 enzyme, 2 µg to 8 µg SuSy enzyme, 0 mM to 15 mM $MgCl_2$, 1 mM to 4 mM CBD, and 1 day to 5 days of reaction. The buffer potassium phosphate pH, 7.2, was based on a previous study (Hardman et al., 2017). The whole volume for a reaction was 10 µl. The reaction was incubated at 30°C for 24h, except the time factor. The suitable condition for synthesis of CBD glycosides was used to vary time of reaction. The samples were collected and checked in TLC with butanol: acetic acid: water (3:1:1 (v/v/v)) as the mobile phase.

5.3.4 Ultra-performance liquid chromatography – electrospray ionization mass spectrometry (LC-ESI-MS)

The 5 ml sample of CBD glycosides synthesis reaction at condition 2 was prepared to purify based on TLC manual purification. The sample was spotted to TLC

and run with butanol: acetic acid: water 3:1:1 v/v/v as mobile phase. The TLC area with CBD glycosides product was cut off. And then, it was eluted again in methanol to extract CBD glycosides. The sample in methanol was evaporated and concentrated it again until dry. After that, the 2 ml water was added to dissolve CBD glycosides and filtered with 0.22 µm PVDF filter (Millipore-sigma, Burlington, MA, USA). And then, it was used for LC-ESI-MS sample injection.

The analyses were performed on the Dionex Ultimate 3000 UHPLC system (Dionex, USA) coupled with an electrospray ionization (ESI) tandem mass spectrometer (microOTOF-Q II) (Bruker, Germany). The injection volume for the sample was 20 µl. LC separation was performed via a Zorbax SB-C18 column, (250 mm × 4.6 mm × 3.5 µm, Agilent Technologies, USA). The conditions were as follows: column temperature 35°C, flow rate 0.5 ml/min, running time 70 min, solvent A water with 0.1% formic acid (FA), solvent B acetonitrile with 0.1% formic acid (FA). The gradient elution was performed using the following solvent gradient: starting with 10% B for 5 min, then ramping to 30% B over 10 min; then increasing to 99% B over 40 min, and holding at 99% for 5 min before ramping down to 10% over 5 min and holding at 10% for 5 min. The eluted components were ionized by ESI source and detected in the mass scanning mode in the range of 50 m/z to 1,500 m/z at positive ion polarity. The nebulizer gas (N_2) was 2 Bar, drying gas was 8 L/min, the dry heater temperature was 180°C, and the capillary voltage was 4.5kV. The LC-QTOF data were collected and processed by Compass 1.3 software (Bruker).

5.4 Results and discussions

5.4.1 Suitable conditions for the CBD glycosides

In a previous study, CBD was a substrate for SrUGT76G1 glycosylation of the hydroxyl groups (Hardman et al., 2017). With the objective of production and purification of CBD glycosides, in this study, 50 mM potassium phosphate buffer (pH 7.2) was applied, and some conditions were varied, including solvent for CBD, $MgCl_2$ concentration, CBD concentration, and the enzymes concentration in 10 µl scale as proof of concept. The CBD glycosides have no commercially available standards, so

the TLC was used to vary the suitable conditions for CBD glycosides production. The CBD glycosides were named CBD-G1, CBD-G2, CBD-G3, CBD-G4, and CBD-G5, following their increasing mobility in TLC (Figure 5.1).

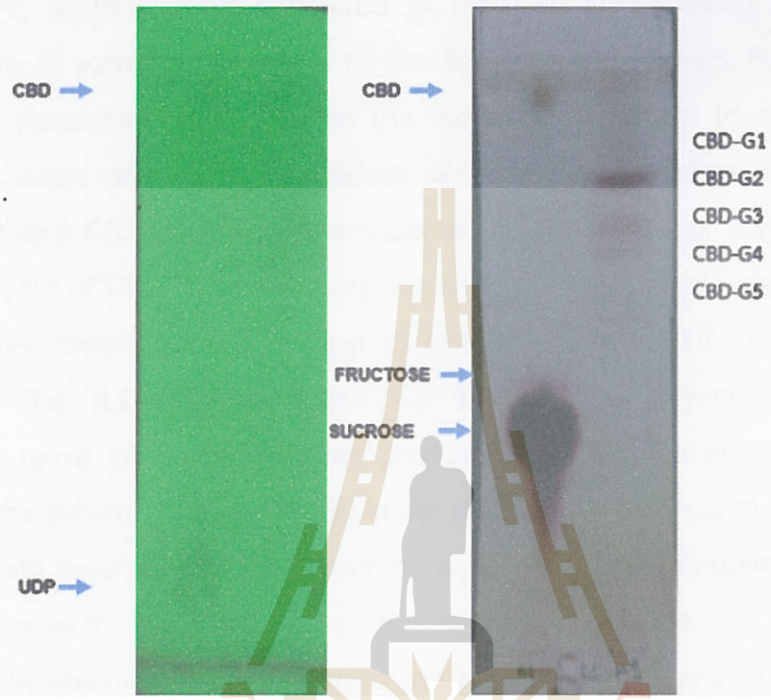

Figure 5.1 The mobility of CBD-G1, CBD-G2, CBD-G3, CBD-G4, and CBD-G5 in TLC using butanol: acetic acid: water (3:1:1 (v/v/v)) as the mobile phase.

5.4.1.1 CBD glycosides reaction condition with SrUGT76G1 enzyme

Given that cannabidiol (CBD) is a hydrophobic molecule, the solvent of choice for dissolving the CBD substrate for the reaction must be chosen. According to the previous review, CBD has varying solubility in different solvents. For example, it can dissolve in ethanol at 35 mg/ml, methanol at 30 mg/ml, DMSO at 60 mg/ml, and dimethylformaminde at 50 mg/ml (Ian Parkes, 2020). However, the solvent was selected with the intention of diluting CBD to aid in the setup of the reaction; the solvent may also have an impact on the enzyme and subsequent purification. As an example, DMSO has a dissolves for CBD well, but it will interfere with the analysis by TLC, making the purification step more difficult. Acetone is a

solvent that, at low concentrations, stabilizes the enzyme; this finding allowed for its use in purification and crystallization of enzymes (Takemori et al., 1967). Therefore, acetone was examined as a solvent for CBD stock reaction. In addition, a previous paper used methanol as a solvent for CBD stock. Consequently, in this study, methanol and acetone were compared in the CBD glycosylation process with concentrations of solvents from 0.5% to 2%. Based on the findings, the SrUGT76G1 enzyme can glycosylate methanol on the alcohol's OH group to create methyl glycosides in cases of high concentrations of methanol. Therefore, it was turned down for use as a CBD solvent. Furthermore, as the percentage of acetone grew, so did the amounts of CBD glycoside compounds (Figure 5.2). there were identified in TLC with three clearly spots from top to bottom: CBD-G1; CBD-G2, and CBD-G3, respectively. The TLC results showed that the acetone solvent is superior to methanol in terms of producing clear products spots. In the end, acetone was selected as the solvent to dissolve CBD in the reaction. Hardman et al.'s earlier work employed 0.5% methanol in their reaction, which is a small amount of methanol that did not cause the detectable production of methyl glycoside.

By electrostatically stabilizing the growing negative charge, $MgCl_2$ acts as a cofactor in the reaction to enable full activity of glycosyltrasferases and sugar nucleotidyltransferases, facilitating the departure of the nucleotide diphosphate leaving group. However, some glycosyltransferases, such as GT42 and β-1,6-GlcNAc transferase C2GnT-L from family GT14, do not need Mg^{2+} (Lairson et al., 2008). However, in previous study, 3 mM $MgCl_2$ was used for CBD glycosides production with SrUGT76G1 enzyme (Hardman et al., 2017). Therefore, the concentration of $MgCl_2$ was investigated starting with 3 mM $MgCl_2$. The TLC result (Figure 5.3) indicated that there was no discernible difference in the CBD glycosides products between 3 mM to 9 mM $MgCl_2$. In order to increase the number of CBD glycosides products, the condition of $MgCl_2$ was considered at 9 mM.

In Hardman et al.'s study (2017), the CBD glycosides synthesis reaction was set up with 0.075 μg/μl enzyme concentration, 0.005 μg/μl CBD, and 2.5mM UDP-Glc that proceeded to >95% substrate conversion with $K_{eq} \approx 24$. In our case, the SrUGT76G1 enzyme was used at 1 μg/μl to 9 μg/μl enzyme concentration, 1 mM CBD, and 1 mM UDP-Glc. The CBD glycosides products increased when the enzyme

concentration increased (Figure 5.4). To increase the CBD-G3 product, the enzyme concentration was chosen at 9 µg/µl. However, CBD has a low solubility in the reaction, and on the surface of the reaction as an oil, the CBD spot in TLC results, which may interfere percent CBD substrate conversion.

Due to its low solubility in water, the concentration of CBD was varied as well, from 1 mM to 5 mM. From TLC (Figure 5.5), the results indicated that CBD-G1 was increasing from 1 mM CBD to 5 mM CBD, but CBD-G2, and CBD-G3 were decreased. Therefore, with a high percent of CBD in reaction, the lowest polarity product CBD-G1 was produced more than CBD-G2, and CBD-G3. However, the percent conversion of CBD substrate decreased with too much CBD excess in the reaction. Based on the TLC results, 2 mM CBD was the best choice for the CBD glycosides synthesis reaction.

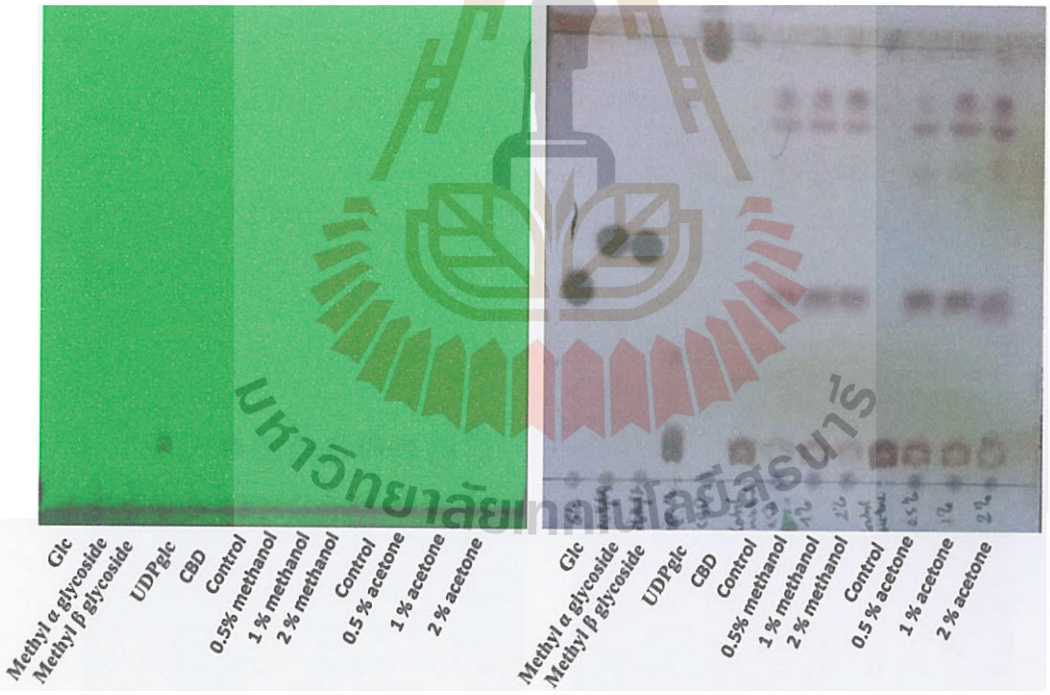

Figure 5.2 The effect of varying solvents for CBD in the CBD glycosides synthesis reaction (1 mM UDP-Glc, 1 mM CBD, 6 ug enzyme, 50 mM buffer potassium phosphate, pH 7.2, 6 mM $MgCl_2$, incubated at 30°C for 18 h).

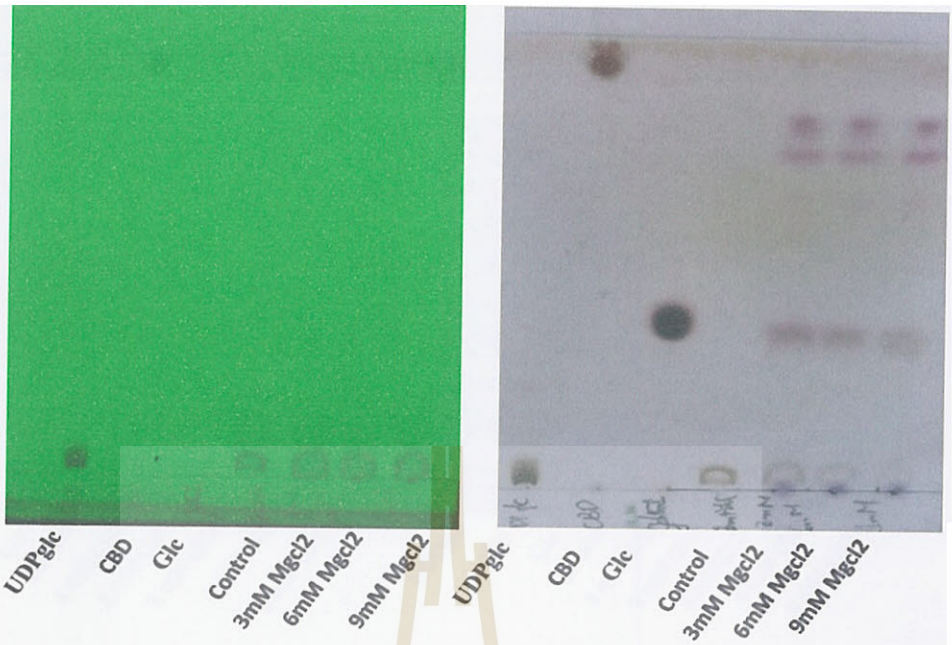

Figure 5.3 The effect of varying $MgCl_2$ concentration in the CBD glycosides synthesis reaction (1 mM UDP-Glc, 1 mM CBD, 6 ug enzyme, 50 mM buffer potassium phosphate, pH 7.2, 2% acetone, incubated at 30°C for 18 h).

Figure 5.4 The effect of varying SrUGT76G1 enzyme concentration in the CBD glycosides synthesis reaction (1 mM UDP-Glc, 1 mM CBD, 50mM buffer potassium phosphate, pH 7.2, 9 mM $MgCl_2$, incubated at 30°C for 18h).

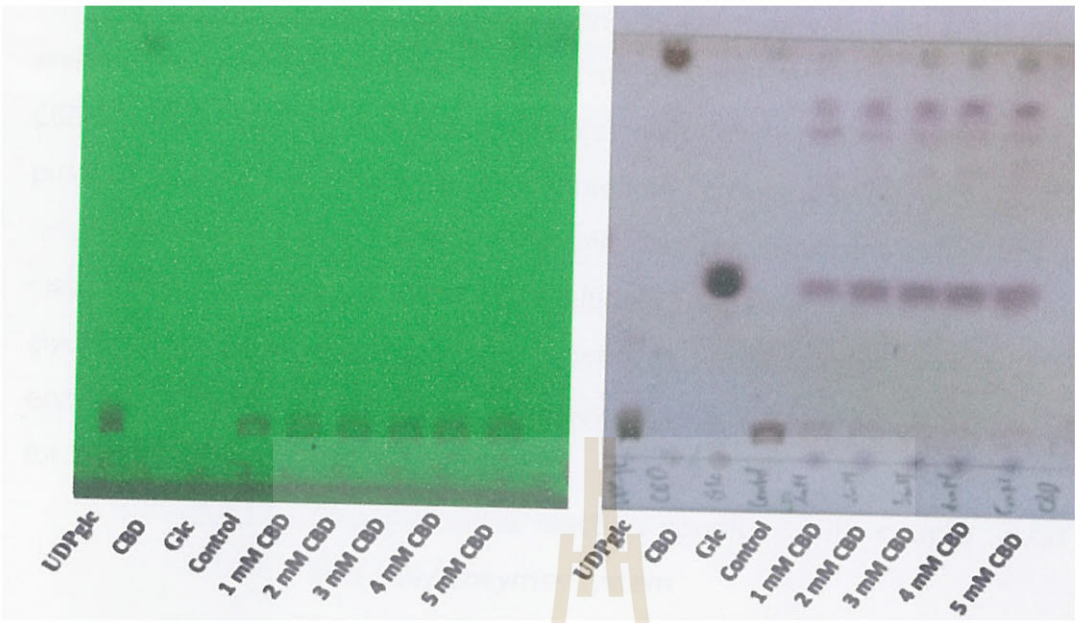

Figure 5.5 The effect of varying CBD concentration in the CBD glycosides synthesis reaction (1 mM UDP-Glc, 9 ug enzyme, 50 mM buffer potassium phosphate, pH 7.2, 9 mM $Mgcl_2$, incubated at 30°C for 18 h).

Figure 5.6 The effect of varying time in the CBD glycosides synthesis reaction (1 mM UDP-Glc, 2 mM CBD, 9 µg enzyme, 50 mM buffer potassium phosphate, pH 7.2, 9 mM $Mgcl_2$, incubated at 30°C for 18 h).

The time for CBD glycosylation was varied as well, from 1 h to 48 h. TLC analysis (Figure 5.6) indicated that CBD-G1 decreased from 1 h CBD to 48 h CBD, but CBD-G2 and CBD-G3 increased. Therefore, with long reaction time, the CBD-G1 product appeared to be further glycosylated to produce CBD-G2, and CBD-G3. The results of CBD glycosides at 48h and 24h was not significant difference, so the reaction can be stopped at 24h for time efficiency. Based on the TLC results, the CBD glycosides condition can be set up as follows: 1 mM UDP-Glc, 2 mM CBD, 9 ug enzyme, 50 mM buffer potassium phosphate, pH 7.2, 9 mM $MgCl_2$, incubated at 30°C for 24 h.

5.4.1.2 CBD glycosides reaction condition with couple SrUGT76G1 and SuSy enzymes system

As a sugar donor, the uridine diphosphate glucose (UDP-Glc) is an expensive substrate. To reduce this expense, researchers have applied sucrose synthase (SuSy) to regenerate UDP-Glc in situ (Bungaruang et al., 2013), SuSy catalyzes the formation of UDP-Glc by reversibly breaking the α-1,2 glycosidic bond in sucrose and transferring the glucose to UDP. SuSy's characteristic allows for the application of coupled enzyme reactions, such as SrUGT76G1 and SuSy, to reduce the cost of producing CBD glycosides. From previous studies, the coupling of SuSy and UGT enzymes has been applied in conditions with pH 6 to 8, low UDP concentration, and to UGT enzyme that are inhibited when the UDP concentration is above 4 mM (Schmölzer et al., 2016) (Dai et al., 2018) (Chu et al., 2021).

From the results of the CBD glycosides synthesis reaction with SrUGT76G1, methanol was rejected for use in CBD stock due to the glycosylation of methanol with glucose form UDP-Glc. In addition, as a good solvent for CBD glycosylation, acetone from 0.5% to 2% increased the amount of CBD glycoside products. However, in this case of multiple the enzymes reaction, the concentration of acetone in reaction might inhibit the enzymes, so the acetone concentration was examined again to see how much acetone can be included in the CBD glycoside reaction without affecting the enzyme activity. Therefore, the acetone solvent was varied, with a concentration ranging from 2% to 20%. The TLC result (Figure 5.7) indicated that CBD-G1 increased from 2% to 20% acetone, but the CBD-G2, and CBD-G3 decreased. It was consistent with the hypothesis that increased acetone led to an

increased soluble of CBD concentration in reaction. with more soluble CBD in the reaction, the enzyme can glycosylate more molecules with the same amount of UDP-Glc, so each glycoside may ten to get fewer glucosyl residues. From these results, CBD-G1 can be produced with a high percent of acetone, making CBD highly soluble in the reaction. However, the enzymes can be precipitated in the case of long-term reaction time at high acetone concentration (no data show). Therefore, the percent of acetone varied with the CBD concentration in reaction with 50 mM CBD in acetone stock.

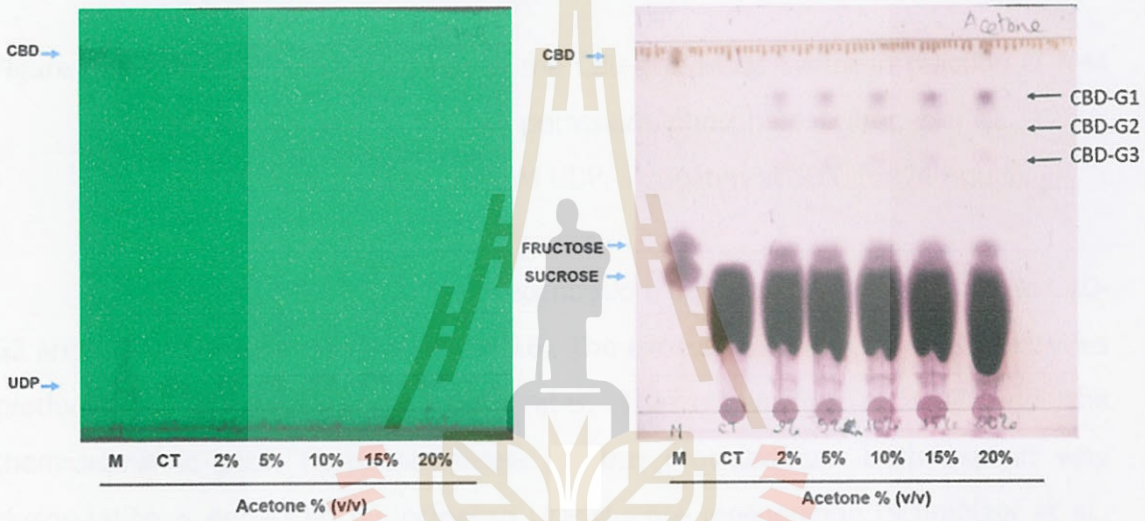

Figure 5.7 Effects of varying acetone solvents for CBD in the CBD glycosides synthesis reaction (1 mM CBD, 8 mM $MgCl_2$, 50 mM potassium phosphate buffer, pH 7.2, 100 mM sucrose, 12 µg SrUGT76G1, 4 µg Susy, 0.3 mM UDP, incubated at 30°C for 24 hours).

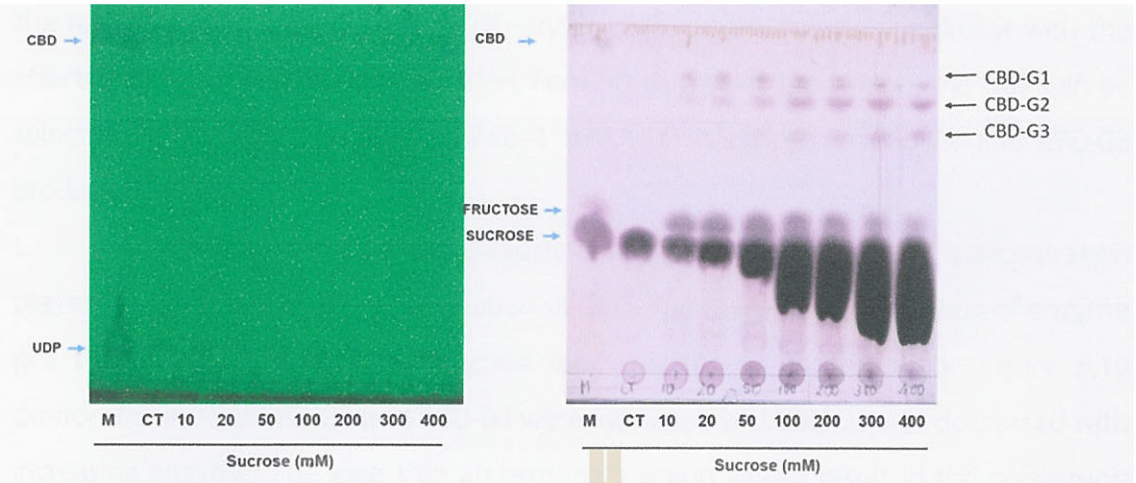

Figure 5.8 Effects of varying sucrose in the CBD glycosides synthesis reaction (1 mM CBD, 8 mM $MgCl_2$, 50 mM potassium phosphate buffer, pH 7.2, 12 µg SrUGT76G1, 4 µg Susy, 0.3 mM UDP, incubated at 30°C for 24 hours).

With increasing sucrose concentration, CBD-G1 was decreased while CBD-G2 and CBD-G3 were increased (Figure 5.8). The excess sucrose in the CBD glycosides products led to higher conversion rates. The elimination of UDP and the thermodynamic push from the excess sucrose provided can both explain why glycosylation is enhanced by increased UDP-glucose regeneration (Schmölzer et al., 2016). However, sucrose is also a large impurity that needs to be removed after finishing the reaction. Consequently, the sucrose content can be selected according to the CBD glycosides product that is being targeted, while avoiding adding excess, for instance, CBD-G1 can be produced with 20 mM sucrose, and CBD-2, and CBD-G3 can be synthesized with 100 mM.

According to earlier research, the UDP concentration has a significant impact on the percentage of conversion to glycosides during glycosylation. Rebaudioside A was found to have a 78% yield conversion using a low UDP concentration of 0.006mM (Wang et al., 2016). However, high UDP concentrations have also inhibited the UGT enzyme in reactions at 4 mM (Schmölzer et al., 2016). In this study, it was determined that the concentration of UDP could range from 0.002 mM to 2 mM in order to change the CBD glycosides reaction. It was discovered that, whereas CBD-G2 and CBD-G3 were increased, CBD-G1 was decreased with increasing UDP. From

the results (Figure 5.9), the effects of varying UDP concentrations was similar with the effects of varying sucrose concentration. For CBD glycosides production, the UDP can be selected at 0.3 mM for CBD-G1, while 1 mM UDP is utilized in CBD-G2 and CBD-G3 production.

In addition to the previously listed variables, SrUGT76G1 concentration played a crucial role in the glycosylation of CBD. The range of 6 µg to 18 µg of enzyme per total 10µl volume of a reaction was investigated in this work. Figure 5.10 demonstrates that CBD-G2 and CBD-G3 were increased and CBD-G1 was decreased with increasing enzyme. The idea that an enzyme's action would result in the conversion of CBD-G1 in the reaction to higher glycosylation forms made it possible. Similar to previous factors, the amount of enzyme can be selected at a low concentration for CBD-G1 production and a high concentration can be used for CBD-G2 and CBD-G3, depending on which CBD glycosides are being targeted.

SuSy, an additional enzyme in the reaction, determines the quantity of UDP-Glc in the reaction that can be used as a sugar donor for the glycosylation of CBD. SuSy was varied in the range of 2 µg to 8 µg. The findings indicated that CBD-G1 and CBD-G2 were decreased, and CBD-G3, CBD-G4 were elevated with increased SuSy (Figure 5.11). It was noteworthy in light of the earlier discussion of sucrose and UDP, the high concentrations of which encourage the production of CBD glycosides with high solubility and higher numbers of glucosyl residues. Based on the intended product, the SuSy concentration can be selected based on these results.

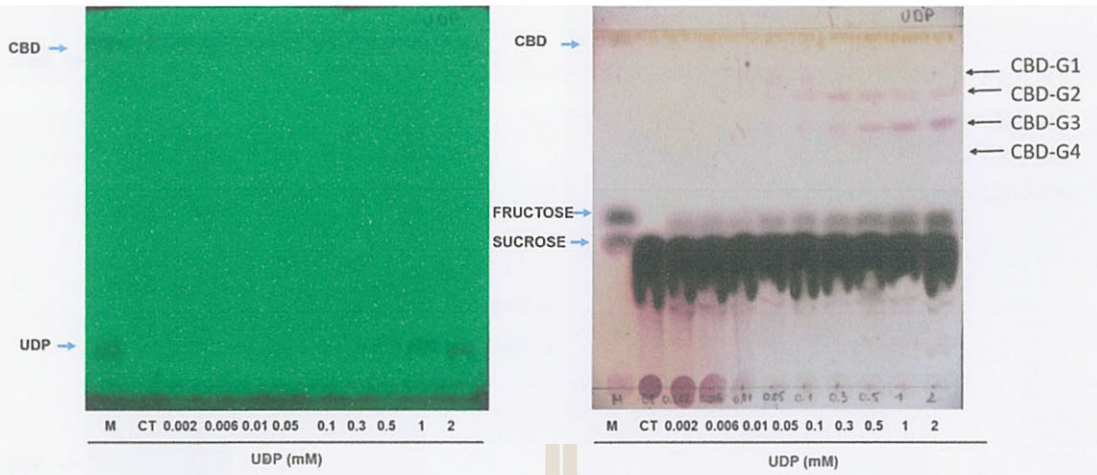

Figure 5.9 Effect of varying the UDP concentration in the CBD glycosides synthesis reaction (1 mM CBD, 8 mM $MgCl_2$, 50 mM potassium phosphate buffer, pH 7.2, 100 mM sucrose, 12 µg SrUGT76G1, 4 µg Susy, incubated at 30°C for 24 hours).

Figure 5.10 Effect of varying SrUGT76G1 for CBD glycosides synthesis reaction (1 mM CBD, 8 mM $MgCl_2$, 50 mM potassium phosphate buffer, pH 7.2, 100 mM sucrose, 4 µg Susy, 0.3 mM UDP, incubated at 30°C for 24 hours).

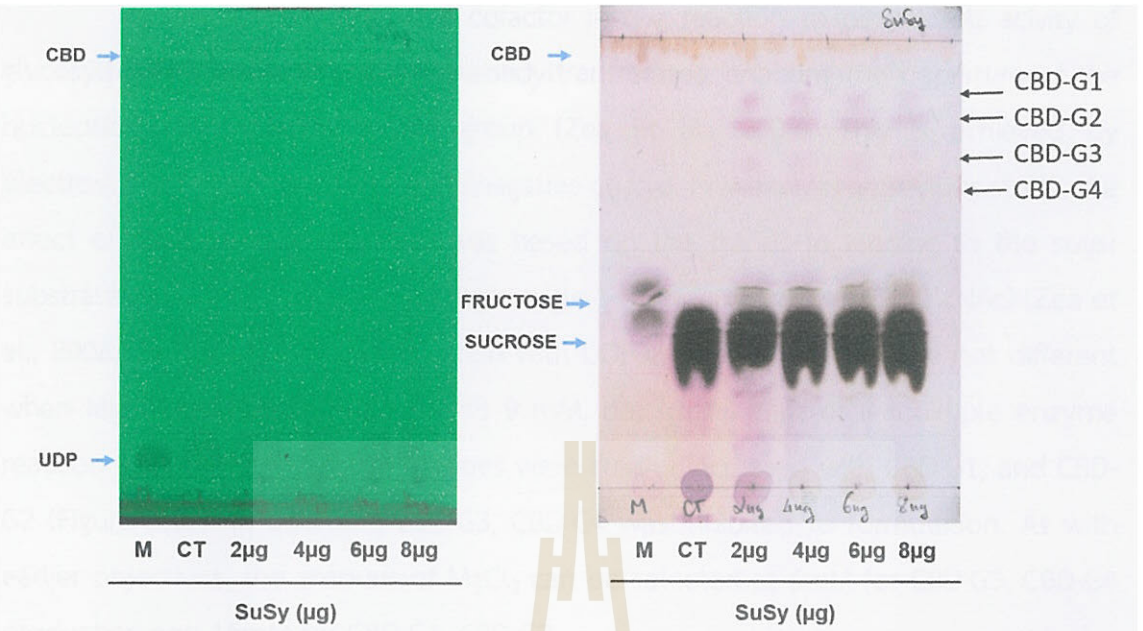

Figure 5.11 Effect of varying SuSy for CBD glycosides synthesis reaction (1 mM CBD, 8 mM $MgCl_2$, 50 mM potassium phosphate buffer, pH 7.2, 100 mM sucrose, 0.3 mM UDP, 10 µg SrUGT76G1 incubated at 30°C for 24 hours).

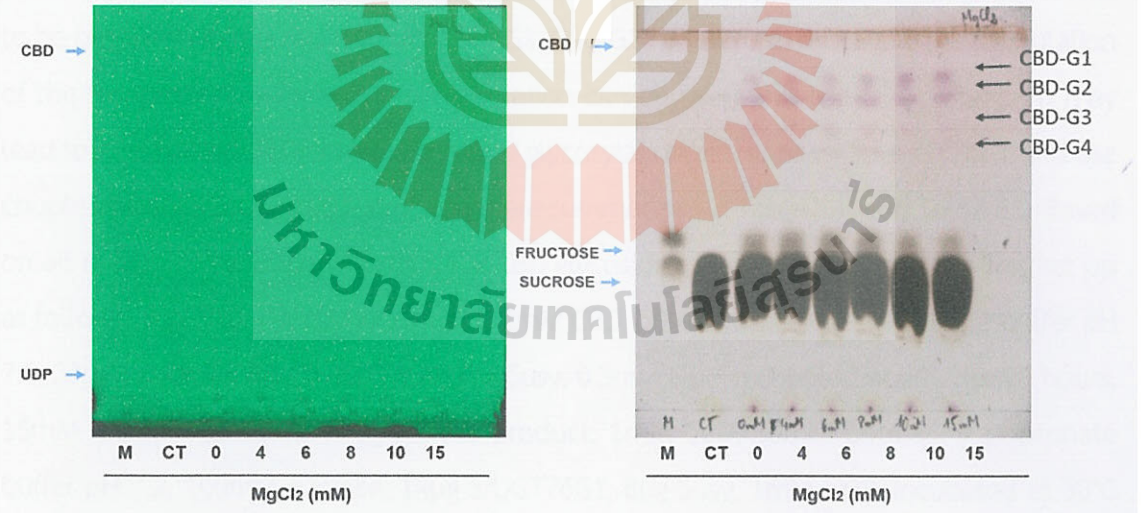

Figure 5.12 Effect of varying $MgCl_2$ for CBD glycosides synthesis reaction (1 mM CBD, 50 mM potassium phosphate buffer, pH 7.2, 100 mM sucrose, 10 µg SrUGT76G1, 4 µg Susy, 0.3 mM UDP, incubated at 30°C for 24 hours).

$MgCl_2$ functions as a cofactor in the reaction to permit full acivity of glycosyltransferases and sugar nucleotidyltransferases, enabling the departure of the nucleotide diphosphate leaving group (Zea et al., 2008). This is achieved by electrostatically stabilizing the rising negative charge. However, in a previous study, the effect of Mg^{+2} on the substrate was based on the trends in binding to the sugar substrates (UTP> UDP> UMP ≈ UDP-glc ≈ glc-1-P ≈ GlcNAc-1-P > UDP-GlcNAc) (Zea et al., 2008). In the case of glycosylation with UDP-glc, the products were not different when $MgCl_2$ increased from 3mM to 9 mM, but in the case of a muiltiple enzyme reaction with UDP, the CBD glycosides were clearly increased with CBD-G1, and CBD-G2 (Figure 5.12). In addition, CBD-G3, CBD-G4 was inhibited to formulation. As with earlier objectives, the amount of $MgCl_2$ can be selected at 6mM for CBD-G3, CBD-G4 production and 15mM for CBD-G1, CBD-G2.

As mentioned earlier, CBD is low-soluble in water, so a high CBD concentration may be excessed or separated on the surface of the reaction. Therefore, the CBD concentration range 0.5mM to 4mM in the glycosylation reaction was significant, showing an increase in the effect of the CBD-G1 formulation while CBD-G2 formulation was constant (Figure 5.13). Due to high concentration of $MgCl_2$, the CBD glycosides were forced to be produced in the top product (CBD-G1, CBD-G2). Therefore, by forcing the formulation of the top product, a high CBD concentration can be used, but the CBD conversion may lead to a reduction. All the factors in CBD glycosylation reactions with SrUGT76G1 and the couple enzymes SrUGT76G1 and SuSy were summarized in Table 5.1, and Table 5.2. Based on all results of variation of factors for CBD glycosides reaction, the condition was set up as follows: top CBD glycosides product: 2mM CBD, 50mM potassium phosphate buffer pH 7.2, 20mM sucrose, 8µg SrUGT76G1, 4µg Susy, 0.3mM UDP, incubated at 30°C for 24 hours, 15mM $MgCl_2$; bottom CBD glycosides product: 1mM CBD, 50mM potassium phosphate buffer pH 7.2, 100mM sucrose, 14µg SrUGT76G1, 8µg Susy, 1mM UDP, incubated at 30°C for 24 hours, 6mM $MgCl_2$.

SuSy enzyme has high stability at temperatures below 30°C (Schmölzer et al., 2016). Therefore, the CBD glycosylation reaction was varied from day 1 to day 5 to check stability of SrUGT76G1 enzyme. The results indicated that at condition 1, CBD glycosides product was forced to produce at CBD-G1, CBD-G2; at condition 2 was gained more product in the bottom. It was significant with hypothesis in optimization

discussion. From Figure 5.14, Figure 5.15, the results indicated that at day 5 of reaction, the CBD glycosides can be collected to move to purification step.

Table 5.1 Effect of factors on the CBD glycosylation reaction with SrUGT76G1 alone.

Factors	Solvents		$MgCl_2$	SrUGT76G1	CBD	Time
CBD Glycosides	Methanol	Acetone				
CBD-G1	↑	↑	CT	↑	↑	↓
CBD-G2	CT	↑	CT	↑	↑	↑
CBD-G3	↓	↑	-	↑	↓	↑

Table 5.2 Effect of factors on the CBD glycosylation reaction with SrUGT76G1 and SuSy.

Factors	Solvents	Sucrose	UDP	SrUGT76G1	SuSy	$MgCl_2$	CBD	Time
CBD-G1	↑	↓	↓	↓	↓	↑	↑	↓
CBD-G2	↓	↑	↑	↑	↑	CT	CT	↑
CBD-G3	↓	↑	↑	↑	↑	↓	-	↑
CBD-G4	-	-	-	-	↑	↓	-	↑
CBD-G5	-	-	-	-	-	-	-	↑

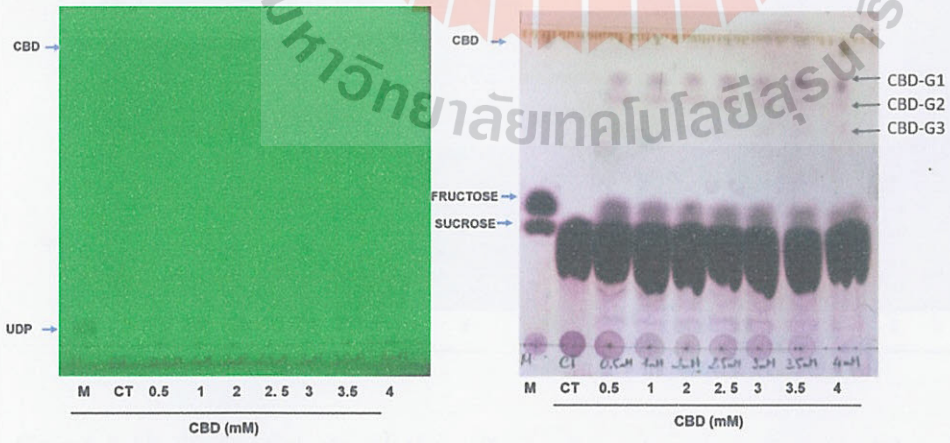

Figure 5.13 Effects of varying CBD for CBD glycosides synthesis reaction (50 mM potassium phosphate buffer, pH 7.2, 100 mM sucrose, 10 µg SrUGT76G1, 4 µg Susy, 0.3 mM UDP, 15 mM $MgCl_2$, incubated at 30°C for 24 hours).

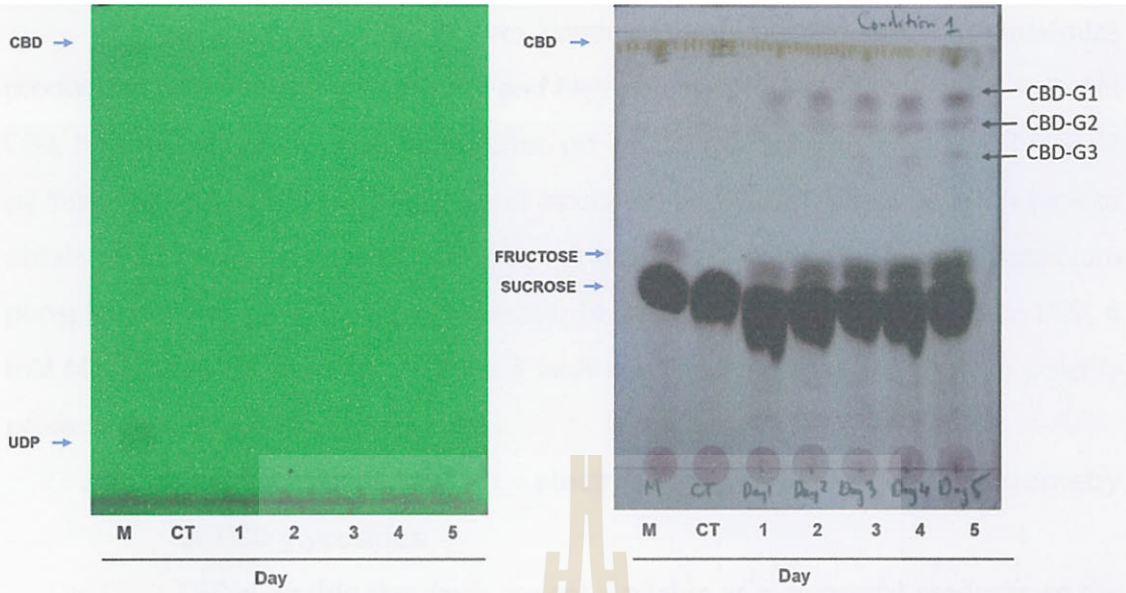

Figure 5.14 TLC analysis of the effects of varying time for condition 1 of the CBD glycosides synthesis reaction (2 mM CBD, 50 mM potassium phosphate buffer, pH 7.2, 20 mM sucrose, 8 µg SrUGT76G1, 4 µg Susy, 0.3 mM UDP, and 15 mM $MgCl_2$, incubated at 30°C for 24 hours).

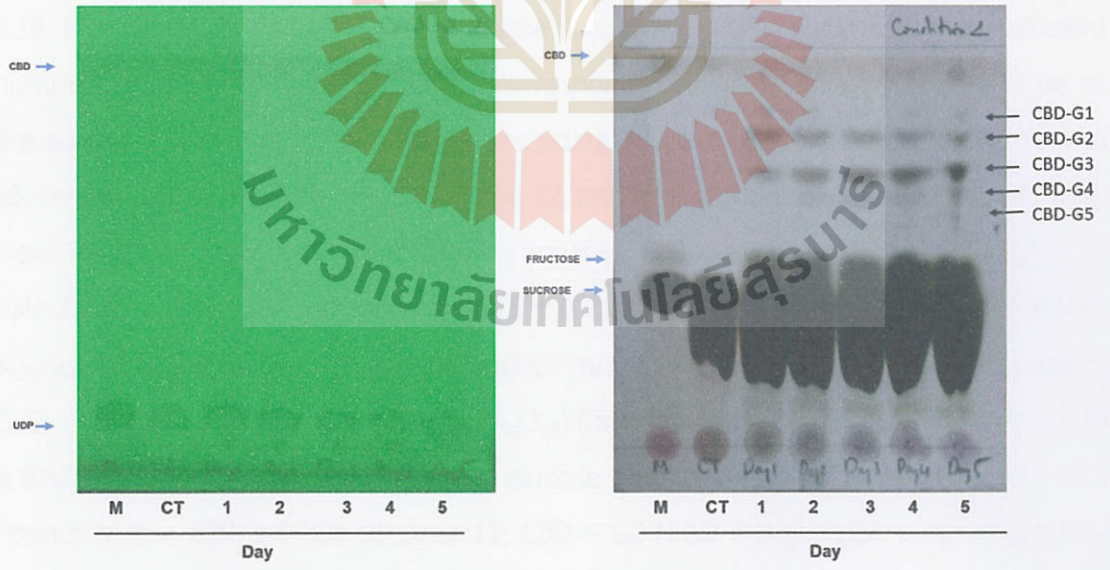

Figure 5.15 TLC analysis of the effect of varying time for condition 2 of the CBD glycosides synthesis reaction (1 mM CBD, 50 mM potassium phosphate buffer, pH 7.2, 100 mM sucrose, 14 µg SrUGT76G1, 8 µg Susy, 1 mM UDP, 6 mM $MgCl_2$, and incubated at 30°C for 24 hours).

Based on all results, two conditions can be concluded to maximize production targeting the low polarity and high polarity products. Condition 1 is 2 mM CBD, 50 mM potassium phosphate buffer, pH 7.2, 20 mM sucrose, 8 µg SrUGT76G1, 4 µg Susy, 0.3 mM UDP, 15mM $MgCl_2$, and incubated at 30°C for 5 days reaction time to obtain low polarity glycosides. Condition 2 includes 1 mM CBD, 50 mM potassium phosphate buffer, pH 7.2, 100 mM sucrose, 14 µg SrUGT76G1, 8 µg Susy, 1 mM UDP, 6 mM $MgCl_2$, and incubated at 30°C for 5 days reaction time to maximize high polarity products.

5.4.2 Liquid chromatography – electrospray ionization mass spectrometry of CBD glycosides.

CBD glycoside standards are not available as commercial products, so the identification of CBD glycosides was based on LC/MS/MS and comparison with a previous study (Hardman et al., 2017). The suitable CBD glycoside condition was set up and then manual purification by TLC. The CBD glycosides binding in TLC was eluted again in methanol. The sample in methanol was evaporated and concentrated it until dry. And then, LC/MS/MC sample was diluted by water and checked by TLC as shown Figure 5.1. The sample of CBD glycosides was analyzed by LC/MS/MS as shown Figure 5.16. Five peaks: 5, 9, 11, 12, and 13 were identified as CBD glycosides with different numbers of glucose residues. Masses corresponding to the CBD aglycone with up to the addition of four glucose residues, including two glucose residues at peaks 11 and 13, three glucose residues at peaks 9 and 12, and four glucose residues at peak 5. They were identified based on the following masses: CBD aglycone $[CBD + H]^+$ ($C_{21}H_{31}O_2$) Calculated: m/z= 315. Found: m/z = 315 ± 0.23 at peak 14. CBD aglycone $[CBD + Na]^+$ ($C_{21}H_{31}O_2Na$) Calculated: m/z= 501. Found: m/z = 501 ± 0.196 at fraction of peak 5; CBD – G1 $[CBD + 2\ glucose + H]^+$ ($C_{33}H_{51}O_{12}$) Calculated: m/z= 639. Found: m/z = 639 ± 0.338 at peak 13; CBD – G3 $[CBD + 2\ glucose + H]^+$ ($C_{33}H_{51}O_{12}$) Calculated: m/z= 639. Found: m/z = 639 ± 0.336 at peak 11; CBD – G2 $[CBD + 3\ glucose + H]^+$ ($C_{39}H_{61}O_{17}$) Calculated: m/z= 801. Found: m/z = 801 ± 0.386 at peak 12; CBD – G4 $[CBD + 3\ glucose + H]^+$ ($C_{39}H_{61}O_{17}$) Calculated: m/z= 801. Found: m/z = 801 ± 0.390 at peak 9; CBD – G5 $[CBD + 4\ glucose + H]^+$ ($C_{45}H_{71}O_{22}$) Calculated: m/z= 964. Found: m/z = 963 ± 0.442 at peak 5. With long-term separation in LC chromatography, the retention times of all peaks were as follows: peak 5 at 22 min, peak 9 at 23.5 min and peak 10 on its tail at

23.75 min, peak 11 at 25.5 min, peak 12 at 31.5 min, peak 13 at 34 min. The Zorbax SB-C18 was used to separate CBD glycosides, so the polarity of the CBD glycosides can hypothesize that peak 5 > peak 9 > peak 11 > peak 12 > peak 13. Using the Hardman et al. (2017) study as a reference, the structure of CBD glycosides can predict peak 5 with four glucose residues with two on each OH group, peak 9 with three glucose residues with one or two on each OH group, peak 11 with two glucose residues, one on each OH group, peak 12 with three glucose residues with one on each OH group, peak 13 with two glucose residues at one OH group. That was consistent with the mass spectra (fragment masses) of all the peaks. In the case of CBD glycosides, the observed O-linked glycosides contained 1-3 glycosidic linkages per glycon (Hardman et al., 2017). Therefore, the breakdown of the glycon could be the same at 1-3 glycosidic linkage bonds, resulting in the loss in mass corresponding to 1 to 3 glucosyl residues. Moreover, the CBD glycosides with two or three glucose residues on one OH side could be broken down in the same way in mass spectra as well, or could be released by breakage of the glycosidic bond to CBD, which appears to break more easily. Figure 5.17 shows peak 5 – CBD-G5 with 4 glucoses, the fragment mass followed two main peaks (CBD with four glucose residues (963.442), CBD with two glucose residues (639.336), and CBD (315.23)). It was the same pattern of breakdown as peak 9 – CBD-G4 (both OH groups glycosylated- CBD with three glucose residues (801.39), CBD with two glucose residues (639.33), CBD with one glucose residue (477.287), and CBD (315.23)) (Figure 5.18), peak 11 – CBD-G3 (both OH glycosylated - CBD with two glucose residues (639.336), CBD with one glucose residue (447.284), and CBD (315.23)) (Figure 5.19), but peak 12 – CBD-G2 (one side OH glycosylated – CBD with three glucose residues (801.386), and CBD (315.23)) (Figure 5.20), peak 13 – CBD –G1 (one side OH glycosylated – CBD with two glucose residues (639.338), and CBD (315.235)) (Figure 5.21). From the results of optimization in TLC and the results of the structure of CBD glycosides, a deep understanding of CBD glycosylation was obtained. The SrUGT76G1 preferred to glycosylate on another glucose residue more than on the second OH group on the other side of the CBD structure. It was significant because glucose has more OH groups available. In the case of targeting the OH groups both sides, the reaction can be set up with high sucrose, high UDP, and SrUGT76G1 as discussed above. In addition, the rotational freedom of CBD along the C1' axis allows the resorcinol ring

to rotate and swing the second hydroxyl group towards the catalytic site of SrUGT76G1 (Hardman et al., 2017). Therefore, two isomers of CBD-G1, CBD-G2, and CBD-G4 are the same in structure (Figure 5.22).

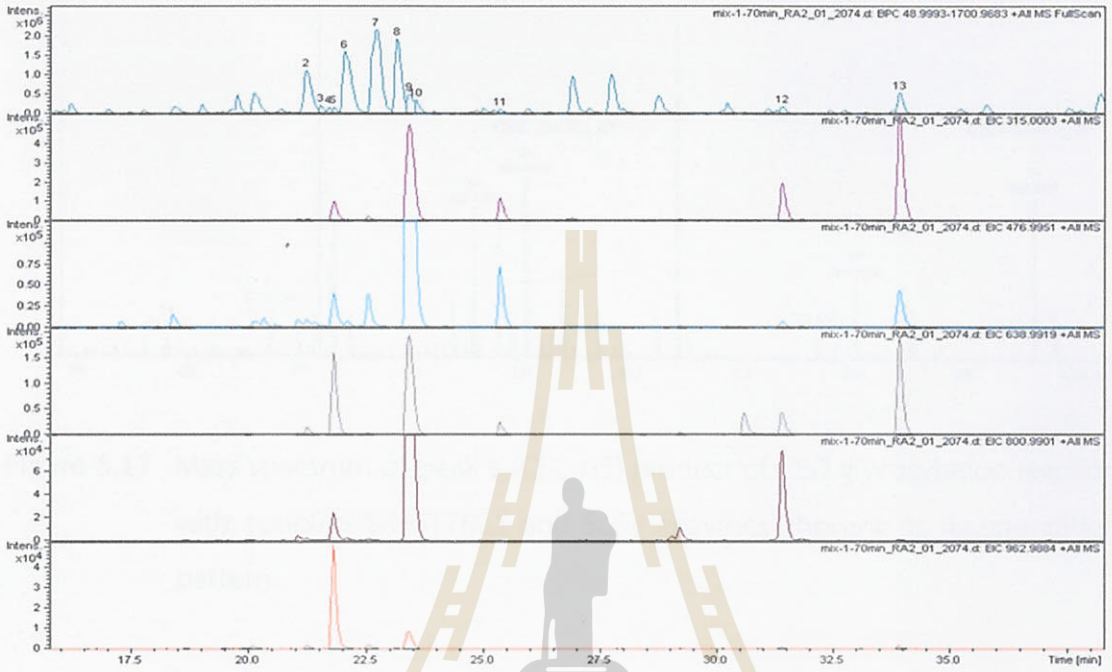

Figure 5.16 LC-MS/MS analysis of CBD glycosides sample and extract peak from their spectrum (A) and extraction peak based on mass 315 (B), 477 (C), 639 (D), 801 (E), 963 (F).

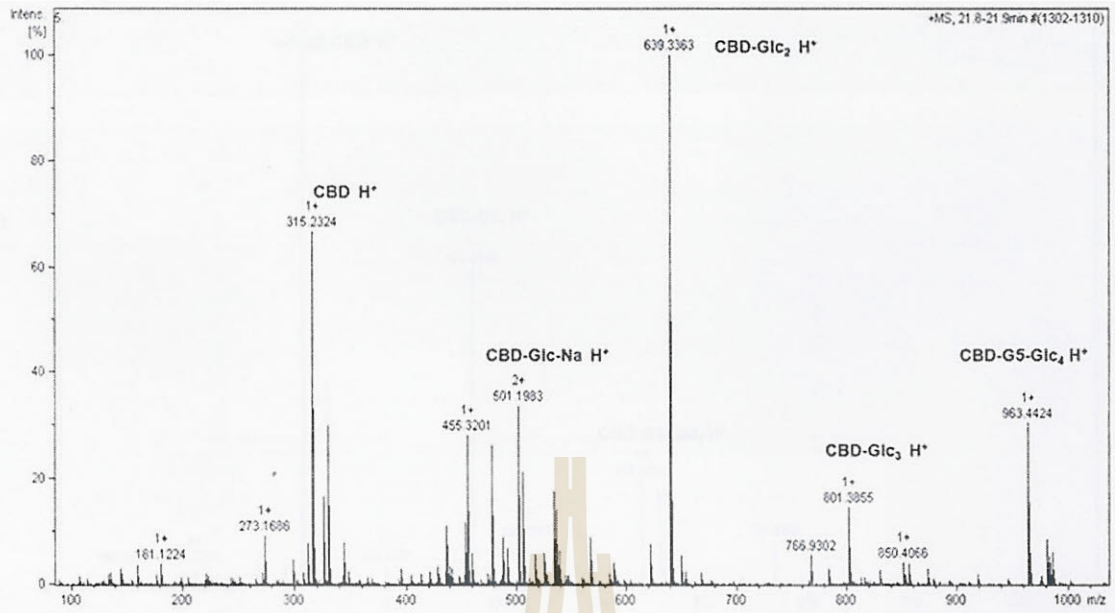

Figure 5.17 Mass spectrum of peak 5 (CBD-G5) product of CBD glycosylation reaction with coupled SrUGT76G1 and SuSy enzymes showing its fragmentation pattern.

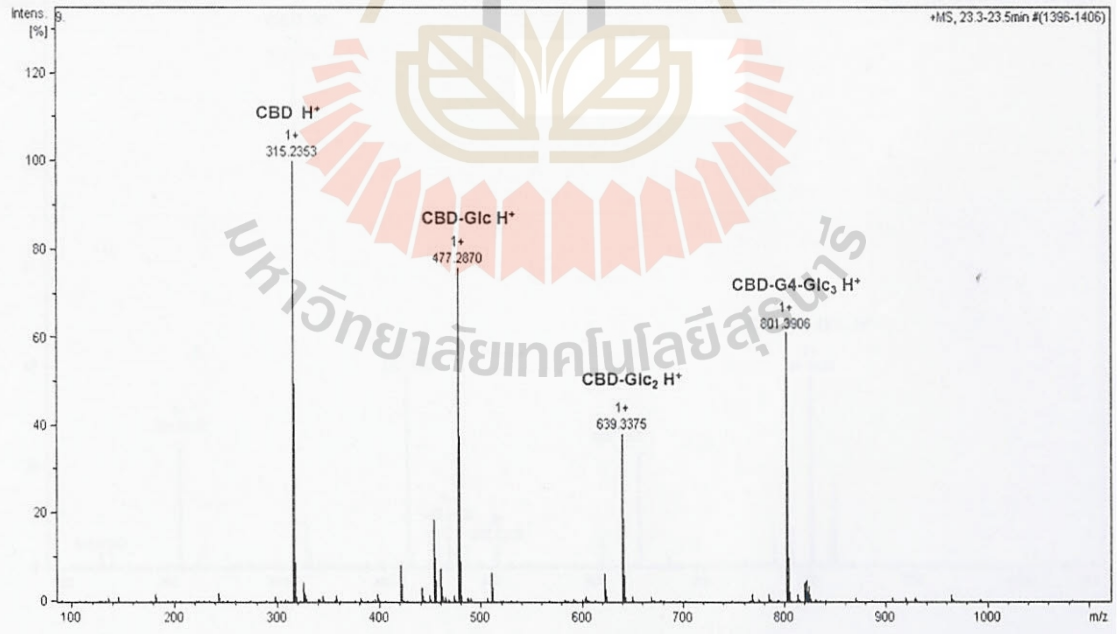

Figure 5.18 Mass spectrum of peak 9 (CBD-G4) product of CBD glycosylation reaction with coupled SrUGT76G1 and SuSy enzymes showing its fragmentation pattern.

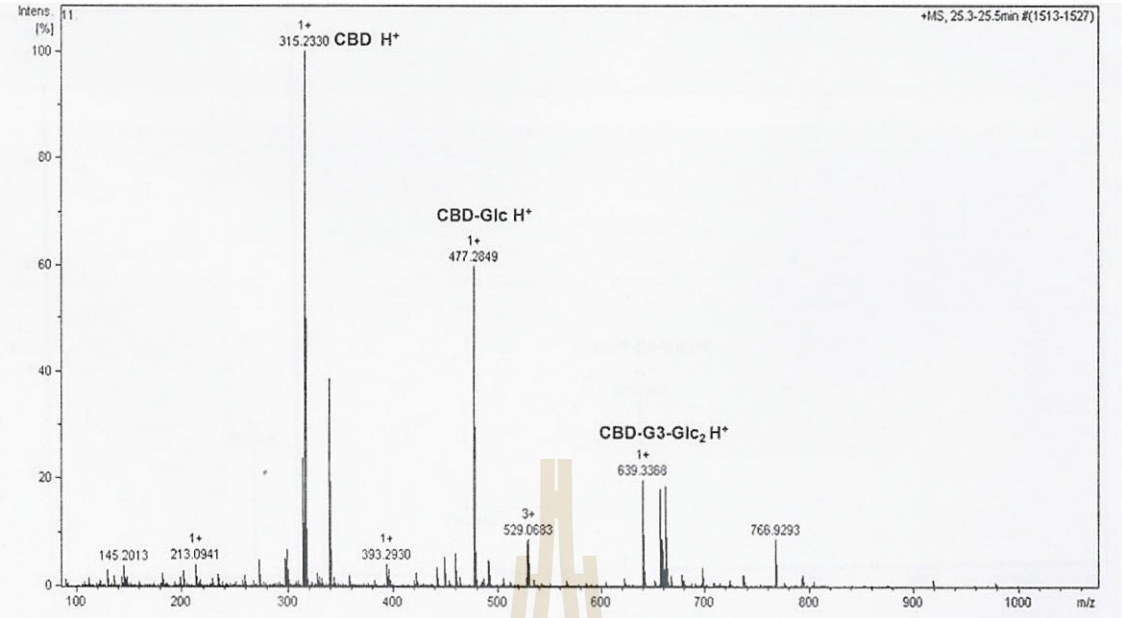

Figure 5.19 Mass spectrum of peak 11 (CBD-G3) product of CBD glycosylation reaction with coupled SrUGT76G1 and SuSy enzymes showing its fragmentation pattern.

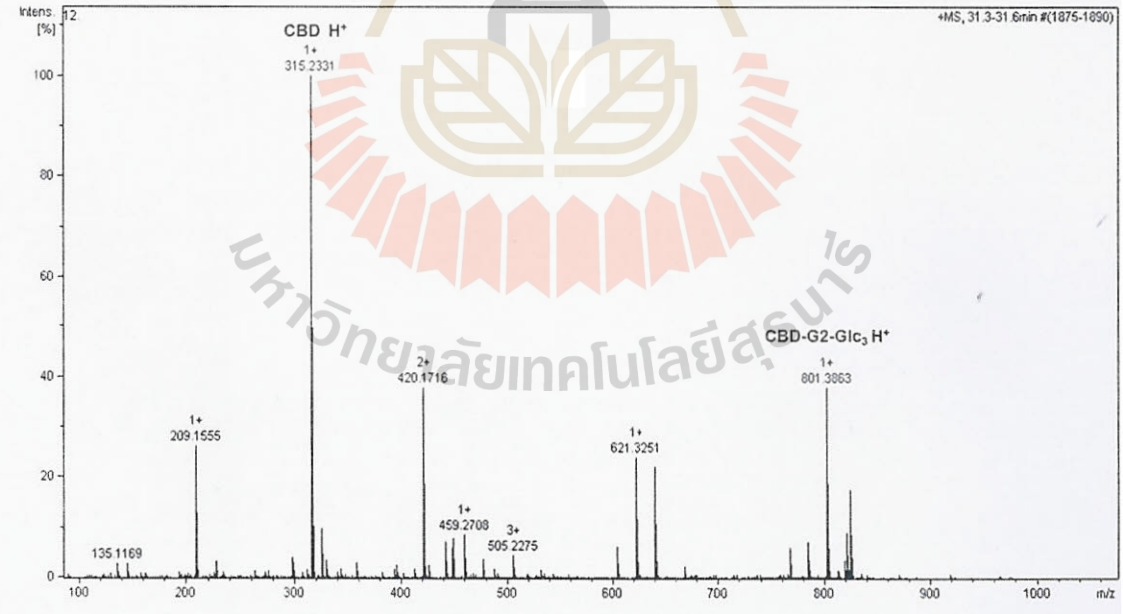

Figure 5.20 Mass spectrum of peak 12 (CBD-G2) product of CBD glycosylation reaction with coupled SrUGT76G1 and SuSy enzymes showing its fragmentation pattern.

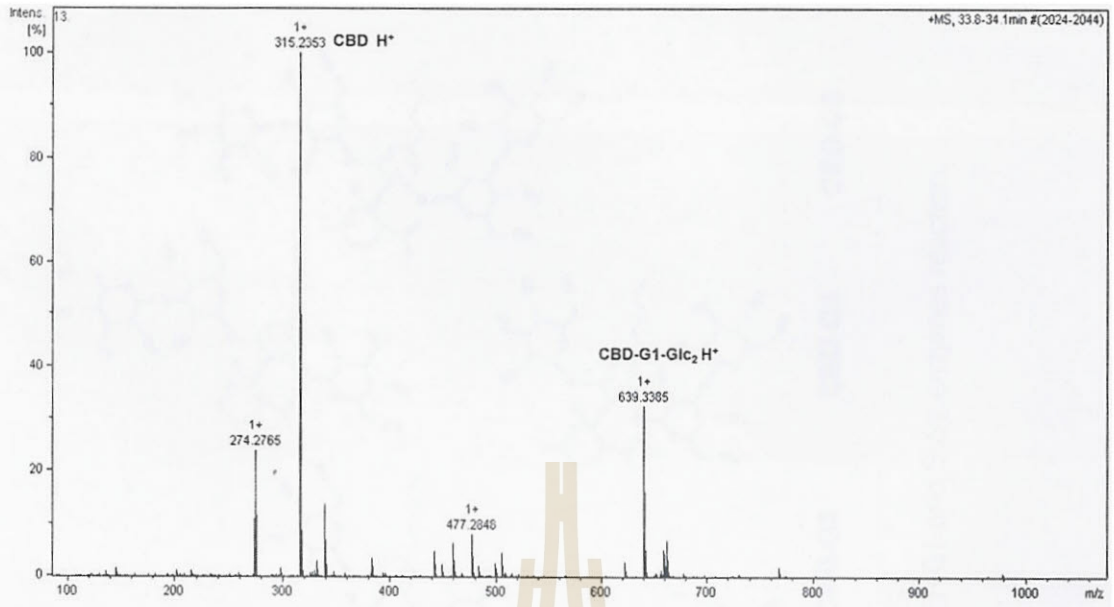

Figure 5.21 Mass spectrum of peak 13 (CBD-G1) product of CBD glycosylation reaction with coupled SrUGT76G1 and SuSy enzymes showing its fragmentation pattern.

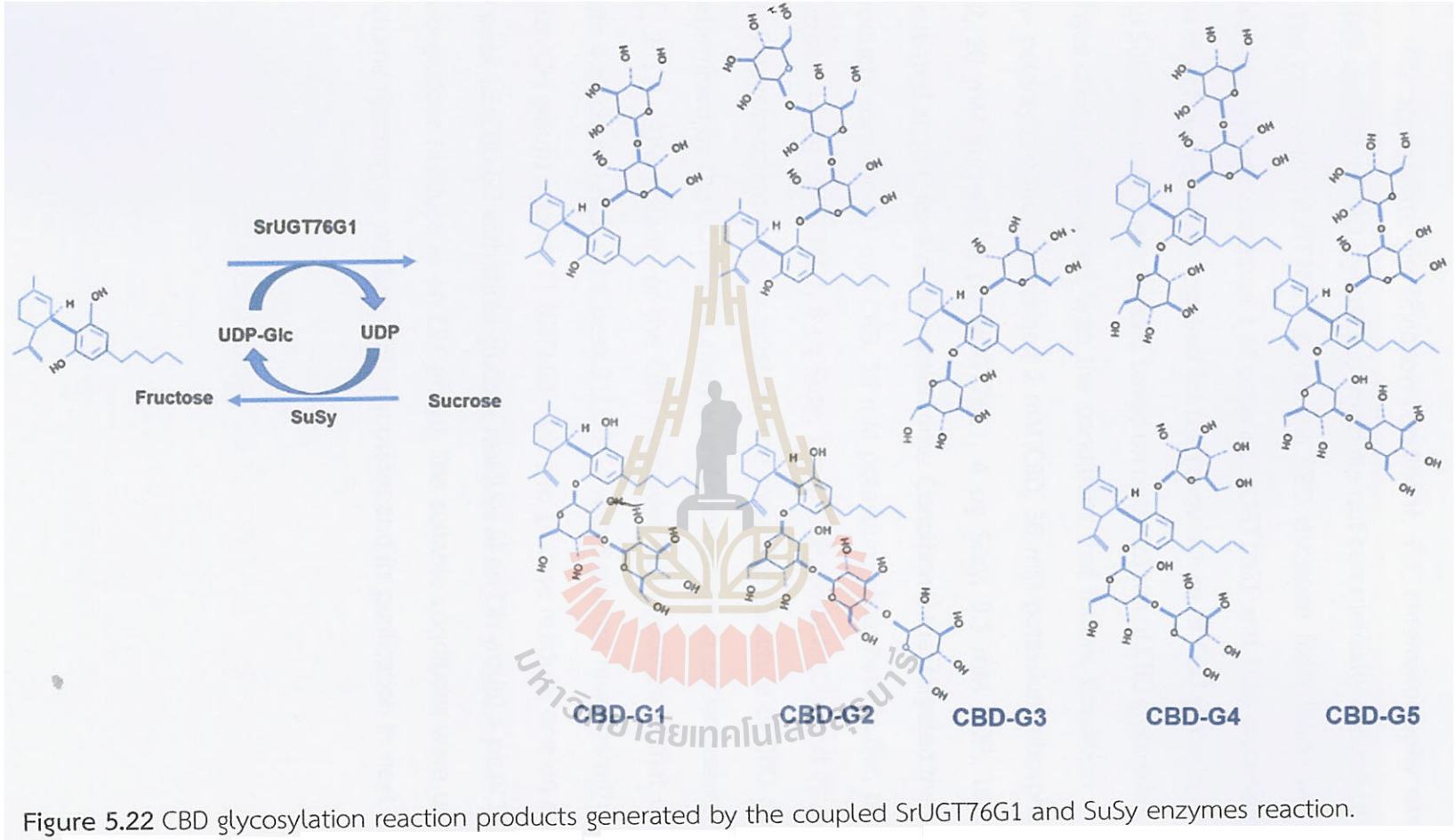

Figure 5.22 CBD glycosylation reaction products generated by the coupled SrUGT76G1 and SuSy enzymes reaction.

5.5 Conclusion

For appropriate glycosylation conditions, TLC chromatography can be used to obtain qualitative CBD glycosides, which are not commercially accessible as standards. In the case with SrUGT76G1 alone, the CBD glycoside formulation was low polarity which similar with condition 1 of coupled SrUGT76G1 and SuSy glycosylation reaction. The direct glycosylation required for the manufacture of CBD glycoside by SrUGT76G1 and SuSy was well characterized based on optimization of CBD glycosides. Two product ranges could be targeted, with the conditions that follow. Condition 1 that targeted low polarity products contained 2 mM CBD, 50 mM potassium phosphate buffer, pH 7.2, 20 mM sucrose, 8 µg SrUGT76G1, 4 µg Susy, 0.3 mM UDP, 15mM $MgCl_2$ and incubated at 30°C for 5 days reaction time. Condition 2 that targeted the higher polarity products contained 1 mM CBD, 50 mM potassium phosphate buffer, pH 7.2, 100 mM sucrose, 14 µg SrUGT76G1, 8 µg Susy, 1 mM UDP, 6mM $MgCl_2$, and incubated at 30°C for 5 days reaction time. In addition, the mass and structure of CBD glycosides were determined by the LC/MS/MS analysis and comparison to earlier research (Hardman et al., 2017). The polarity of the CBD glycosides can hypothesize that peak 5 (CBD-G5 with 4 glucoses residues) > peak 9 (CBD-G4 with 3 glucose residues with one or two on each OH group) > peak 11 (CBD-G3 with two glucose residues one on each OH group) > peak 12 (CBD-G2 with three glucose residues at on OH group) > peak 13 (CBD-G1 with two glucose residues at on OH group). The suitable conditions were used to increase volume reaction to produce CBD glycosides and its purification in next step.

CHAPTER VI

PURIFICATION OF CANNABIDIOL GLYCOSIDES

6.1 Abstract

Using silica gel chromatography and flash/preparative HPLC, this chapter reports the partial removal of most impurities from CBD glycosides after synthesis reaction. From silica gel chromatography, the most impurities were removed, especially sucrose, which was hardly eluted all in C18-resin column. In addition, the CBD-G1 was isolated by 5% methanol in ethyl acetate fractions of silica gel chromatography and purified more by a mini C18-resin column. For flash/preparative HPLC, the mixed CBD glycosides formulation was found in fractions 23 and 24 at around 27-28% acetonitrile in water and the CBD-G2 was eluted at fractions 31 and 32 at around 40% acetonitrile in water.

6.2 Introduction

The cannabidiol glycosides are prodrugs with many advantages over the original cannabidiol, such as improving the solubility, stability, bioavailability, and pharmacokinetic characteristics (Zipp et al., 2017). In addition, the CBD glycosides were produced by the SrUGT76G1 enzyme from *Stevia rebaudiana* in a previous study (Hardman et al., 2017). Furthermore, *Glycine max* sucrose synthase (SuSy) is highly active in the synthesis of UDP-glc. The coupled SrUGT76G1 and SuSy enzymes cascade reaction was developed to synthesize glycoside compounds using cheap sucrose as the expedient glucosyl donor (Pei et al., 2017) (Hu et al., 2020). The optimization of CBD glycosides synthesis was successfully done by coupled SrUGT76G1 and SuSy enzymes in Chapter 5. However, with many substrates in the reaction as impurities, so the isolation and purification of CBD glycosides was challenging. In the case of CBD glycosides, their formulas were closely similar, with 2 glucose residues, 3 glucose residues, and 4 glucose residues. The most common techniques for purification include C18-resin column and silica gel column,

precipitation based on polarity of solvent, and so on. In the previous paper, CBD glycosides compounds (VB110, and VB104) could be purified with the HyperSep™ C18 cartridge column at 60% methanol in water (Hardman et al., 2017). However, the high concentration of sucrose is hardly eluted all by water in the C18 column.

In this study, the combination of silica gel chromatography and flash/ preparative HPLC was successfully used to partially purify CBD glycosides. The solvent with 0% to 20% methanol in ethyl acetate was applied to the purification of CBD glycosides in silica gel chromatography. The solvent with 5% methanol in ethyl acetate was isolated mostly CBD-G1, which was then further purified using a mini C18-resin column. In addition, the formulation of CBD-G2 was also isolated in flash/preparative HPLC with around 40% acetonitrile in water. The mixed CBD glycosides was partially purified in fractions 23 and 24 with solvent composition of around 28% acetonitrile in water.

6.3 Materials and Methods

6.3.1 Materials

The CBD glycosides produced in the coupled SrUGT76G1 and SuSy enzymes system in chapter 5 (15 ml volume reaction of condition 1 and 15 ml volume reaction of condition 2), were used to purification. Thin-layer chromatography was purchased from Chemical Express Co., Ltd. (Bangkok, Thailand). All chemicals used in this study were of analytical grade from various suppliers.

6.3.2 Silica gel column chromatography

The reaction was dried by a freeze dryer and then diluted again with ethyl acetate. Based on precipitation of polarity of ethyl acetate solvent, the most hydrophilic compound was not diluted in solvent. After several times wash with ethyl acetate for extraction of CBD glycosides, the sample was evaporated and mixed with methanol and 3 spoons of silica gel as silica gel sample preparation. Due to silica gel dissolving in methanol, the compound was mixed well with silica gel. And then, the sample was evaporated until dry again. After that, the sample adsorbed onto silica gel and was applied to the top of a silica gel column chromatography and eluted with a solvent system of ethyl acetate: methanol. The CBD, and CBD glycosides were eluted by 0%, 5%, 7%, 8%, 10%, 20% methanol. The fractions were monitored by

silica gel TLC 60 F254 using butanol: acetic acid: water (3:1:1 v/v/v) as mobile phase. The process of silica gel chromatography is shown Figure 6.1.

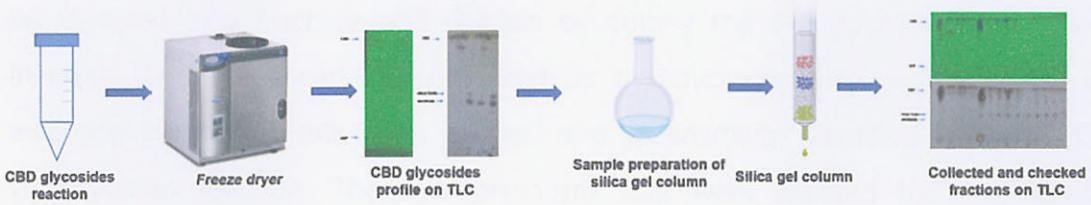

Figure 6.1 Process of silica gel chromatography.

6.3.3 Flash/Preparative HPLC

The sample of CBD glycosides was checked in TLC and further fractionated on a BUCHI Pure Flash/Prep HPLC Model C-850 (Flawil, Switzerland) in flash mode with A water and B acetonitrile as the mobile phase. The gradient elution was performed using the following solvent gradient: starting with DI water for 10 min, then ramping to 20% solvent B over 5 min, and then increasing to 35% B over 10 min, ramping again to 42% B over 5 min, increasing to 50% B over 5 min, and then ramping again to 70% in 5 min, and then ramping to 100% B in 3 min and holding at 100% for 7 min. The sample was injected as liquid sample into the HPLC system with an FP ECOFLEX C18 4g column. The flow rate was 10 ml/min, and the analysis wavelengths were 200, 210, 220, and 240 nm. The fractions were monitored and confirmed by silica gel TLC 60 F254, as described above.

6.4 Results and discussions

In the CBD glycosides reaction, the impurities are UDP, UDP-Glc, sucrose, fructose, excess CBD, enzymes, and salts. The strategy was set up to remove all impurities and take off the CBD glycosides, and included invertase microorganisms, silica gel chromatography, and flash/preparative HPLC.

6.4.1 Invertase microorganism isolation for sugar digestion

The sugars contained in the CBD glycoside synthesis reaction products were sucrose, and glucose, or fructose which are nutrients for microorganisms to grow. However, the sugar in CBD glycosides was also an impurity which must be

removed after finishing the reaction. In the CBD glycosylation, sucrose was used as the main substrate with high concentration in the reaction, with final concentrations of 20 mM and 100 mM. Based on invertase microorganism characteristics, sucrose can be digested into fructose and glucose by cutting the 1-2 glycoside linkage with invertase and these can be consumed by the microorganism. In this study, the invertase microorganisms were isolated and preliminarily identified from the CBD glycosylation reaction. The microorganisms that were isolated by streaking the reaction solution from which sucrose had disappeared onto an LB agar plate, 7 colonies were isolated and cultured in Basal medium with 10 g/L sucrose, 2.5 g/L $NaNO_3$, 0.5 g/L $MgSO_4.7H_20$, 1.5 g/L KH_2PO_4. The culture conditions were 5 mL medium, 30°C, and 200 rpm, orbital shaking overnight. All supernatants from culture of 7 colonies were collected and tested with sucrose. The reaction was 50% v/v culture supernatants, 20 mM sucrose, and 50 mM sodium phosphate buffer, pH 7.2. The reaction was incubated at 60 degrees for 1 hour. The DNS assay was used to compare the activities of the incubated at seven colonies. Based on the absorbance wavelength at 540 nm, the invertase enzyme activity (Figure 6.2) showed that all colonies had activity, with the highest in colony 1. It was chosen for sugar digestion in the CBD glycosides reaction. The Gram staining technique for bacteria was used to identify the microorganism, which was a Gram negative bacterium with a red color that was observed under a microscope (Figure 6.2). However, the concentration of sucrose at 100 mM inhibited the invertase microorganism. Therefore, the invertase microorganism can only be used with 20 mM sucrose condition. However, the byproduct (under UV 254nm) was formed during sugar digestion (Figure 6.2).

6.4.2 Purification of CBD glycosides by silica gel column chromatography

The CBD glycoside samples, after drying in a freeze dryer, were dissolved again in ethyl acetate solvent. The CBD glycosides product were diluted well in ethyl acetate solvent (it was checked ratio in TLC, data no shown), but the hydrophilic compounds were less dissolved in ethyl acetate. The results are shown in Figure 6.3. The reaction for synthesis of CBD glycosides was set up in 10 ml at condition 1 of CBD glycosides synthesis reaction (Chapter 5) and then using sugar removed by microorganism, 5 ml at condition 2 of CBD glycosides synthesis reaction (Chapter 5), 5 ml at condition 1 of CBD glycosides synthesis reaction, 10 ml volume

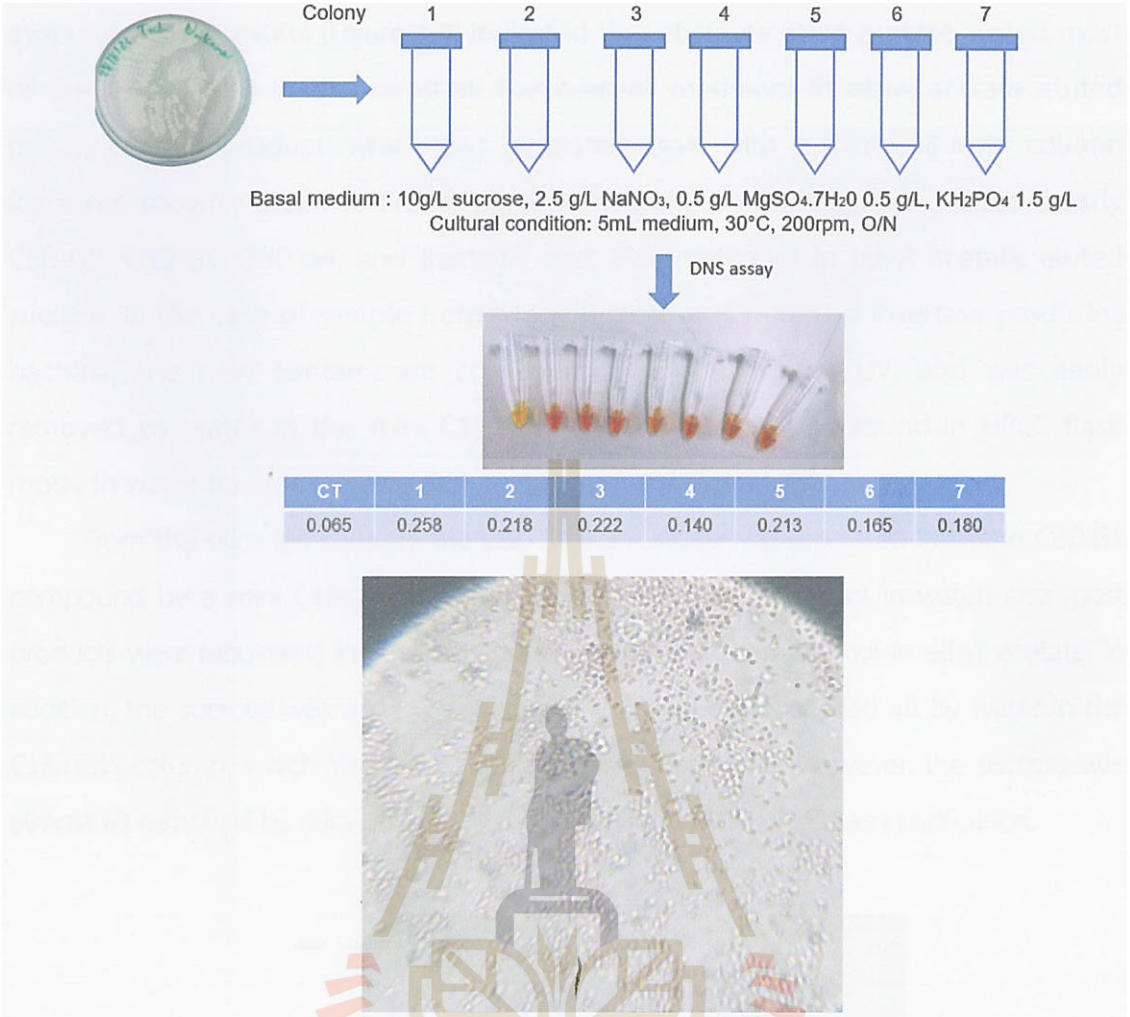

Figure 6.2 DNS assay for invertase microorganism and itself under microscope with gram dyeing technique.

reaction at condition 2 of CBD glycosides synthesis reaction following 1, 2, 3, and 4 in Figure 6.3, respectively. The objective of the silica gel column was to separate almost hydrophilic compounds, especially sucrose, salts, enzymes, UDP and UDP-Glc, and some forms of CBD glycosides. The hydrophilic compounds are tightly absorbed by silica gel. That is a principle for applying silica gel to CBD glycosides purification. All the samples were mixed together with silica gel and methanol. The silica gel can dissolve in methanol that make a change for hydrophilic compound absorbed to the first amount of silica gel sample. The solvents with 0% - 20% methanol in ethyl acetate were used as the mobile phase for CBD glycosides elution. The elution fractions for the silica gel column were collected and concentrated by rotary

evaporator. The results (Figure 6.4) indicated that absolute ethyl acetate eluted most of the excess CBD in the samples; five percent methanol in ethyl acetate eluted mostly CBD-G1 product, which was separated again with a mini C18-resin column (data not shown); seven to fifteen percent methanol in ethyl acetate eluted mostly CBD-G2, CBD-G3, CBD-G4, and fructose; and 20% methanol in ethyl acetate eluted sucrose. In the case of sample from which sucrose was removed invertase producing bacteria, the new contaminant compound was seen under UV, and was easily removed by water in the mini C18-resin column. It was also found in HPLC flash mode in water fractions (Figure 6.5).

From the silica gel column, the CBD-G1 fractions can be separated from the CBD-G1 compound by a mini C18-resin column at 50% and 60% methanol in water, and most products were recovered in fractions containing 5% to 20% methanol in ethyl acetate. In addition, the sucrose was a sticky compound that was hardly eluted all by water in the C18-resin column, which interfered with the purification result. However, the sucrose was almost all removed by silica gel, which supported further for HPLC flash purification.

Figure 6.3 CBD glycosides sample with difference condition. (1. 10 ml sample at condition 1 of CBD glycosides synthesis reaction and then using sugar removed by microorganism, 2. 5 ml sample at condition 2 of CBD glycosides synthesis reaction, 3. 5 ml sample at condition 1 of CBD glycosides synthesis reaction, 4. 10 ml sample condition 2 of CBD glycosides synthesis reaction.

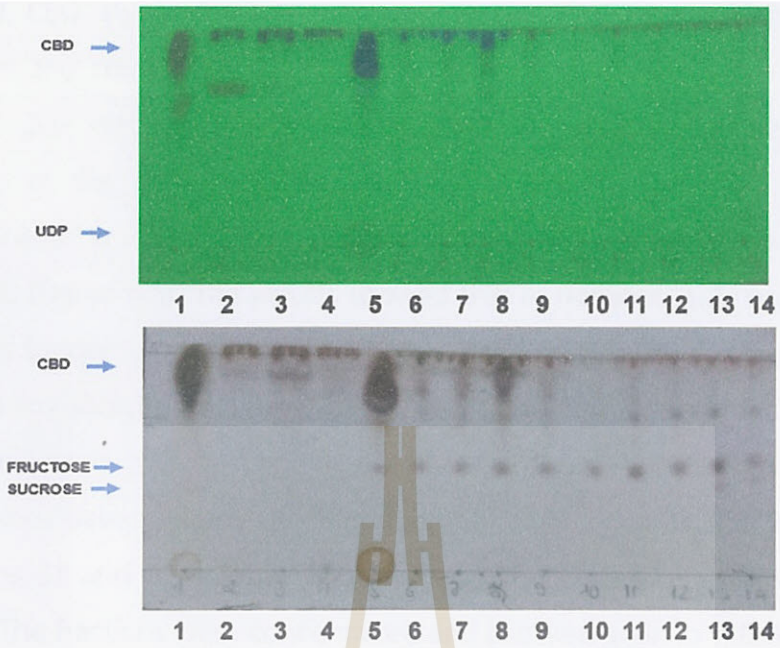

Figure 6.4 TLC of fractions from silica gel chromatography eluted with 0% to 20% methanol in ethyl acetate. (1. 100 ml Absolute ethyl acetate; 2. 100 ml of 5% methanol in ethyl acetate; 3. 100 ml of 5% methanol in ethyl acetate; 4. 100 ml of 5% methanol in ethyl acetate; 5. 100 ml of 5% methanol in ethyl acetate; 6. 100 ml of 7% methanol in ethyl acetate; 7. 100 ml of 8% methanol in ethyl acetate; 8. 100 ml of 10% methanol in ethyl acetate; 9. 100 ml of 10% methanol in ethyl acetate; 10. 100 ml of 10% methanol in ethyl acetate; 11. 100 ml of 15% methanol in ethyl acetate; 12. 100 ml of 15% methanol in ethyl acetate; 13. 100 ml of 20% methanol in ethyl acetate; 14. 100 ml of 20% methanol in ethyl acetate).

6.4.3 Purification of CBD glycosides using HPLC flash/preparative

The fractions of 5% to 20% from silica gel chromatography were used for further purification by flash/preparative HPLC. The mixed fractions were evaporated to remove the solvent and eluted with water. The most of the excess CBD was turned into oil and easily removed by the phase separation with water. The sample was filtered and injected into an HPLC. The profile of the CBD glycosides sample was checked by TLC (Figure 6.6), which showed CBD excess, CBD glycosides, fructose and a very small amount of sucrose, along without unknown compound (under UV). The

separation of CBD glycosides was reported in previous paper using water and acetonitrile as the mobile phase (Hardman et al., 2017). With a flow rate of 10 ml/min, and 200 nm, 210 nm, 220 nm, 240 nm absorbance detection, the characteristics of the compound sample after undergoing the flash mode HPLC process are shown in Figure 6.7. An aliquot of 10 µl of each fraction were checked again with TLC (Figure 6.5). The results showed that in fractions 2, 3, and 4, fructose and impurities (under UV) were washed out as early peak in HPLC chromatography. The TLC scanning showed fractions 11, 23, 24, 31, and 32 contained CBD glycosides. The results indicated that fraction 11 was sucrose. However, CBD glycoside forms were not obvious detectable by UV, and all eluted at fractions 23, and 24, with CBD-G2 at fractions 31 and 32. All the CBD glycosides fractions was dried again with a freeze dryer. The fractions were concentrated and checked again in TLC (Figure 6.8).

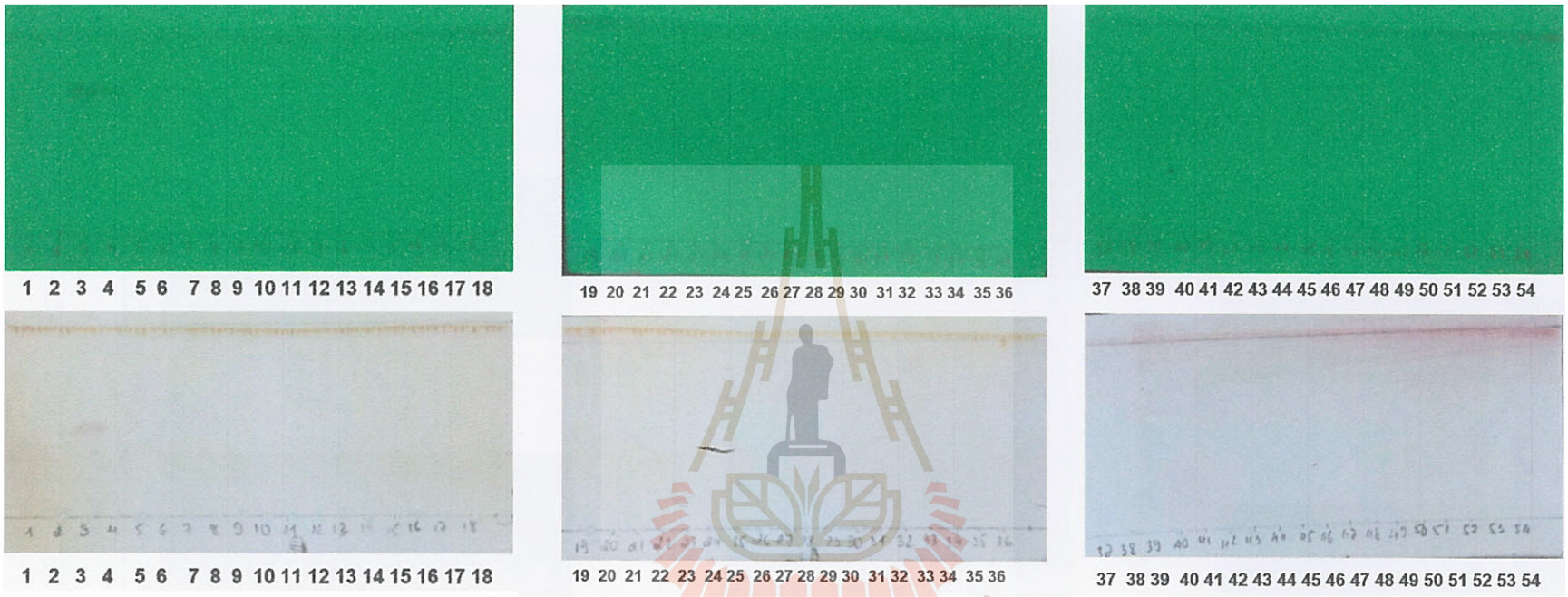

Figure 6.5 The fraction of flash mode HPLC in TLC.

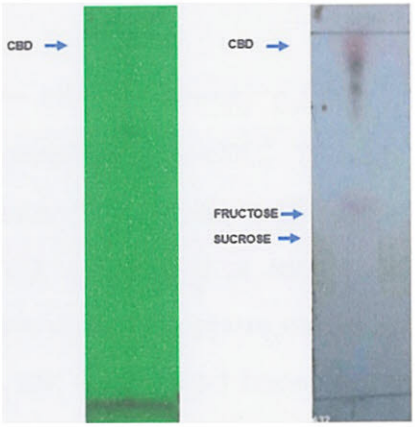

Figure 6.6 TLC profile of CBD glycosides samples for flash/preparative HPLC.

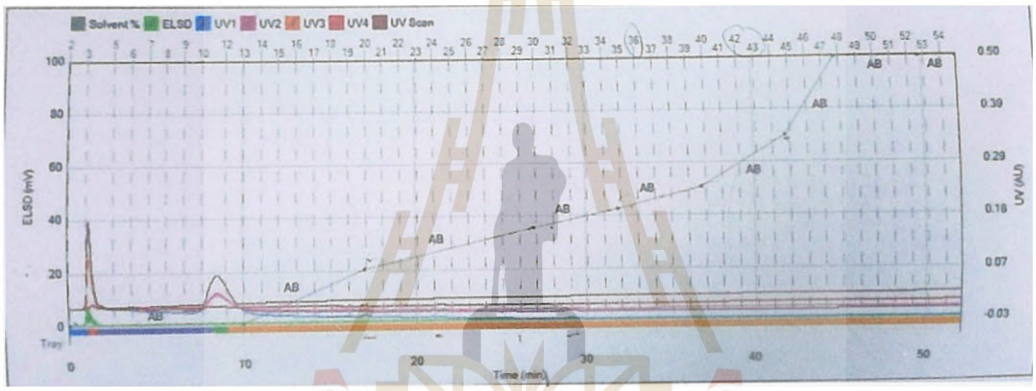

Figure 6.7 The chromatography of CBD glycosides purification in flash mode HPLC.

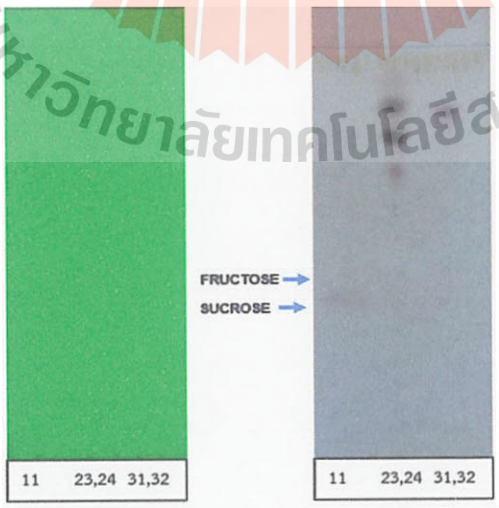

Figure 6.8 The fractions 11, 23+24, and 31+32 of CBD glycoside after HPLC flash on TLC.

6.5 Discussion

The CBD glycosides can be partially purified by a combination of silica gel chromatography and flash/preparative HPLC. Through the use of silica gel and 5% methanol in ethyl acetate, the CBD-G1 was separated from the CBD glycosides synthesis reaction. CBD-G2 was eluted at roughly 40% acetonitrile in water. The mixed CBD glycosides were eluted in approximately 27-28% acetonitrile in water. The lowest polarity CBD-G1 can be purified based on the control time for synthesis reaction of the condition 1 and silica gel chromatography. However, due to similar formulation of CBD glycosides, the mix CBD glycosides may be further purification with other methods.

CHAPTER VII

CONCLUSIONS

7.1 Screening media and suitable expression conditions for SrUGT76G1 and SuSy enzyme production from recombinant *E. coli* BL21(DE3)

The SrUGT76G1 was successfully cloned into pET32a(+) and expressed in *E. coli* BL21(DE3) host cells, in which it had good expression with induction by 0.2 mM IPTG at 20°C overnight. LB broth was a good medium for expression of both SrUGT76G1 and SuSy enzymes compared with TB, SOB, M9 modified, and FM – auto induction media. The suitable expression conditions for SrUGT76G1 and SuSy enzymes were significant in a 2 L shake flask, 5 L fermenter, 50 L fermenter cultures with production yields of 14 mg/L, 15 mg/L, 17.3 mg/L, and 7.3 mg/L, 10.8 mg/L, 14.9 mg/L respectively. These conditions were obtained from Box-Behnken design with five center points and three factors, including temperature, lactose, and time. These findings demonstrate the potential of suitable expression condition as a good condition for enhancing soluble enzymes in *E. coli* BL21(DE3).

7.2 Promise of microfluidization technique for SuSy and SrUGT76G1 enzyme extraction

The microfluidic enzyme extraction method is a substitute for the lysozyme extraction method with many advantages such as applicability to large scale, simple sample preparation, easy management, and protection of the enzyme activity with low temperature. The microfluidic extraction condition was 25 g/L cell concentration, 69 Mpa pressure, used in a single pass to give 86% disruption efficiency, which can benefit the extraction of all enzymes. It was calculated that those parameters can be increased to 150 g/L at 69 Mpa, for 2 time passes with disruption efficiency of 91.33%. The scanning electron microscopy was used to observe the cell shredding to 400-500 nm particles at 86% disruption efficiency.

7.3 Suitable conditions for cannabidiol glycosides production

The suitable CBD glycosylation conditions were obtained with SrUGT76G1 alone and with a coupled SrUGT76G1 and SuSy enzyme system, which reduces the cost of sugar donors by using SuSy to regenerate UDP-Glc. Thin layer chromatography was used to monitor optimization of the CBD glycosides synthesis reaction, which helped to clearly understand the trend of formation of CBD glycosides based on adjusting factors, including $MgCl_2$, CBD, UDP, sucrose, SrUGT76G1, SuSy, acetone concentrations and time. The result of LC/MS/MS was used to confirm the mass of CBD glycosides and based on that the structures were elucidated by comparison with a previous study (Hardman et al., 2017).

7.4 Purification of CBD glycosides using silica gel chromatography and flash/preparative HPLC

Most hydrophilic impurities were removed by silica gel chromatography, including, sucrose, salts, and so on. CBD-G1 was separated by 5% methanol in ethyl acetate, and it was purified with a mini C18 column. In the flash/preparative HPLC, CBD-G2 was isolated at 29 min elution time with 40% acetonitrile in water. The mixed CBD glycosides were eluted at 27-28% acetonitrile in water. The CBD glycosides were partially purified from the CBD glycosides synthesis reaction.

These results provided new insight into the expression conditions for both enzymes for production, the microfluidic extraction enzyme, the coupled SrUGT76G1, SuSy enzyme system to gain more polar glycoside products, and partially purification of CBD glycosides. Future research should look at the fusion for enhancement of the enzymes-soluble and other ways to purify each form of CBD glycosides. The characteristic of each CBD glycoside form may allow more use of CBD glycosides in medical applications, such as cancer and brain disease treatment.

REFERENCES

Aliferis, K.A., Bernard-Perron, D., 2020. Cannabinomics: application of metabolomics in annabis (*Cannabis sativa L.)* research and development. Front. Plant Sci. https://doi.org/10.3389/fpls.2020.00554.

Ashton, C.H., 2001. Pharmacology and effects of cannabis: A brief review. Br. J. Psychiatry 178, 101–106. https://doi.org/10.1192/bjp.178.2.101.

Bernaerts, T.M.M., Gheysen, L., Foubert, I., Hendrickx, M.E., Van Loey, A.M., 2019. Evaluating microalgal cell disruption upon ultra-high pressure homogenization. Algal Res. 42. https://doi.org/10.1016/j.algal.2019.101616.

Black, N., Stockings, E., Campbell, G., Tran, L.T., Zagic, D., Hall, W.D., Farrell, M., Degenhardt, L., 2019. Cannabinoids for the treatment of mental disorders and symptoms of mental disorders: a systematic review and meta-analysis. The Lancet Psychiatry 6. https://doi.org/10.1016/S2215-0366(19)30401-8.

Boyle, J., 2005. Lehninger principles of biochemistry (4th ed.): Nelson, D., and Cox, M. Biochem. Mol. Biol. Educ. 33. https://doi.org/10.1002/bmb.2005.494033010419.

Brandley, B.K., Schnaar, R.L., 1986. Cell-surface carbohydrates in cell recognition and response. J. Leukoc. Biol. https://doi.org/10.1002/jlb.40.1.97.

Bungaruang, L., Gutmann, A., Nidetzky, B., 2013. Leloir glycosyltransferases and natural product glycosylation: Biocatalytic synthesis of the C-glucoside nothofagin, a major antioxidant of redbush herbal tea. Adv. Synth. Catal. 355, 2757–2763. https://doi.org/10.1002/adsc.201300251.

Calapai, F., Cardia, L., Sorbara, E.E., Navarra, M., Gangemi, S., Calapai, G., Mannucci, C., 2020. Cannabinoids, blood–brain barrier, and brain disposition. Pharmaceutics. https://doi.org/10.3390/pharmaceutics12030265.

Cerino, P., Buonerba, C., Cannazza, G., D'Auria, J., Ottoni, E., Fulgione, A., Di Stasio, A., Pierri, B., Gallo, A., 2021. A review of hemp as food and nutritional supplement. Cannabis Cannabinoid Res. https://doi.org/10.1089/can.2020.0001.

Chen, F., Huang, G., 2019. Application of glycosylation in targeted drug delivery. Eur. J. Med. Chem. https://doi.org/10.1016/j.ejmech.2019.111612.

Chen, Fang, Huang, G., Huang, H., 2020. Sugar ligand-mediated drug delivery. Future Med. Chem. https://doi.org/10.4155/fmc-2019-0114.

Chen, L., Cai, R., Weng, J., Li, Y., Jia, H., Chen, K., Yan, M., Ouyang, P., 2020. Production of rebaudioside D from stevioside using a UGTSL2 Asn358Phe mutant in a multi-enzyme system. Microb. Biotechnol. 13, 974–983. https://doi.org/10.1111/1751-7915.13539.

Chen, L., Sun, P., Li, Y., Yan, M., Xu, L., Chen, K., Ouyang, P., 2017. A fusion protein strategy for soluble expression of Stevia glycosyltransferase UGT76G1 in *Escherichia coli*. 3 Biotech 7. https://doi.org/10.1007/s13205-017-0943-y.

Chu, J., Yue, J., Qin, S., Li, Y., Wu, B., He, B., 2021. Biocatalysis for rare ginsenoside rh2 production in high level with co-immobilized UDP-glycosyltransferase bs-yjic mutant and sucrose synthase atsusy. Catalysts 11. https://doi.org/10.3390/catal11010132.

Corroon, J., MacKay, D., Dolphin, W., 2020. Labeling of cannabidiol products: A public health perspective. Cannabis Cannabinoid Res. https://doi.org/10.1089/can.2019.0101.

Cristino, L., Bisogno, T., Di Marzo, V., 2020. Cannabinoids and the expanded endocannabinoid system in neurological disorders. Nat. Rev. Neurol. https://doi.org/10.1038/s41582-019-0284-z.

Dai, L., Liu, C., Li, J., Dong, C., Yang, J., Dai, Z., Zhang, X., Sun, Y., 2018. One-pot synthesis of ginsenoside Rh2 and bioactive unnatural ginsenoside by coupling promiscuous glycosyltransferase from *Bacillus subtilis 168* to sucrose synthase. J. Agric. Food Chem. 66. https://doi.org/10.1021/acs.jafc.8b00597.

De Graaf, M., Pinedo, H.M., Quadir, R., Haisma, H.J., Boven, E., 2003. Cytosolic β-glycosidases for activation of glycoside prodrugs of daunorubicin. Biochem. Pharmacol. 65. https://doi.org/10.1016/S0006-2952(03)00183-7.

De Winter, K., Dewitte, G., Dirks-Hofmeister, M.E., De Laet, S., Pelantová, H., Křen, V., Desmet, T., 2015. Enzymatic glycosylation of phenolic antioxidants: Phosphorylase-mediated synthesis and characterization. J. Agric. Food Chem. 63. https://doi.org/10.1021/acs.jafc.5b04380.

Dewitte, G., Walmagh, M., Diricks, M., Lepak, A., Gutmann, A., Nidetzky, B., Desmet, T., 2016. Screening of recombinant glycosyltransferases reveals the broad

acceptor specificity of stevia UGT-76G1. J. Biotechnol. 233. https://doi.org/10.1016/j.jbiotec.2016.06.034.

Duman-Özdamar, Z.E., Ünlü, A., Ünal, H., Woodley, J.M., Binay, B., 2021. High-yield production of active recombinant *S. simulans lysostaphin* expressed in *E. coli* in a laboratory bioreactor. Protein Expr. Purif. 177. https://doi.org/10.1016/j.pep.2020.105753.

Elferink, H., Titulaer, W.H.C., Derks, M.G.N., Veeneman, G.H., Rutjes, F.P.J.T., Boltje, T.J., 2022. Chloromethyl glycosides as versatile synthons to prepare glycosyloxymethyl-prodrugs. Chem. - A Eur. J. 28. https://doi.org/10.1002/chem.202103910.

Ferrazzano, G.F., Cantile, T., Alcidi, B., Coda, M., Ingenito, A., Zarrelli, A., Di Fabio, G., Pollio, A., 2016. Is *Stevia rebaudiana bertoni* a non cariogenic sweetener? A review. Molecules. https://doi.org/10.3390/molecules21010038.

Fraw-doktor, 2016. *Glycine max* [WWW Document]. URL https://plantsam.com/glycine-max/.

Fride, E., 2005. Endocannabinoids in the central nervous system: From neuronal networks to behavior. Curr. Drug Targets CNS Neurol. Disord. https://doi.org/10.2174/156800705774933069.

Gan, S., Rozhon, W., Varga, E., Halder, J., Berthiller, F., Poppenberger, B., 2021. The acyltransferase PMAT1 malonylates brassinolide glucoside. J. Biol. Chem. 296. https://doi.org/10.1016/j.jbc.2021.100424.

Geogre Mouratidis, 2020. Cannabis plant anatomy: A beginner's guide [WWW Document]. URL https://cannigma.com/plant/cannabis-plant-anatomy.

Ghosh, A.K., Khan, S., Marini, F., Nelson, J.A., Farquhar, D., 2000. A daunorubicin β-galactoside prodrug for use in conjunction with gene- directed enzyme prodrug therapy. Tetrahedron Lett. 41. https://doi.org/10.1016/S0040-4039(00)00742-5.

Goyal, D., Sahni, G., Sahoo, D.K., 2009. Enhanced production of recombinant streptokinase in *Escherichia coli* using fed-batch culture. Bioresour. Technol. 100, 4468–4474. https://doi.org/10.1016/j.biortech.2009.04.008.

Haberl Meglič, S., Janež, N., Peterka, M., Flisar, K., Kotnik, T., Miklavčič, D., 2020. Evaluation and optimization of protein extraction from *E. coli* by

electroporation. Front. Bioeng. Biotechnol. 8, 543187. https://doi.org/10.3389/fbioe.2020.543187.

Hamada, Hiroki, Nakayama, T., Shimoda, K., Matsuura, N., Hamada, Hatsuyuki, Iwaki, T., Kiriake, Y., Saikawa, T., 2020. Curcumin oligosaccharides (gluco-oligosaccharides) penetrate the blood-brain barrier in mouse brain: glycoside (polysaccharide) modification approach for brain drug delivery across the blood-brain barrier and tumor drug delivery. Nat. Prod. Commun. 15. https://doi.org/10.1177/1934578X20953653.

Hardman, J.M., Brooke, R.T., Zipp, B.J., 2017. Cannabinoid glycosides: In vitro production of a new class of cannabinoids with improved physicochemical properties. bioRxiv. https://doi.org/10.1101/104349.

Hu, Y., Min, J., Qu, Y., Zhang, X., Zhang, J., Yu, X., Dai, L., 2020. Biocatalytic synthesis of calycosin-7-o-β-D-glucoside with uridine diphosphate–glucose regeneration system. Catalysts 10 (2), 258. https://doi.org/10.3390/catal10020258.

Hua, T., Li, X., Wu, L., Iliopoulos-Tsoutsouvas, C., Wang, Y., Wu, M., Shen, L., Brust, C.A., Nikas, S.P., Song, F., Song, X., Yuan, S., Sun, Q., Wu, Y., Jiang, S., Grim, T.W., Benchama, O., Stahl, E.L., Zvonok, N., Zhao, S., Bohn, L.M., Makriyannis, A., Liu, Z.J., 2020. Activation and signaling mechanism revealed by cannabinoid receptor-Gi complex structures. Cell 180. https://doi.org/10.1016/j.cell. 2020. 01.008.

Humphrey, T. V., Richman, A.S., Menassa, R., Brandle, J.E., 2006. Spatial organisation of four enzymes from *Stevia rebaudiana* that are involved in steviol glycoside synthesis. Plant Mol. Biol. 61. https://doi.org/10.1007/s11103-005-5966-9.

Lan Parkes, 2020. The solubility and stability profiles of cannabidiol. CBD world news.

Idrees, H., Zaidi, S.Z.J., Sabir, A., Khan, R.U., Zhang, X., Hassan, S.U., 2020. A review of biodegradable natural polymer-based nanoparticles for drug delivery applications. Nanomaterials. https://doi.org/10.3390/nano10101970.

Jansson, D., Dieriks, V.B., Rustenhoven, J., Smyth, L.C.D., Scotter, E., Aalderink, M., Feng, S., Johnson, R., Schweder, P., Mee, E., Heppner, P., Turner, C., Curtis, M., Faull, R., Dragunow, M., 2021. Cardiac glycosides target barrier inflammation of the vasculature, meninges and choroid plexus. Commun. Biol. 4. https://doi.org/10.1038/s42003-021-01787-x.

Kienzl, M., Kargl, J., Schicho, R., 2020. The immune endocannabinoid system of the tumor microenvironment. Int. J. Mol. Sci. https://doi.org/10.3390/ijms21238929.

Kim, M., Park, M.H., Nam, G., Lee, M., Kang, J., Song, I.S., Choi, M.K., Jin, H.K., Bae, J.S., Lim, M.H., 2021. A Glycosylated prodrug to attenuate neuroinflammation and improve cognitive deficits in Alzheimer's Disease transgenic mice. Mol. Pharm. 18. https://doi.org/10.1021/acs.molpharmaceut.0c00677.

Kim, M.J., Zheng, J., Liao, M.H., Jang, I.C., 2019. Overexpression of SrUGT76G1 in Stevia alters major steviol glycosides composition towards improved quality. Plant Biotechnol. J. 17. https://doi.org/10.1111/pbi.13035.

Kleinig, A.R., Mansell, C.J., Nguyen, Q.D., Badalyan, A., Middelberg, A.P.J., 1995. Influence of broth dilution on the disruption of *Escherichia coli*. Biotechnol. Tech. 9, 759–762. https://doi.org/10.1007/BF00159244.

Koley, D., Bard, A.J., 2010. Triton X-100 concentration effects on membrane permeability of a single HeLa cell by scanning electrochemical microscopy (SECM). Proc. Natl. Acad. Sci. U. S. A. 107, 16783–16787. https://doi.org/ 10.1073/ pnas.1011614107.

Kulmer, S.T., Gutmann, A., Lemmerer, M., Nidetzky, B., 2017. Biocatalytic cascade of polyphosphate kinase and sucrose synthase for synthesis of nucleotide-activated derivatives of glucose. Adv. Synth. Catal. 359, 292–301. https://doi.org/10.1002/adsc.201601078.

Kurze, E., Ruß, V., Syam, N., Effenberger, I., Jonczyk, R., Liao, J., Song, C., Hoffmann, T., Schwab, W., 2021. Glucosylation of (±)-menthol by uridine-diphosphate-sugar dependent glucosyltransferases from plants. Molecules 26. https://doi.org/ 10.3390/molecules26185511.

Kweon, D.H., Han, N.S., Park, K.M., Seo, J.H., 2001. Overproduction of Phytolacca insularis protein in batch and fed-batch culture of recombinant *Escherichia coli*. Process Biochem. 36, 537–542. https://doi.org/10.1016/S0032-9592(00) 00237-5.

Lairson, L.L., Henrissat, B., Davies, G.J., Withers, S.G., 2008. Glycosyl transferases: Structures, functions, and mechanisms. Annu. Rev. Biochem. https://doi.org/ 10.1146/annurev.biochem.76.061005.092322.

Lu, H.C., MacKie, K., 2016. An introduction to the endogenous cannabinoid system. Biol. Psychiatry. https://doi.org/10.1016/j.biopsych.2015.07.028.

Madan, S., Ahmad, S., Singh, G.N., Kohli, K., Kumar, Y., Singh, R., Garg, M., 2010. *Stevia rebaudiana (Bert.) Bertoni* - A Review. Indian J. Nat. Prod. Resour.

Madhav, H., Bhasker, S., Chinnamma, M., 2013. Functional and structural variation of uridine diphosphate glycosyltransferase (UGT) gene of *Stevia rebaudiana*-UGTSr involved in the synthesis of rebaudioside A. Plant Physiol. Biochem. 63. https://doi.org/10.1016/j.plaphy.2012.11.029.

Mao, Y., Zhang, Y., Luo, Z., Zhan, R., Xu, H., Chen, W., Huang, H., 2018. Synthesis, biological evaluation and low-toxic formulation development of glycosylated paclitaxel prodrugs. Molecules 23. https://doi.org/10.3390/molecules23123211.

Martin, H., Lázaro, L.R., Gunnlaugsson, T., Scanlan, E.M., 2022. Glycosidase activated prodrugs for targeted cancer therapy. Chem. Soc. Rev. 9694–9716. https://doi.org/10.1039/d2cs00379a.

Mawson, R., Gamage, M., Terefe, N.S., Knoerzer, K., 2011. Ultrasound in enzyme activation and inactivation, in: Food Engineering Series. pp. 369–404. https://doi.org/10.1007/978-1-4419-7472-3_14.

McGilveray, I.J., 2005. Pharmacokinetics of cannabinoids. Pain Res. Manag. https://doi.org/10.1155/2005/242516.

Menzella, H.G., Ceccarelli, E.A., Gramajo, H.C., 2003. Novel *Escherichia coli* strain allows efficient recombinant protein production using lactose as inducer. Biotechnol. Bioeng. 82, 809–817. https://doi.org/10.1002/bit.10630.

Mestrom, L., Przypis, M., Kowalczykiewicz, D., Pollender, A., Kumpf, A., Marsden, S.R., Bento, I., Jarzębski, A.B., Szymańska, K., Chruściel, A., Tischler, D., Schoevaart, R., Hanefeld, U., Hagedoorn, P.L., 2019. Leloir glycosyltransferases in applied biocatalysis: A multidisciplinary approach. Int. J. Mol. Sci. https://doi.org/10.3390/ijms20215263.

Middelberg, A.P.J., 2000. 2 Microbial cell disruption by high-pressure homogenization. pp. 11–21. https://doi.org/10.1007/978-1-59259-027-8_2.

Millar, S.A., Maguire, R.F., Yates, A.S., O'sullivan, S.E., 2020. Towards better delivery of cannabidiol (Cbd). Pharmaceuticals 13, 1–15. https://doi.org/10.3390/ph13090219.

Millar, S.A., Stone, N.L., Yates, A.S., O'Sullivan, S.E., 2018. A systematic review on the pharmacokinetics of cannabidiol in humans. Front. Pharmacol. https://doi.org/10.3389/fphar.2018.01365.

Mistry, S., 2021. Glycosides [WWW Document]. URL https://solutionpharmacy.in/classification-of-glycosides.

Monshouwer, K., Van Laar, M., Vollebergh, W.A., 2011. Buying cannabis in "coffee shops." Drug Alcohol Rev. 30. https://doi.org/10.1111/j.1465-3362.2010.00268.x.

Murota, K., Matsuda, N., Kashino, Y., Fujikura, Y., Nakamura, T., Kato, Y., Shimizu, R., Okuyama, S., Tanaka, H., Koda, T., Sekido, K., Terao, J., 2010. α-Oligoglucosylation of a sugar moiety enhances the bioavailability of quercetin glucosides in humans. Arch. Biochem. Biophys. 501. https://doi.org/10.1016/j.abb.2010.06.036.

Navarro, P.P., Vettiger, A., Ananda, V.Y., Llopis, P.M., Allolio, C., Bernhardt, T.G., Chao, L.H., 2022. Cell wall synthesis and remodelling dynamics determine division site architecture and cell shape in *Escherichia coli*. Nat. Microbiol. 7, 1621–1634. https://doi.org/10.1038/s41564-022-01210-z.

Nawaz, N., Wen, S., Wang, F., Nawaz, S., Raza, J., Iftikhar, M., Usman, M., 2022. Lysozyme and its application as antibacterial agent in food industry. Molecules. https://doi.org/10.3390/molecules27196305.

Nidetzky, B., Gutmann, A., Zhong, C., 2018. Leloir glycosyltransferases as biocatalysts for chemical production. ACS Catal. 8, 6283–6300. https://doi.org/10.1021/acscatal.8b00710.

Oberbarnscheidt, T., Miller, N.S., 2020. The impact of cannabidiol on psychiatric and medical conditions. J. Clin. Med. Res. 12. https://doi.org/10.14740/jocmr4159.

Pamplona, F.A., Da Silva, L.R., Coan, A.C., 2018. Potential clinical benefits of CBD-Rich cannabis extracts over purified CBD in treatment-resistant epilepsy: Observational data meta-analysis. Front. Neurol. https://doi.org/10.3389/fneur.2018.00759.

Pan, H., Xie, Z., Bao, W., Zhang, J., 2008. Optimization of culture conditions to enhance cis-epoxysuccinate hydrolase production in *Escherichia coli* by response surface methodology. Biochem. Eng. J. 42, 133–138. https://doi.org/10.1016/j.bej.2008.06.007.

Pei, J., Chen, A., Zhao, L., Cao, F., Ding, G., Xiao, W., 2017. One-pot synthesis of hyperoside by a three-enzyme cascade using a UDP-Galactose regeneration system. J. Agric. Food Chem. 65. https://doi.org/10.1021/acs.jafc.7b02320.

Ponton, J.A., Smyth, K., Soumbasis, E., Llanos, S.A., Lewis, M., Meerholz, W.A., Tanguay, R.L., 2020. A pediatric patient with autism spectrum disorder and epilepsy using cannabinoid extracts as complementary therapy: A case report. J. Med. Case Rep. 14. https://doi.org/10.1186/s13256-020-02478-7.

Rezaei, L., Shojaosadati, S.A., Farahmand, L., Moradi-Kalbolandi, S., 2020. Enhancement of extracellular bispecific anti-MUC1 nanobody expression in *E. coli BL21 (DE3)* by optimization of temperature and carbon sources through an auto-induction condition. Eng. Life Sci. 20, 338–349. https://doi.org/10.1002/elsc.201900158.

Richman, A., Swanson, A., Humphrey, T., Chapman, R., McGarvey, B., Pocs, R., Brandle, J., 2005. Functional genomics uncovers three glucosyltransferases involved in the synthesis of the major sweet glucosides of *Stevia rebaudiana*. Plant J. 41. https://doi.org/10.1111/j.1365-313X.2004.02275.x.

Rimmington, F., 2020. Pharmacokinetics and pharmacodynamics. South. African J. Anaesth. Analg. 26. https://doi.org/10.36303/SAJAA.2020.26.6.S3.2562.

Rosano, G.L., Ceccarelli, E.A., 2014. Recombinant protein expression in *Escherichia coli*: Advances and challenges. Front. Microbiol. 5. https://doi.org/10.3389/fmicb.2014.00172.

Sacco, P., Cok, M., Scognamiglio, F., Pizzolitto, C., Vecchies, F., Marfogliá, A., Marsich, E., Donati, I., 2020. Glycosylated-chitosan derivatives: A systematic review. Molecules. https://doi.org/10.3390/molecules25071534.

Sarkandy, S.Y., Khalilzadeh, R., Shojaosadati, S.A., Sadeghizadeh, M., Farnoud, A.M., Babaeipour, V., Maghsoudi, A., 2010. A novel amino acid supplementation strategy based on a stoichiometric model to enhance human IL-2 (interleukin-2) expression in high-cell-density *Escherichia coli* cultures. Biotechnol. Appl. Biochem. 57, 151–156. https://doi.org/10.1042/ba20100320.

Schmölzer, K., Gutmann, A., Diricks, M., Desmet, T., Nidetzky, B., 2016. Sucrose synthase: A unique glycosyltransferase for biocatalytic glycosylation process development. Biotechnol. Adv. https://doi.org/10.1016/j.biotechadv.2015.11.003.

Shchegravina, E.S., Sachkova, A.A., Usova, S.D., Nyuchev, A. V., Gracheva, Y.A., Fedorov, A.Y., 2021. Carbohydrate systems in targeted drug delivery: Expectation and reality. Russ. J. Bioorganic Chem. https://doi.org/10.1134/S1068162021010222.

Shimizu, R., Shimabayashi, H., Moriwaki, M., 2006. Enzymatic production of highly soluble myricitrin glycosides using β-galactosidase. Biosci. Biotechnol. Biochem. 70. https://doi.org/10.1271/bbb.70.940.

Shu, W., Zheng, H., Fu, X., Zhen, J., Tan, M., Xu, J., Zhao, X., Yang, S., Song, H., Ma, Y., 2020. Enhanced heterologous production of glycosyltransferase ugt76g1 by co-expression of endogenous prpd and malk in *Escherichia coli* and its transglycosylation application in production of rebaudioside. Int. J. Mol. Sci. 21, 1–12. https://doi.org/10.3390/ijms21165752.

Sivashanmugam, A., Murray, V., Cui, C., Zhang, Y., Wang, J., Li, Q., 2009. Practical protocols for production of very high yields of recombinant proteins using *Escherichia coli.* Protein Sci. 18, 936–948. https://doi.org/10.1002/pro.102.

Spleman, L., Sinclair, R., Freeman, M., Davis, M., Gebauer, K., 2018. 1061 The safety of topical cannabidiol (CBD) for the treatment of acne. J. Invest. Dermatol. 138. https://doi.org/10.1016/j.jid.2018.03.1074.

Stein, O., Granot, D., 2019. An overview of sucrose synthases in plants. Front. Plant Sci. 10. https://doi.org/10.3389/fpls.2019.00095.

Stinchcomb, A.L., Lexington, K.Y., Lee, S., 2010. Formulations of cannabidiol and prodrugs of cannabidiol and methods of using the same. Us 2010/0273895 a1 61.

Takemori, S., Furuya, E., Suzuki, H., Katagiri, M., 1967. Stabilization of enzyme activity by an organic solvent [37]. Nature. https://doi.org/10.1038/215417a0.

Tan, S.C., Yiap, B.C., 2009. DNA, RNA, and protein extraction: The past and the present. J. Biomed. Biotechnol. https://doi.org/10.1155/2009/574398.

Tanasescu, R., Constantinescu, C.S., 2010. Cannabinoids and the immune system: An overview. Immunobiology 215. https://doi.org/10.1016/j.imbio.2009.12.005.

Trad-Paulo Gómzer, 2017. How THC gets into your brain – and how to increase it [WWW Document]. URL http://profofpot.com/thc-blood-brain-barrier/ (accessed 5.21.17)..

Tripathi, N.K., 2016. Production and purification of recombinant proteins from *Escherichia coli*. ChemBioEng Rev. 3, 116–133. https://doi.org/10.1002/cben.201600002.

Tzadok, M., Uliel-Siboni, S., Linder, I., Kramer, U., Epstein, O., Menascu, S., Nissenkorn, A., Yosef, O.B., Hyman, E., Granot, D., Dor, M., Lerman-Sagie, T., Ben-Zeev, B., 2016. CBD-enriched medical cannabis for intractable pediatric epilepsy: The current Israeli experience. Seizure 35. https://doi.org/10.1016/j.seizure.2016.01.004.

Voeks, R., 2014. ' Cannabis: evolution and ethnobotany. AAG Rev. Books 2. https://doi.org/10.1080/2325548x.2014.901859.

Wakshlag, J.J., Schwark, W.S., Deabold, K.A., Talsma, B.N., Cital, S., Lyubimov, A., Iqbal, A., Zakharov, A., 2020. Pharmacokinetics of cannabidiol, cannabidiolic Acid, Δ9-tetrahydrocannabinol, tetrahydrocannabinolic acid and related metabolites in canine serum after dosing with three oral forms of hemp extract. Front. Vet. Sci. 7. https://doi.org/10.3389/fvets.2020.00505.

Wang, H., Yang, R., Hua, X., Zhang, Z., Zhao, W., Zhang, W., 2011. Expression, enzymatic characterization, and high-level production of glucose isomerase from *Actinoplanes missouriensis CICIM B0118(A)* in *Escherichia coli*. Zeitschrift fur Naturforsch.-Sect. C J. Biosci. 66. https://doi.org/10.1515/znc-2011-11-1210.

Wang, X., 2009. Structure, mechanism and engineering of plant natural product glycosyltransferases. FEBS Lett. https://doi.org/10.1016/j.febslet.2009.09.042.

Wang, Y., Chen, L., Li, Yan, Li, Yangyang, Yan, M., Chen, K., Hao, N., Xu, L., 2016. Efficient enzymatic production of rebaudioside A from stevioside. Biosci. Biotechnol. Biochem. 80. https://doi.org/10.1080/09168451.2015.1072457.

Wouters, M., Benschop, A., van Laar, M., Korf, D.J., 2012. Cannabis use and proximity to coffee shops in the Netherlands. Eur. J. Criminol. 9. https://doi.org/10.1177/1477370812448033.

Wu, J.Y., Ding, H.Y., Wang, T.Y., Tsai, Y.L., Ting, H.J., Chang, T.S., 2021. Improving aqueous solubility of natural antioxidant mangiferin through glycosylation by maltogenic amylase from *parageobacillus galactosidasius DSM 18751*. Antioxidants 10. https://doi.org/10.3390/antiox10111817.

Xu, W., Ling, P., Zhang, T., 2013. Polymeric micelles, a promising drug delivery system to enhance bioavailability of poorly water-soluble drugs. J. Drug Deliv. 2013. https://doi.org/10.1155/2013/340315.

Yasmin-Karim, S., Moreau, M., Mueller, R., Sinha, N., Dabney, R., Herman, A., Ngwa, W., 2018. Enhancing the therapeutic efficacy of cancer treatment with cannabinoids. Front. Oncol. 8. https://doi.org/10.3389/fonc.2018.00114.

Yoon, S.K., Kang, W.K., Park, T.H., 1994. Fed-batch operation of recombinant *Escherichia coli* containing trp promoter with controlled specific growth rate. Biotechnol. Bioeng. 43, 995–999. https://doi.org/10.1002/bit.260431013.

Yu, J., Tao, Y., Pan, H., Lin, L., Sun, J., Ma, R., Li, Y., Jia, H., 2022. Mutation of Stevia glycosyltransferase UGT76G1 for efficient biotransformation of rebaudioside E into rebaudioside M. J. Funct. Foods 92. https://doi.org/10.1016/j.jff.2022.105033.

Yu, N., Liu, T., Zhang, X., Gong, N., Ji, T., Chen, J., Liang, X.J., Kohane, D.S., Guo, S., 2020. Dually enzyme- and acid-triggered self-immolative ketal glycoside nanoparticles for effective cancer prodrug monotherapy. Nano Lett. 20. https://doi.org/10.1021/acs.nanolett.0c01973.

Zea, C.J., Camci-Unal, G., Pohl, N.L., 2008. Thermodynamics of binding of divalent magnesium and manganese to uridine phosphates: Implications for diabetes-related hypomagnesaemia and carbohydrate biocatalysis. Chem. Cent. J. 2. https://doi.org/10.1186/1752-153X-2-15.

Zhang, S., Liu, Q., Lyu, C., Chen, Jinsong, Xiao, R., Chen, Jingtian, Yang, Y., Zhang, H., Hou, K., Wu, W., 2020. Characterizing glycosyltransferases by a combination of sequencing platforms applied to the leaf tissues of *Stevia rebaudiana*. BMC Genomics 21. https://doi.org/10.1186/s12864-020-07195-5.

Zhang, X.Q., Lund, A.A., Sarath, G., Cerny, R.L., Roberts, D.M., Chollet, R., 1999. Soybean nodule sucrose synthase (nodulin-100): Further analysis of its phosphorylation using recombinant and authentic root-nodule enzymes. Arch. Biochem. Biophys. 371, 70–82. https://doi.org/10.1006/abbi.1999.1415.

Zipp, B.J., Hardman, J.M., Brooke, R.T., 2017. Cannabinoid glycoside prodrugs and methods of synthesis.

Zou, S., Kumar, U., 2018. Cannabinoid receptors and the endocannabinoid system: Signaling and function in the central nervous system. Int. J. Mol. Sci. https://doi.org/10.3390/ijms19030833.

BIOGRAPHY

Miss Le Thi Thuy Trinh was born on the 8th of May, 1995, in Quang Nam, Vietnam. She graduated with the Bachelor's degree in Food Technology from Hue University of Agriculture and Forestry. Then, she pursued a Master's degree in the School of Biotechnology at Suranaree University of Technology (SUT) in 2020. Then, she received the scholarship from Suranaree University of Technology (SUT) through the One Grant One Graduate Scholarship for Graduate Students (OROG) program. She is currently pursuing her doctoral degree under the supervision of Associate Professor Apichat Boontawan, Co-Advisor Prof. James Ketudat-Cairns, and Co-Advisor Assoc. Prof. Mariena Ketudat-Cairns. Her research topic focuses on production and purification of cannabidiol glycosides using SrUGT76G1 Glycosyltransferase and sucrose synthase enzyme catalysts.